Studies on Transalkylation over modified Zeolite Catalysts

Submitted in partial fulfillment of the requirement

for the Degree of

Doctor of Philosophy

by

RUCHIKA THAKUR
(Roll No. 901009007)

Under the supervision of

Dr. Sanghamitra Barman
Associate Professor

Dr. Raj Kumar Gupta
Associate Professor

Department of Chemical Engineering
Thapar University
Patiala

SCHOOL OF CHEMISTRY AND BIOCHEMISTRY
THAPAR UNIVERSITY
PATIALA – 147004, PUNJAB, INDIA
2016

DEDICATED TO

MY

BELOVED PARENTS

ACKNOWLEDGEMENTS

This thesis owes its existence to the support, help and inspiration of several people. I would like to extend my gratitude to many people who helped to bring this research project to fruition. I would like to express my deepest gratitude to my Supervisors and mentors Dr. Sanghamitra Barman & Dr. Raj Kumar Gupta, Department of Chemical Engineering and Technology, Thapar University, Patiala for their immense unwavering support, guidance and encouragement from the preliminary to the concluding levels of my Doctoral Research. They supported me throughout my work with patience and knowledge whilst allowing me the room to work in my own way. Their commitment and sense of mission has moulded my work to provide it direction and substance.

I am extremely thankful to the Director, Thapar University, Dean (Research & Sponsored Projects), Head, School of Chemistry & Biochemistry and Head, Department of Chemical Engineering and Technology for extending the opportunity to undertake this doctoral research.

A particular thanks goes to the members of Doctoral Committee for monitoring my research work from time to time and giving their valuable feedback. I am highly obliged to Dr. Susheel Mittal for his help, professionalism, valuable guidance and financial support throughout my entire program of doctrol study that I do not have enough words to express my deep and sincere appreciation. I am also indebted to Dr. Manmohan Chibber who has been a constant source of encouragement and enthusiasm. In addition I am deeply grateful to Dr. Rajeev Mehta who guided me through all these years.

I owe my sincere thanks to Dr. Bonamali Pal (Head, School of Chemistry and Biochemistry) for providimg support and faciliaction. A special thanks to Dr Amjad Ali who has always been available to answer my questions and giving valueable suggestions

regarding my work. I would also like to thank Dr Ranjana Prakash for unfailing support and continuous encouragement.

Grateful acknowledgement is made to my other friends Amu, Shilpa Narang, Navjot Kaur, Taranpreet Kaur, Sumit, Harkirat Sandhu, Nitin Goyal and Dr Gaurav Madhu. I am also thankful to all the teaching and non-teaching staff members of the department for their invaluable cooperation and help during the entire tenure of my studies in the department. Mr. Chander Singh, a fine technician, in School of Chemistry and Biochemistry has always helped me out in case my instrument needs some repairs. I would also like to thank Mr Amit, Mr Munish, Mr Shubham, Mr Krishan, Mr Rana for their constant help and support throughout this doctoral research.

At the end, I wish to express my profound gratitude to my parents. No matter where they are, they are always with me. It is power of their blessings, which has given me the courage, confidence and zeal for hard work. My brother, Mr Ankur Thakur, also deserves a very deep acknowledgement for supporting and encouraging me at every step of my work.

Date: 14th JULY 2016
Place: PATIALA

Ruchika Thakur

Ruchika Thakur

CERTIFICATE

This is to certify that the thesis entitled "Studies on Transalkylation over modified Zeolite Catalysts" being submitted by Ruchika Thakur, to the School of Chemistry and Biochemistry, Thapar University , Patiala for the award of degree of DOCTOR OF PHILOSOPHY, is a record of bonafide research work carried out by her. Ms. Ruchika Thakur has worked under my guidance and supervision and has fulfilled the requirements for submission of thesis, which to my knowledge has reached the requisite standard.

The results embodied in the thesis have not been submitted in part or full to any other University or Institute for the award of any degree or diploma.

Dr. Sanghamitra Barman
Associate Professor
Department of Chemical Engineering
Thapar University
Patiala

Dr. Raj Kumar Gupta
Associate Professor
Department of Chemical Engineering
Thapar University
Patiala

TABLE OF CONTENTS

LIST OF ABBREVIATIONS

Abbreviation	*Description*
atm	Atmosphere
BET	Brunauer- Emmett-Teller
Ce	Cerium
CeB	Cerium modified Hbeta zeolite
CeB_{10}	Cerium modified Hbeta zeolite with 10% cerium solution
CeB_{12}	Cerium modified Hbeta zeolite with 12% cerium solution
CeX	Cerium modified NaX zeolite
CeX_2	Cerium modified NaX zeolite with 2% cerium solution
CeX_5	Cerium modified NaX zeolite with 5% cerium solution
CeX_6	Cerium modified NaX zeolite with 6% cerium solution
CeX_7	Cerium modified NaX zeolite with 7% cerium solution
CeX_8	Cerium modified NaX zeolite with 8% cerium solution
CeX_{10}	Cerium modified NaX zeolite with 10% cerium solution
$CeX1_2$	Cerium modified NaX zeolite with 12% cerium solution
C_{A0}	Initial concentration
C_A	Final concentration
DIPB	Diisopropylbenzene
DIPT	Diisopropyltoluene
EDS	Energy Dispersive X-ray spectroscopy
FAU	Faujasite
Hbeta	Beta zeolite
J/ mol K	Joule per mole per Kelvin
k_1,k_2,k_3	kinetic rate constant, kmol/kg h
K_B	Adsorption constant for benzene, atm^{-1}
Kc	Adsorption constant for cumene, atm^{-1}
K_{DIPB}	Adsorption constant for DIPB, atm^{-1}
kJ/ mol	Kilojoule per mole
K_t	Adsorption constant for toluene, atm^{-1}
$K_{1,2,4TMB}$	adsorption constant for Trimethylbenzene, atm^{-1}
La	Lanthanum

LaB	Lanthanum modified beta zeolite
LaX	Lanthanum modified NaX zeolite
LHHW	Langmuir Hinshelwood Hougen Watson model
l/h	litre per hour
mg/ L	milligram per litre
min	minute
mmol/g	millimole per gram
mol%	mole%
ml/min	millilitre per minute
m^2/g	metre square per gram
NaX	X zeolite
N_2	Nitrogen
NH_3-TPD	Ammonia Temperature Programmed Desorption
P	Total pressure, atm
p_A	partial pressure of aliphatics, atm
p_B	partial pressure of benzene, atm
p_{cumene}	partial pressure of cumene, atm
p_{cymene}	partial pressure of cymene, atm
p_{DIPB}	partial pressure of DIPB, atm
p_{DIPT}	partial pressure of DIPT, atm
p_T	partial pressure of toluene, atm
p_{TMB}	partial pressure of TMB, atm
p_{Temb}	partial pressure of TeMB, atm
p_{xyl}	partial pressure of xylene, atm
Pr	Praseodymium
PrB	Praseodymium modified beta zeolite
PrB_{10}	Praseodymium modified beta zeolite with 10% praseodymium solution
PrX	Praseodymium modified NaX zeolite
$-r_{cum}$	Experimental rate of cumene conversion
SEM	Scanning electron microscopy
TMB	Trimethylbenzene
TeMB	Tetramethylbenzene

X_c	moles of cumene reacted, kmol
X_{expt}	Experimental fractional conversion
X_{pred}	Predicted fractional conversion
X_A	moles of aliphatics produced, kmol
X_{DIPT}	moles of DIPT produced, kmol
X_{ben}	moles of benzene produced, kmol
X_{cymene}	moles of cymene produced, kmol
X_{xyl}	moles of xylene produced, kmol
XRD	X-ray diffraction
X_t	moles of toluene reacted, kmol

LIST OF SYMBOLS

Symbols	*Description*
Å	Angstrom
A	Pre–exponential factor
E_a	Activation energy
ΔH	Enthalpy
ΔS	Entropy
g	gram
H	Hour
K	Kelvin
K	rate constant
Kg	Kilogram
M	metre
mm	millimetre
%	percentage
μ	micro
θ	Theta
α	Alpha
°	Degree
°C	Degree Celsius
S	second
T	Temperature
t	Time
X	Conversion
Y	Yield

LIST OF FIGURES

LIST OF TABLES

ABSTRACT

Alkyl-transfer of alkyl aromatics like toluene and benzene were studied for the purpose of understanding the principles that governs them. Transalkylation of low valued alkyl aromatics was done so as to convert these aromatics to industrially important products like xylene, cumene and cymene. Transalkylation of aromatics ranging from mono to polyalkyl-benzenes was studied in a fixed bed reactor system on solid acid catalysts (zeolites).

In order to replace highly toxic, corrosive and non renewable traditional catalysts with nontoxic as well as renewable catalysts zeolites were used as catalysts for transalkylation of aromatics. In present thesis two different types of large pore zeolites, namely, Hbeta and NaX zeolites were modified using various rare earth metals and were used as catalysts for different transalkylation reactions in heterogeneous mode. The catalysts were refluxed with rare earth nitrate solution at specific conditions to carry out the ion exchange. The chemical analysis of catalysts was done by EDS to find the metal ion incorporated into the zeolite while the catalysts structure and crystallinity was established by powder XRD characterization technique. The surface morphology and particle size was determined by SEM studies. The quantity and strength of acidic sites present in catalysts were found using TPD results.

The rare earth metal ions chosen for the modification of Hbeta and NaX zeolites were lanthanum (La), cerium (Ce) and Praseodymium (Pr). The catalyst activity was found to be a function of its acidity which in turn depends on the rare earth metal ion type and its concentration in the catalyst. The modified zeolites were able to catalyze the transalkylation reaction more effectively than the parent zeolites. These rare earth metal ions modified zeolite catalyst have shown excellent stability on time-on-stream without significant loss in activity. However, the parent catalyst was found to be less active and stable to carry out the transalkylation of aromatics.

Transalkylation reactions were studied at temperatures up to 500°C. Results showed that alkyl-transfer reactions seemed to be dominant at higher temperatures. In transalkylation reactions, the reactant conversion depends on the type of alkyl substituent/s, ring conjugation of the aromatic moiety and the number of alkyl groups on the aromatic ring/s and the chain length. The outlined mechanism showed that the catalyst pore sizes and the type of pores as

well as the feed composition of binary mixtures play important roles in the transfer of alkyl groups between aromatic molecules. The activity of the zeolites also depends on type of ions exchanged with the H^+ or Na^+ ions present in the framework of the zeolite.

Besides evaluating the catalyt performance, kinetics and thermodynamic parameters of the reactions were also evaluated. A suitable kinetic model was developed following several mechanisms such as dual site, single site mechanism with surface reaction as the rate controlling step. Activation energy for various transalkylation reactions were found to be in range of 50-130 kJ/mol.

Zeolitic catalysts are deactivated through molecular retention which is dominant at lower temperatures. Bulkier alkylaromatics readily available in petroleum liquids can be transformed to commercially valuable products through transalkylation reactions with the help of a suitable catalyst. Thus, the transalkylation reactions have promising future applications in petrochemical and related industries;

Keywords: Benzene, Cerium, Cumene, Cymene, DIPB, Deactivation, Friedel-Crafts, Hbeta zeolite, Kinetics, Kinetic Modelling, Lanthanum, LHHW model, Mass transfer, NaX zeolite, Praseodymium, Rare earth metal ions, Transalkylation, Toluene, TMB, Xylene.

CHAPTER- 1

Introduction

This chapter deals with the general introduction of alkylation and transalkylation reactions. The transalkylation reactions investigated in the present work are also introduced. A brief introduction to various catalysts used for transalkylation reaction is also given. As large pore zeolites (NaX and Hbeta) are used as catalysts in this study; therefore, a detail description of zeolite composition, its structure and properties is included.

1.1 TRANSALKYLATION REACTIONS

Alkylation reactions are one of the most fundamental and commercially important organic reactions in the chemical industry as they are used to synthesize various commercial aromatic compounds. Transalkylation reactions represent a class of alkylation reactions which involve the introduction of an alkyl group via transfer route between two dissimilar aromatic moieties [Maity *et al*., 2006; Kondamudi and Upadhyayula, 2008; Odedario and Khattaf, 2011]. Transalkylation reactions are different from disproportionation reactions in a way that the former involve alkyl transfer within two dissimilar molecules while in the later case the transfer occurs between two similar molecules. These two major practical processes for utilisation of aromatics are coined as "alkyl group transfer reactions" or "alkyl-transfer reactions" [Al-Zahrani *et al*., 2003]. Transalkylation reactions are commercially very interesting as these reactions lead to the production of monosubstituted or disubstituted homologues of higher value from low valued polyalkylated byproducts [Cejka and Wicheterlova, 2002; Maity *et al*., 2006; Kondamudi and Upadhyayula, 2008; Krejci *et al*., 2010]. It is a challenging task in industrial research to find the cost effective catalytic transalkylation processes.

Early research in the field of transalkylation was reported for xylene production from toluene [Brown and Nelson, 1953]. Since then, a number of transalkylation reactions have been practiced industrially for the production of valuable chemical products such as 4-alkyl-or 4,4'-dialkyl biphenyls, 4-alkyl naphthalenes, cumene, cymene, ethylbenzene [Cavani *et al*., 2002; Maity *et al*., 2006]. Different undesirable products are formed during the direct alkylation of molecules. However, transalkylation reactions of aromatics involve extremely bulky transition states and hence are highly shape selective [Maity *et al*., 2006]. Xylene, cumene and cymene are important commercial products. Transalkylation reaction of toluene and trimethylbenzene for production of xylene is one of the most important commercial reaction [Chao and leu, 1989; Dumitriu *et al*., 1996; Hulea *et al*., 1997; Lee *et al*., 1998;

Dumitriu *et al*., 2002; Sulikowski and Rachwalik, 2003]. Cumene and cymene production by transalkylation of benzene and toluene respectively are other commercially important transalkylation reactions [Odedario and Khattaf, 2011].

1.1.1 Transalkylation of toluene to produce xylene

Global demand for xylene remains at a high level and is growing sharply. Para-xylene is the most useful product followed by *ortho*-and *meta*-xylene [Khattaf *et al*., 2007]. Xylene has numerous applications and is used in the production of polyethylene terephthalate, phthalic anhydride and terephthalic acid. It is also used as octane additive for fuels in petroleum industry [Waziri *et al*., 2010]. It also finds many uses as sterilizer, thinner for paints, solvent for paraffins, varnishes, as cleansing agent for steel and in pharmaceuticals. Reforming and pryolysis of gasoline are one of the major sources of these aromatic hydrocarbons in petrochemical industry [Dumitriu *et al*., 2002]. Toluene-methanol alkylation under harsh Friedel-Crafts conditions is the industrial route for xylene production. [Dumitriu *et al*., 2002; Borgna *et al*., 2004]. Xylene industry has now switched over from the alkylation route to transalkylation route as the later uses environment friendly catalysts. Low value toluene and trimethylbenzene being available in abundance can be utilized for the production of monoalkylated xylene by using zeolite catalysts.

1.1.2 Transalkylation of toluene to produce cymene

Cymene (isopropyltoluene) is used for the production of cresols, pharmaceuticals, fungicides, pesticides, perfumery [Welstead, 1978; Frankel and Levy, 1989], heat transfer media [Derfer and Derfer, 1978], polymers, special solvents, etc. Among the isomers of cymene, *meta* and *para* isomers are of great demand. Alkylation of toluene with propene or isopropanol over liquid acids is traditional route for cymene production. Various catalyst like H_2SO_4 [Meyer and Bernhauer, 1929], $TiC1_4$ [Cullinane and Leyshan, 1954], $FeSO_4$-HC1 [Hino and Arata, 1977] and other solid acids like BF_3 supported alumina, silica-alumina supported titania [Sabu *et al*., 1973] and different zeolites were being used in the alkylation process. More recently, commercial production of cymene by transalkylation reaction has become more popular than alkylation reactions.

1.1.3 Transalkylation of benzene to produce cumene

Cumene, also known by cumol or isopropylbenzene, is commercially utilised for the production of phenol and acetone [Maity *et al*., 2006]. About 90% of the world's demand of phenol is met through cumene [Arshadi and Ghiaci, 2010]. The main end uses for cumene, as a phenol intermediate, are bisphenol A, phenolic resins, and caprolactam. Cumene is also used for the production of α-Methylstyrene, enamels, thinner for paints and acetophenone and as a solvent for fats.

Friedel-Crafts alkylation of benzene with propene is the conventional route for industrial scale cumene production. Various acid catalysts like $AlCl_3$-HCl, H_2SO_4, SPA (Solid phosphoric acid) are used to catalyze this reaction [Bandhopdhyay *et al*., 1996]. Isopropylation of benzene to cumene is accompanied by the formation of 5-10 wt% diisopropylbenzene (DIPB) isomers [Pradhan and Rao, 1993; Maity *et al.*, 2006; Kondamudi and Upadhyayula, 2008]. This is a major concern when cumene yield and selectivity is of much importance. These byproducts are diverted to the fuel pool in the commercial plants leading to additional raw material consumption which affects the economy of the whole process. The byproduct DIPB can be converted to main product cumene by transalkylation with benzene.

Any chemical industry which manufactures cumene can carry out alkylation and transalkylation reaction in the same or different reactor where the byproduct like DIPB can be recycled to transalkylation zone for further reaction. Combining both alkylation and transalkylation reaction can thus maximize yield of cumene and also includes various advantages which include capital and operating cost savings, smaller overall unit size, and uses a lesser quantity of catalyst.

1.2 CATALYSTS FOR TRANALKYLATION REACTIONS

The first alkylation reaction of benzene with alkyl chlorides using $AlCl_3$ as a catalyst was reported by Friedel and Crafts in 1877 [Friedel and Crafts, 1877]. Over the past decades, with modifications in this pathbreaking discovery, vast number of synthetic compounds has been produced. Friedel-Crafts alkylation and transalkylation was carried out in the presence of both bronsted and lewis acid catalyst. Anhydrous aluminium chloride was preferred as a catalyst for the liquid phase alkylation reactions, although a co-catalyst or promoter like

hydrogen chloride is usually needed to obtain efficient results. In the vapor phase alkylation, phosphoric acid supported on keiselgurh (solid phosphoric acid) was reported as a commonly used catalyst.

Besides these catalysts, various other catalysts have also been employed for the alkylation and transalkylation reaction of hydrocarbons [Patkin and Friedmann, 1964]. These include lewis acids such as weak metal halides ($AlCl_3$, BF_3, $FeCl_3$, $TiCl_4$, $SnCl_4$ or $ZnCl_2$), protonic acids (bronsted acids such as HF, H_2SO_4) and inorganic acidic oxides such as phosphorous pentoxide on alumina. Unfortunately, many of these traditional Friedel-Crafts catalysts are in liquid phase which involve number of disadvantages like the process requires more amount of catalyst than stoichiometric amounts, due to the configuration of a complex between the product and the catalyst. Moreover, the hydrolysis of the catalyst leads to the loss of the catalyst. The use of these liquid catalysts imposes other limitations like handling, safety, equipment corrosion, toxicity, and waste disposal. Moreover, these catalysts do not meet the environmental protection and safety standards. Meanwhile, environmentally benign chemical production, has initiated efforts in green chemistry [Anastas and Warner, 2000]. As a possible solution, significant efforts have been made to eliminate the hazardous liquid acid catalyst with solid acid catalysts [Clarck, 2002; Gates, 2003]. Vast number of solid acid catalysts have been developed, which include metal halides and triflates [Olah and Molnar, 2003], clays [Balogh and Laszlo, 1993; Nikaljeet *et al*., 2000; Verma, 2002, Dasgupta and Torok, 2008], metal oxides [Ushikubo, 2000; Wachs *et al*., 2000; Hutchings *et al*., 2003], cationic resin sulfonic acids [Olah, 1964; Molnar, 2008], supported reagents [Mahajan and Ghatpande, 2005], heteropolyacids [Kozhevnikov, 2003; Misono, 2003], and zeolite [Janssens *et al*., 1997; Csicsery and Kiricsi, 2003]. The fundamental demand is to identify novel, recyclable, stable and environmentally safe catalysts which can replace the traditional liquid acids catalysts for industrial alkylation and transalkylation processes. From this perspective, zeolites are catalysts which offer numerous advantages over liquid acid catalysts [Chen, 1988; Chen and Degnan, 1988] as they are free from environmental and corrosion problems. Furthermore, the combination of acidity and shape selectivity in zeolite makes them potential catalysts for various alkylation and transalkylation reactions. Some of the important and interesting organic reactions can now be commercially practiced using solid zeolite catalysts which were not feasible earlier due to low activity, selectivity and stability of liquid catalysts.

1.2.1 Zeolite catalysts

1.2.1.1 Zeolite structure

Zeolites molecular sieves are similar to clay minerals in composition but they possess well defined three dimensional structures [Breck, 1974]. Zeolites are crystalline aluminosilicates and have an extensive three dimensional network of SiO_4 and AlO_4 tetrahedral building blocks. In each tetrahedra, silica and alumina are the tetrahedral central atoms (T atoms) while apical oxygen is shared with adjacent tetrahedra. Each tetrahedral atoms occupy four connected vertices of a three dimensional network and the oxygen occupy two connected positions between the four connected vertices [Lobo, 2003]. As the zeolites are derived from silicate type network structures, the oxygen to tetrahedral atom ratio in a zeolite structure is two [Lobo, 2003]. The O-T-O bond angle is close to the ideal tetrahedra bond angle of 109.5° and is less flexible than T-O-T bond angle which is usually around 140° to 165° [Lobo, 2003]. These tetrahedra are referred as the primary building units (PBU) of zeolite which join together to form secondary building units (SBU) by condensation. Such building units basically consist of n-ring structures which contain tetrahedra units. Secondary building units further interconnect with themselves to produce a wide range of tertiary building units or building polyhedral. These building units in turn are arranged in a three dimensional fashion to form extended characteristic frameworks of the various zeolite crystal structures (Figure 1.1). In these structural diagram the corners of polyhedra represent Si or Al atoms and the connecting lines show shared oxygen atoms.

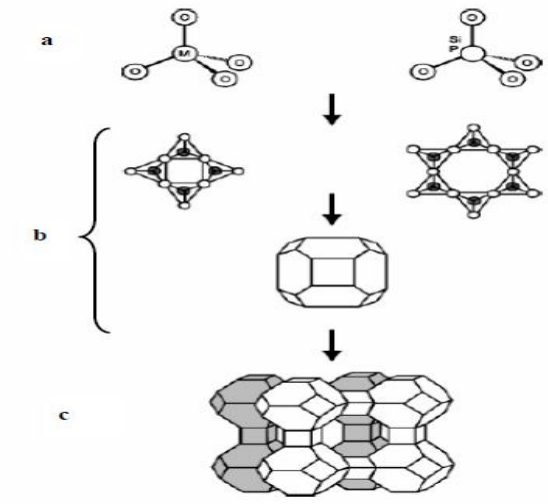

Figure 1.1: Primary, secondary and tertiary units in zeolite structure [Meier, 1996]

Zeolites are composed of channel and cavities of molecular dimensions ranging from 3-10 Å in diameter. The unit cell of the zeolites is represented by the following formula [Szostak, 1989]:

$$M_{x/n}[(AlO_2)_x(SiO_2)_y]\,zH_2O$$

The negative charge of the framework is same as the number of aluminium atoms and this charge is balanced by exchangeable charge compensating cations M of valency n. The most common cations include alkali metals (Na^+, K^+), alkaline earth metal (Ca^{2+}, Ba^{2+}) and other cations like NH_4^+ or H^+ [Breck, 1974]. The water molecules (z) present in the zeolites do not occur as a gas or liquid rather as clusters bonded to the zeolite wall. The water molecules in the zeolites have higher density than liquid water causing the motion of water molecules inside the intracrystalline volume different from that of liquid water. The value of x + y represents total number of tetrahedra in the unit cell of zeolite. In general, the ratio y/x is greater than 1, which controls the acidity, and to a lesser extent, the morphology of zeolites. These primary building blocks contain large vacant spaces (cages) that can accommodate cations (Na^+, K^+, Ba^{2+}, Ca^{2+}), as well as large molecules and cation groups (H_2O, NH_4^+). The cations are mobile throughout the structure and play a charge balancing role with the AlO_4^- tetrahedral. Further, it is interesting to observe that the charge balancing cations (Na^+, K^+, Ba^{2+}, Ca^{2+}), can be exchanged with other cations in aqueous solution, without affecting the aluminosilicate framework [Elliot and Zhang, 2005].

1.2.1.2 Zeolite Properties

Zeolites have numerous applications as catalysts due to some of their important properties which are listed below:

- Synthetic zeolites have uniform pores, well defined crystal structure and pure phase composition available in discrete sizes and having very large surface area ranging from 300-600 m^2/g.
- Owing to its high thermal stability, zeolites have gained much importance in catalytic reactions with high reaction temperature.
- Zeolite catalysts can be recovered and regenerated easily eliminating the catalyst disposal problems. Thus, they are environment friendly.
- Separation process is convenient and inexpensive, thus simplifying their repeated use.

- High concentration of active sites (acid sites), whose number and strength can be modified by ion exchange process in a wide range.

Apart from the above listed properties, zeolites have some very important properties such as acidity, ion exchange and adsorption properties which play very crucial role in determining their selectivity and activity as catalysts.

Acidity of zeolites

The catalytic activity of zeolite depends upon the acidity of the catalyst. The reactivity of zeolite is influenced by the active sites provided by the imbalance of the charge between aluminium and silicon ions in the framework. Thus, each aluminium ion represents an active site within the zeolite framework [Haag et al., 1984]. Both bronsted and lewis acidity are used to classify the active sites present in zeolite structure (Figure 1.2). Whenever a proton acts as a charge balancing cation for the anionic framework the bronsted acidity arises in the zeolite. Differences in acidic strength of different zeolites are often related to Al content of that zeolite, T-O-T bond angles, bond lengths, and crystal resonance energy [Szostak, 1989].

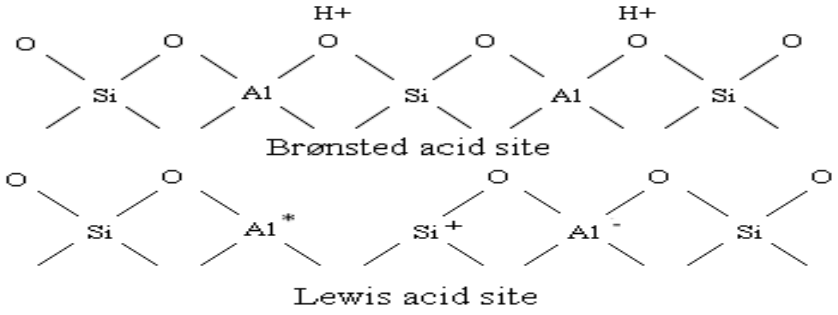

Figure 1.2: Acidic sites in zeolites [Barrer, 1982]

A trigonally co-ordinated aluminium atom, which acts as an electron acceptor, behaves as a lewis acid. It is observed that at higher temperature (>773 K) can result in the conversion of the bronsted acid sites to lewis acid sites by dehydroxylation [Anderson *et al*., 1980]. Hydrothermal treatment, which leads to dealumination of zeolites, also produces Lewis acids sites [Barthomeuf, 1977] thus inducing activity on nearby Bronsted acid sites.

Ion exchange properties

Zeolite frameworks are occupied by different types of ions such as sodium or potassium which can be readily exchanged with ions in the external solutions. These cations serve as counter ions to balance the negative charge which is generated by isomorphous substitution of tetravalent silicon atoms by trivalent aluminium atoms. These positively charged counter ions are very loosely held within the framework and are readily available for exchange with other ions in the contact solution. Thus, the cation exchange capacity (CEC) of the zeolites is usually very high and increases with aluminium content [Pless, 2005]. Barrer (1982) first reported that ion exchange of zeolite considerably affects their molecular sieving properties. The exchangeable cations in zeolite framework can be stoichiometrically exchanged with specific ions to enhance the sorption capacities of zeolites. Ion exchange process can simply be carried out by stirring a zeolite with the salt solution containing the cation to be exchanged at a particular temperature. Ion exchange can also be carried out via solid-solid reaction between the zeolite and the salt or oxide in hydrothermal conditions [Kucherov and Slinkin, 1986; Kucherov *et al*., 1989].

Adsorption properties

Due to highly porous structure, zeolites have high capacity to absorb guest molecules into the voids of the zeolite structure. Zeolite offers numerous applications based on adsorption properties for example drying and separation of mixtures etc. Due to adsorption properties zeolites are used in drying alcohols, benzene, natural gas, ethylene and methanol. It is also used for abatement of pollution etc. Removal of CO_2 from nitrogen rejection plants using 4A zeolite is an important industrial process.

1.2.2 Large pore zeolite as transalkylation catalyst

The uniformity in the pore structure of zeolite allows adsorption and separation of the diffusing molecule on the basis of molecular size and shape. This is known as molecular sieving. The zeolite properties can be altered by ion exchange which may facilitate the adsorption. The molecular shape-selective properties of zeolites make them pioneer among other catalysts. As usually bulky hydrocarbons are involved in transalkylation reactions, large pore zeolites are proved to be promising catalysts for selective transformation. In the last decade, several researchers have used different zeolite catalysts for various alkylation and

transalkylation reactions. Zeolites that possess 12 member ring pore aperture, such as beta, mordenite, USY and X are reported to be the potential catalysts for inter-conversion of alkylbenzenes. Though, many large pore zeolites are reported to transalkylate aromatics efficiently but the BEA and faujasite classes are of great interest as transalkylating catalysts. The structure, properties and applications of the two zeolites, namely beta and X zeolite, used in present study are discussed in the following sections.

1.2.2.1 Zeolite X

In 1784, a well known zeolite has been credited as "faujasite" in the honour of Barthelemy Faujas de Saint-Fond who formulated a nice formalism to identify zeolite. Faujasite (FAU) finds numerous applications in the petroleum industry as most gasoline is processed using faujasite-type zeolites which help in achieving high yield of gasoline and diesel fuel from crude oil. The acidic zeolite helps in catalytic cracking of petroleum residue to low molecular weight olefins and gasoline. It is one of the largest applications of FAU zeolites. Zeolite X belongs to the FAU (faujasite) family of zeolites and is representated as Na_{86} $[(AlO_2)_{86}(SiO_2)_{106}].H_2O$. Zeolite X has Si/Al ratio ranging from 1.25-1.5 and bears one of the largest cavities and entrances of any known zeolites [Szostak, 1989]. It has a three dimensional framework which comprises of sodalite cages connected through hexagonal prisms with pores running perpendicular to each other in x, y, and z planes. The secondary building units are 4-6, and 6-6 having a large pore diameter of 7.4 Å. The 4 and 6 membered rings are joined together to form sodalite cage. A typical sodalite or β cage has six-4 member rings and eight 6-member rings. These cages are connected to each other through 6-member ring. These sodalite cages (truncated octahedra) connected on their hexagonal faces form a central cavity or supercage or α cage (Figure 1.3). The supercage is composed of 18 four-member rings, 4 six-member rings and 4 twelve member rings. The unit cell of FAU has 192 tetrahedra which are arranged in sixteen 6 member rings, eight β cages and eight α cages. The unit cell of zeolite X is cubic (a=b=c=24.7 Å). The extraframework ion usually present in X zeolite is sodium ion. X zeolite has been extensively used in number of processes like for adsorption of various gases (CO_2, NO_2 etc), waste water treatment, as nucleophilic reagent, in catalytic cleavage of many bonds (C=N).

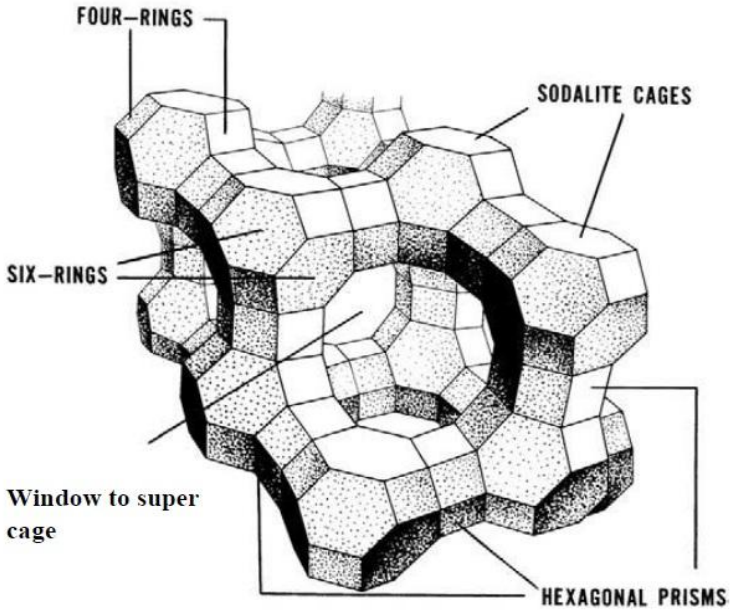

Figure 1.3: Structure of X zeolite [Qinhua andAizhen, 1990]

1.2.2.2 Zeolite beta

Zeolite beta was first synthesized by Wadlinger *et al*. (1967). It represents the first high silica zeolite (Si/Al = 10-100) synthesized from a gel with alkali metal and organic template, tetraethylammonium cations. Zeolite beta can be described by the general formula [Meier *et al*., 1996]:

$Na_n[Al_nSi_{64-n}O_{128}]$, where n = 7

The structure of zeolite beta was described by Treacy *et al*. (1996) and Higgins *et al*. (1998). Zeolite beta is an intergrowth hybrid of two distinct structures [Jansen *et al*., 1997] having tetragonal and monoclinic symmetry. These systems contain straight 12 membered-ring channels present in two crystallographic directions perpendicular to [001] having elliptical openings while the 12 membered-ring in the third direction is sinusoidal having circular openings (5.5 Å). The two polymorphs (polymorphs A and B) are different in the pore dimension of the straight channels. In the tetragonal system, the straight channels have openings of 6.0 x 7.3 Å, whereas in the monoclinic system they are 6.8 x 7.3 Å. Zeolite beta may be represented as shown in Figure 1.4.

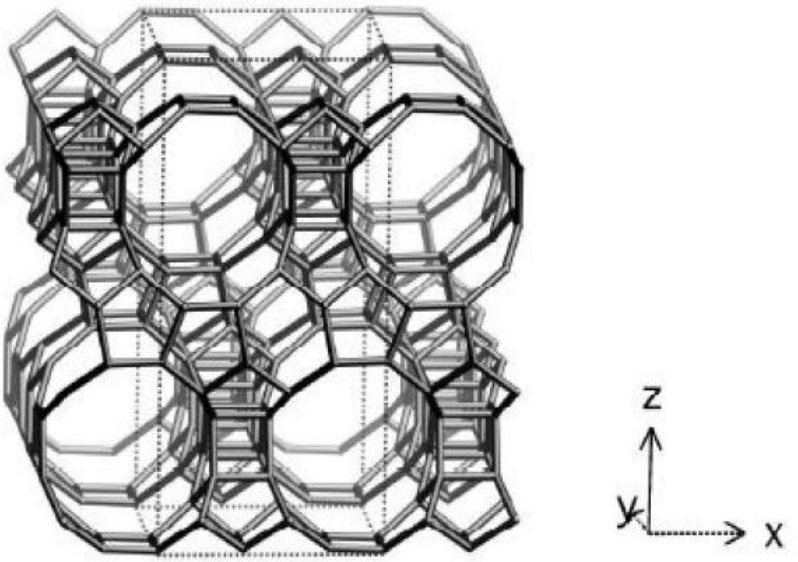

Figure 1.4: Three dimensional structure of beta zeolite [Jansen *et al.*, 1997]

Zeolite beta is a potential acid catalyst due to the presence of large intersecting pores in a highly siliceous framework. It possesses high thermal and acid treatment stability, high strength acidic sites and is hydrophobic in nature [Barrer, 1982].

The thesis is organized into eight chapters. In Chapter 1, a general introduction to transalkylation reactions with special reference to three transalkylation system chosen in the present thesis is provided. The commercial importance of the products and their conventional route of formation are given in the introduction section. A brief introduction for the catalysts including zeolites structure and properties are also introduced in this chapter. As large pore zeolites, NaX and beta zeolites are used as catalysts in present work, therefore, a brief description about both catalysts is included in the introduction chapter.

In Chapter 2, Literature review of transalkylation reaction of toluene with trimethylbenzene, transalkylation reaction of toluene with cumene and transalkylation reaction of benzene with diisopropylbenzene is cited. A comparison of vapor phase and liquid phase conditions for transalkylation reactions is made on basis of literature review. As rare earth metal ions modified zeolites were used as catalysts hence a brief literature on ion exchange in zeolites is also included in literature review. Justification of the present work and objectives set for the present work are listed in the current section.

Chapter 3 deals with materials and methods used in the present thesis. The methods used for modification of NaX and Hbeta zeolite are given. The experimental procedure and product analysis using GC details are also provided.

In Chapter 4, rare earth metal modified large pore zeolites were characterized using various characterization techniques. Different techniques used for characterization are Energy Dispersive Spectra, X-ray Diffraction, Scanning Electron Micrograph and Temperature Programmed Desorption of ammonia.

Chapter 5, 6 and 7 presents detail study on transalkylation of toluene with TMB, transalkylation of toluene with cumene and transalkylation of benzene with DIPB respectively. Rare earth metal modified NaX and Hbeta zeolites were used as catalysts for the transalkylation reactions. Effect of various reaction parameters like metal loading , metal content, catalyst loading, temperature, reactant ratio and space time were studied for all reaction systems. Kinetic models were proposed for the above said reaction systems which were used to carry out kinetic study of the reactions.

Chapter 8 deals with the conclusions drawn from each system and the future recommendations in the research area.

CHAPTER-2

Literature Review

In this present chapter, all the references related to transalkylation reactions are cited. Effort has been made to highlight the contribution of all the prominent researchers in this area of research.

2.1 TRANSALKYLATION REACTIONS

Alkylation and transalkylation are important class of reactions widely used in chemical and petrochemical industries. Due to increase in demand of mono or disubstituted alkyl aromatics transalkylation have attracted much attention in the industry. Transalkylation reactions have been extensively studied over various catalysts. In Friedel-Crafts alkylation reaction, aluminium chloride and hydrogen chloride react with the alkylating agent to form either a carbonium ion or a complex. The ion or complex then attacks the aromatic ring to form the specific product. The aromatic ring to which the olefin gets attached may be of benzene, substituted benzene or more complicated ring systems like naphthalene or anthracene. Another feature of Friedel-Crafts alkylation reaction is polyalkylation. Since alkyl group activate the aromatic ring towards further attack, there is a marked tendency for polysubstitution during the alkylation. This affects the yield of the monoalkylated product. It has been reported in the literature that alkyl group could be transferred from one aromatic ring to another by the catalytic effect. The transfer of alkyl group from one to another similar and dissimilar aromatic ring in the presence of an acid catalyst is known as dispropotionation and transalkylation reaction respectively. The following mechanism (Figure 2.1) was proposed for disproportionation of toluene over zeolites by Csicsery (1971) but it applies to transalkylation also:

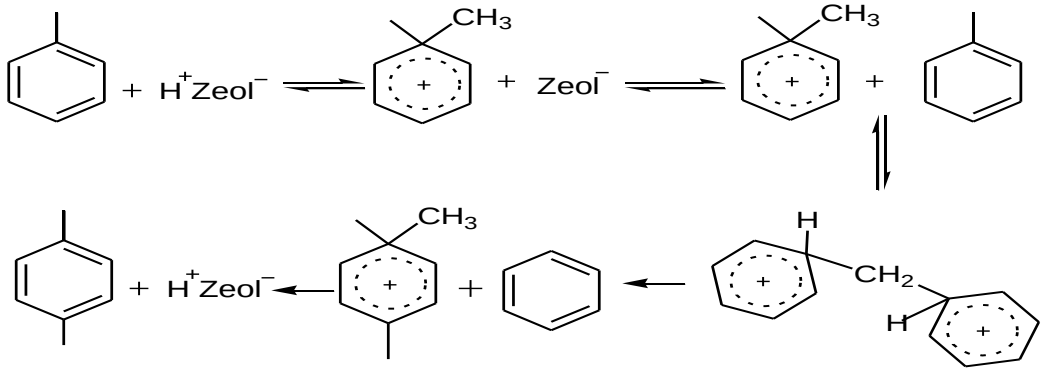

Figure 2.1: Proposed Mechanism of Dispropotionation/Transalkylation [Csicsery, 1971]

In the following sections, the literature on transalkylation of toluene to xylene, toluene to cymene and diisopropyl benzene to cumene, over zeolite catalyst are reviewed.

2.1.1 Transalkylation of trimethylbenzene with toluene

Alkylation of toluene with methanol is the traditional route for xylene synthesis under Friedel-Crafts reactions [Dumitriu *et al*., 2002; Borgna *et al*., 2004]. In the past decades, researchers have however reported studies on transalkylation of toluene with TMB for production of xylene with environmentally friendly catalysts including both unmodified and modified zeolites catalyst. Among the various zeolites used for toluene-TMB transalkylation reaction, beta, Y, SAPO-5 is found to be the promising catalyst. Beta zeolite showed a satisfactory performance as a catalyst for toluene-trimethylbenzene transalkylation due to the great stability of the zeolite (Wang and Tsai, 1990; Crejka and Krejcki, 2000; Hanika *et al*., 2003). Comparative studies have been done to compare the activities of various zeolites. Das *et al*. (1994) studied the transformation of commercial C_9 aromatic stream to xylene by transalkylation route over zeolite beta, mordenite and ZSM-5 catalyst. Crejka and Krejci (2001) investigated the impact of the channel geometry and architecture of large pore zeolites faujasite, beta and mordenite on the activity, selectivity and time-on-stream stability in trimethylbenzene transalkylation with toluene to xylenes. Krejci *et al*. (2010) compared the catalytic activity of three zeolites for toluene-trimethylbenzenes transalkylation. It was found that among the various zeolites chosen zeolite beta gave the highest yield and long-term stability of conversion to xylene due to its intercrossing channel system. Li *et al.* (2015) studied the effect of pore structure of different zeolites on product distribution for toluene-trimethylbenzene transalkylation. It was found that the reaction occurs with diphenylmethane intermediates. Medium-pore ZSM-5 shows low activity; whereas; large pore zeolites like BEA allows fast formation and movement of bulky species. SAPO-5 is also used extensively for toluene-trimethylbenzenes transalkylation (Hulea *et al*., 1997; Dumitriu *et al*., 2002).

Metal modified zeolites are also reported for toluene-TMB transalkylation reaction. Meshram *et al*. (1984) studied toluene-trimethylbenzene transalkylation over ZSM-5 and nickel modified ZSM-5 catalyst. It was found that incorporation of nickel ions prolonged the life of the catalyst. It was reported that transalkylation prevailed on external surface of the H-ZSM-5 whereas the disproportionation of toluene occurred inside the pore. Chao and Leu (1989) investigated transalkylation of toluene with 1,2,4TMB using NaHY zeolites at 460 °C and

400 °C in a fixed-bed continuous and pulse microreactor respectively. Dumitriu *et al*. (2002) carried out transalkylation of toluene with trimethylbenzenes over transition $MeSAPO_4$-5 (metal substituted $SAPO_4$-5) framework. The activity of catalyst was found to vary in the order of SiAPO>MgAPO>MnAPO>ZnAPO>CoAPO. It was found that the activity was directly related to the acidity of the zeolite catalyst which also influenced various reactions occurring during the toluene-TMB transalkylation. In general, transalkylation and disproportionation reaction predominated on strong acidic sites whereas isomerization occured on weak acid sites. Serra *et al*. (2005) examined the conversion of TMB under industrially relevant transalkylation conditions using different acid zeolite catalysts. These zeolites contain different type of channel systems comprising 10, 12 and 10+12 member ring pores. Different metals (Re, Pt, Mo, Ga, Ni, La, Bi) were used to impregnate the zeolites. It was found from these studies that the metal substituted $SAPO_4$-5 catalysts showed better results in terms of catalytic activity, life of catalyst, reactant conversion and product selectivity. Zeolite pore size, geometry, content and nature of metal ions were found to influence dealkylation and transalkylation reactions. Zeolites with intercrossing channels having dual member ring system showed high dealkylation and transalkylation activities.

Dealumination of zeolites is also reported to change the properties of the catalyst. Dumitriu *et al*. (1996) found that dealumination of Y zeolites make them effective catalyst for toluene-trimethylbenzene transalkylation. Degree of dealumination and coke content were found to have direct influence on product distribution. Lee *et al*. (1998) used large pore zeolites like Hbeta, H-mordenite and H-omega for toluene-trimethylbenzene transalkylation. All three catalysts were dealuminated and these dealuminated zeolites were applied as catalyst for transalkylation reactions. Hbeta and H-MOR showed high activity compared to H-omega inspite of its high acidity. The activity and stability of Hbeta decreased after delumination. Dealumination exposed some of the occluded acid sites and make a more open structure. All these changes compensate the loss of acidity and enhanced the activity and stability of H-MOR and H-omega. However, H-omega deactivated rather rapidly than H-MOR; hence, H-MOR was considered as the best acid catalyst among the three zeolites chosen for toluene-1,2,4-trimethylbenzene transalkylation.

Dual zeolite systems has also been used as catalyst for toluene and 1,2,4-trimethylbenzene transalkylation reaction. Aitani *et al*. (2010) investigated the production of various xylenes over H-mordenite, H-ZSM-5 and a dual catalyst consisiting ZSM-5 and mordenite in a riser-

simulator. They studied the effect of various factors like temperature, reaction time and feed composition on product distribution. It was found that at an optimum temperature of 400°C, maximum conversion (25%) of toluene was achieved with significant yield of benzene and xylenes. Wang *et al*. (2010) presented a study for the TMB conversion to xylenes over H-mordenite catalysts. They prepared a dual zeolite catalyst containing the mixture of mordenite and ZSM-5 catalysts and applied dual zeolite as a catalyst for the reaction. Effect of dual catalyst activity and various parameters on C_9 conversion and product distribution were studied. The dual catalyst was found to actively catalyze transalkylation reactions.

Mostly the reaction has been reported using continuous down flow packed bed reactor; however, reactions were also reported using rise simulator and fluidized bed. Khattaf *et al*. (2007) carried out 1,2,4-TMB-toluene transalkylation over USY-zeolite type catalyst in a riser simulator. TMB to toluene molar ratio was maintained at 1. The reaction was found to involve a number of processes like isomerisation and dispropotionation. The reactions were carried out at 400-500 °C. The effect of reaction conditions on the product selectivity was investigated. The experimental results were modeled using quasi-steady state approximation. Waziri *et al*. (2010) performed catalytic transformation of toluene and trimethylbenzene using two different zeolite catalysts (H-mordenite and H-ZSM-5) in a riser simulator. The experiments were performed at 300−400 °C and 5−20 s reaction times. Kinetic models were developed for different reactions involved in the system. Deactivation of the catalyst was modeled using decay function which was based on TOS (time-on-stream). The developed model showed predicted results which correlated with the experimental data. The apparent activation energy for the transalkylation reaction was higher over H-ZSM-5 than H-mordenite (i.e., $E_{app,(H\text{-}ZSM\text{-}5)} > E_{app,(H\text{-}Mordenite)}$). Ali *et al*. (2011) carried out the conversion of heavy reformate in fluidized bed reactor over MOR catalyst. It was found that dealkylation reaction occurs on high acidic sites while the dispropotionation reaction prevails over low acidic sites. Concentration of catalyst acidic site plays a significant role in transalkylation reaction. However, coke formation was favored at high concentation of acid sites. Khattaf *et al.* (2015) carried out toluene-TMB-TeMB transalkylation and found that xylene yield was maximum in toluene-TMB-TeMB system and least in case of dispropotionation of toluene. Kinetic modeling was done and it was found that toluene dispropotionation rate was slower that toluene-TMB transalkylation. A number of patents on the transalkylation of TMB with toluene have been reported in Table 2.1.

Table 2.1- Review of patents on transalkylation reaction of TMB with toluene

	Catalyst	Patent No	Patent Name	Refrences
1.	**Crystalline aluminosilicate**	US3527825	Transalkylation process	Ernest (1970)
2.	**Amorphous and crystalline aluminosilicate**	US3551509	Moving bed process using sieve catalyst to make xylene by toluene dispropotionation and transalkylation with C9-C10 alkylbenzene	Thaomas et al. (1970)
3.	**Mordenite zeolite**	US3677973	Transalkylation of alkylaromatic hydrocarbons in contact with zeolite catalyst composition	Mitche et al. (1972)
4.	**Mordenite zeolite**	US 3780122	Alkylaromatic transalkylation using alumina defecient mordenite	Ernest (1973)
5.	**Mordenite zeolite**	US4127283	Process of selectively hydrodealkylating/ transalkylating heavy reformate	Feinstein and Bertolacini (1979)
6.	**ZSM-35, ZSM-38 zeolite**	US4136128	Catalytic alkylation/ transalkylation	Haag and Olson (1979)
7.	**SSZ-26, SSZ-35, Al-SSZ-33 zeolite**	US5952536	Aromatics and toluene/TMB gas phase transalkylation process	Nacamuli et al. (1999)
8.	**Mordenite zeolite**	US6060417	Catalyst composition for transalkylation of alkylaromatic hydrocarbons and process of production of xylene	Kato et al. (2000)
9.	**Mordenite zeolite**	US6040490	Process of producing aromatic compound by dealkylation, transalkylation and dispropotionation	Ichioka et al. (2000)
10.	**MCM-22, PSH-3, SSZ-25, ZSM-12, and zeolite beta, ZSM-5**	US20050215839	Aromatics transalkylation to ethylbenzene and xylenes	Bogdan et al. (2005)
11.	**ZSM-5**	US20150073187	Toluene methylation with transalkylation of heavy aromatics	Ghosh et al. (2015)
12.	**ZSM, MCM**	US9249068	Process for production of xylenes	Tinger et al. (2016)

To sum up, the acitivity and selectivity of the catalyst was found to be increased by the incorporation of metal ions. It was found that the product distribution depend on the metal-ion content of metal modified zeolites and the composition of feedstocks. It was found that

low SiO_2:Al_2O_3 ratio, gave better rate of transalkylation reaction and hence xylene yield. The transalkylation reaction proceeds with good yields on dealumination of catalyst. Toluene acts as a controlling species in methyl group transfer in transalkylation.

2.1.2 Transalkylation of toluene with cumene

Initially, cymene production was carried out by toluene alkylation with propene or isopropanol using liquid acids but later on, the production process was replaced by transalkylation reactions using safer catalysts. The following literature is reported for cymene production by transalkylation reactions. Reddy *et al*. (1995) studied catalytic activity of beta zeolite for transalkylation of toluene with cumene and compared its activity with mordenite and ZSM-12. It was found that the selectivity of cymenes over zeolite beta was much better than mordenite and ZSM-12. This may be due to the fact that beta zeolite is highly siliceous and possess interconnecting channel system.

Bandyopadhyay *et al*. (1996) compared the catalytic activity of Hbeta, H-Y and H-ZSM-12 zeolites. Hbeta was proved to be a potential catalyst among these three catalysts. The optimum conditions for the highest selectivity of product transalkylation were found to be 473–493 K, 4.2 h^{-1} WHSV and high toluene to cumene ratio. They also compared toluene-cumene transalkylation reaction with toluene-diisopropylbenzene transalkylation reaction (Bandyopadhyay *et al*., 1998). They applied three large pore zeolites for the reactions. The activity and selectivity of Hbeta, H-Y and H-ZSM-12 were evaluated. It was found that large pore zeolites favor bimolecular pathway, and diphenylpropane intermediate is formed during the reaction. Hbeta was found to give better results than H-Y and H-ZSM-12 for the transalkylation reaction. It was observed that the catalytic performance of zeolites was related to their structural properties. They proposed following reaction mechanism for this transalkylation reaction.

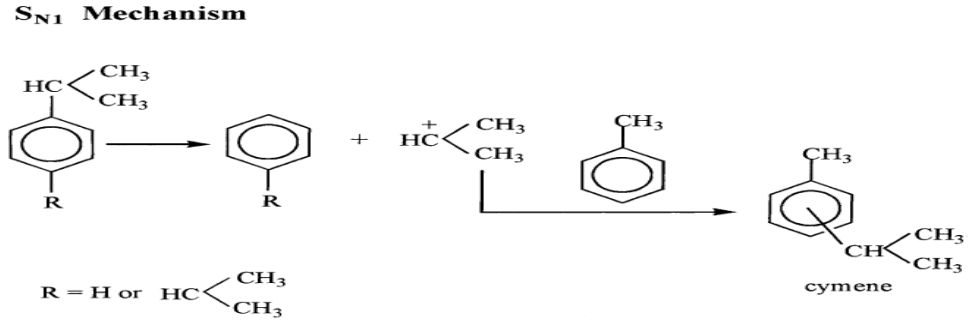

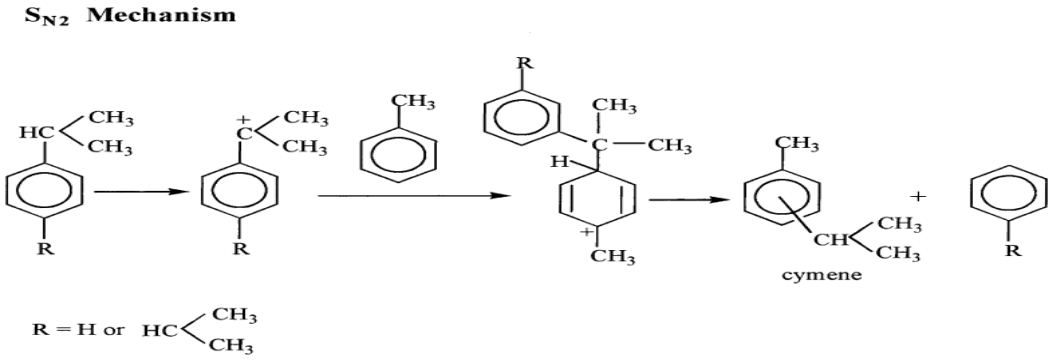

HY zeolite has been reported in both its parent and modified form as an catalyst for toluene-cumene transalkylation reactions. Mavrodinova *et al*. (2003) prepared indium modified HY and USY (ultra stable) zeolite. They investigated the effects of Lewis acid sites on the catalytic behavior of dealuminated HY zeolites. The modified zeolites were found to show superior catalytic activity than HY. Odedairo and Khattaf (2011) investigated gas-phase transalkylation of toluene with cumene at 200°C-300 °C and 5 to 20 s contact time under atmospheric conditions. They compared the catalytic activity over USY zeolite and a dual-zeolite comprising ZSM-5 and mordenite. The dual-zeolite catalyst showed better selectivity than USY catalyst. Cumene was found to show much higher reactivity compared with toluene.

To conclude, the USY zeolite and dual zeolite based catalyst show higher activity than the parent zeolite; however, dual zeolite based catalyst show better results between the two catalysts. Large pore zeolites favor bimolecular pathway and diphenylpropane type intermediate is formed during the reaction. Different activities of various zeolite may be attributed to their structural and acidic properties.

2.1.3 Transalkylation of DIPB with benzene

Production of cumene through benzene-diisopropylbenzene transalkylation has been studied over various catalysts. Variation of different reaction parameters and their effects on DIPB conversion and cumene selectivity are reported in many studies. Conventionally, cumene is produced by isopropylation of benzene. However, DIPB isomers are produced as by-product during isopropylation of benzene to cumene. This DIPB can be converted to cumene by transalkylation with benzene.

Comparative studies have revealed that large pore zeolites are best among various zeolites used for transalkylation studies. Liquid phase benzene-DIPB transalkylation was performed

over large pore zeolites (H-mordenite, La-HY and Hbeta) at 170-210 °C. They carried out the reaction in both atmospheric and high pressure condition (25 kg/cm^2). Effect of zeolite structure and various parameters were studied for these reactions. Zeolite beta was observed to be a very active and selective catalyst for transalkylation reactions (Pradhan and Rao, 1993). Sotelo *et al*. (2006) investigated the effect of supercritical CO_2 on DIPB-benzene transalkylation over different catalysts such as beta, Y and mordenite with different aluminum contents. However, the results showed that the use of supercritical CO_2 did not result in any superior catalytic activity for the Y zeolite. On the other side, a significant product yield was obtained over beta and mordenite zeolites. Yang *et al*. (2010) compared the activity of hierarchical beta zeolite with conventional beta zeolite for DIPB-benzene transalkylation. They prepared hierarchical beta zeolite by the dry gel conversion method. The results indicated that DIPB conversion decreased from 74% to 29% after a reaction time of 32 h over the conventional beta zeolite while, DIPB conversion remains above 60% after 32 h for the hierarchical beta zeolite, under the same reaction conditions. The two zeolites differ in their pore structure, crystal size and acidity. The results revealed that the hierarchical beta zeolite was superior due to the presence of meso/macropores.

Modified large pore Y zeolite has been extensively used for cumene production by benzene transalkylation. Ca^{2+} and RE^{3+} impregnated Y zeolite has been applied both for alkylation and transalkylation for the production of cumene. It was reported that combining alkylation reaction along with transalkylation reaction gives better result for maximizing the product yield (Mirzabekova *et al*., 1977). Lishchiner *et al*. (1983) studied the effect of acidity on activity of impregnated LaCaNiY zeolite catalyst for benzene alkylation by propene and its transalkylation by DIPB. They investigated the stability of metal impregnated zeolite by time-on-stream study and found that catalyst deactivated after 3 h time on stream and thereafter, the formation of cumene declined. However, it was reported that when propene was admitted to the deactivated catalyst, the activity was greatly restored increasing the rate of formation of cumene. This showed that reaction of aromatics proceeds in the active centers of catalytic surface. Bozga *et al*. (2001) presented a study of DIPB transalkylation on a Ca^{2+} modified Y type zeolite. The calcium modified Y zeolite exhibits good activity and selectivity for the diisopropylbenzene transalkylation with benzene. Kinetic model such as Langmuir-Hinshelwood, Eley Rideal and classical power law model were derived following

the reaction scheme. Experimental data was fitted with LHHW model in which the experimental conversion and predicted conversion had a good correlation.

Kaeding and Hollard (1988) and Marvec *et al*. (1992) reported the use of H-ZSM-5 zeolite for transalkylation of benzene with DIPB for cumene production. It was reported that best cumene yield was reported at reaction temperatures ranging from 225-300 °C. It was found that silica to alumina ratio plays a very crucial role in product distribution of transalkylation reactions. H-ZSM-5 zeolite with molar ratio SiO_2/Al_2O_3 of 20 was found to be the best catalyst for the above reaction.

Maity *et al*. (2006) carried out transalkylation reaction of benzene with DIPB over H-MOR catalyst in a fixed-bed laboratory scale reactor. Various process parameters such as temperature, space-time, and benzene/DIPB mole ratio were found to have effect on DIPB conversion. The conversion increased with increase in benzene/DIPB ratio and temperature but higher temperature beyond 513 K lead to secondary reactions with the formation of *n*-Propyl benzene. The selectivity of cumene increases with decrease in space-time and reactor temperature. Kondamudi and Upadhyayula (2008) studied transalkylation of DIPB with benzene over SAPO-5 catalyst and Pt-SAPO-5 catalysts. It was reported that high mole ratio of benzene to DIPB and high space velocities resulted in high cumene selectivity. Platinum modified SAPO-5 showed promising good results in terms of activity and stability. The apparent activation energy and the frequency factor (*A*o) was found to be 130.2 $kJmol^{-1}$ and 1.1×10^{13} respectively. The reaction followed LHHW dual site mechanism which predicted the reaction rate with a standard error estimate of $\pm 3.3 \times 10^{-6}$ for the rate of disappearance of DIPB. Pathak *et al.* (2011) optimize conventional and reactive distillation processes for cumene production. Reactive distillation process due to process integration was found to be more significant than conventional process. Selectivity of reactive distillation process was also better than conventional process and thus appeared to be more promising than the conventional process. Zhixi *et al.* (2015) modified MCM-48 with aluminium and titanium using hydrothermal method. The active sites, which are introduced in the zeolite framework by aluminum and titanium atoms, are utilized for catalytic reaction due to the presence of mesopores in Al-MCM-48 and Ti-MCM-48.

A number of patents on transalkylation of DIPB with benzene over various zeolites have been reported in Table 2.2.

Table 2.2- Review of patents on reaction between DIPB with benzene

	Catalyst	Patent No:	Patent name:	References
1.	**Y, Mg-Y zeolite**	US3385906	Production of cumene	Kauffman (1968)
2.	**Beta zeolite**	US4891458	Liquid phase alkylation and transalkylation process over zeo beta	Innens *et al* . (1990)
3.	**Y zeolite**	US5036033	Alkylation catalyst and processes for preparing cumene	West and Abdo (1991)
4.	**Beta , Y zeolite**	US5081323	Liquid phase alkylation and transalkylation process using zeolite beta	Innens *et al* . (1992)
5.	**Beta zeolite**	EP0538518A1	An improved process for the production of cumene	Rao (1993)
6.	**MCM-49 zeolite**	US5371310	Process for preparing short chain alkyl aromatic compounds	Bennet *et al.* (1994)
7.	**Beta zeolite**	US5600050	Zeolite catalyst for the liquid phase alkylation and transalkylation of benzene	Huang *et al.* (1997, b)
8.	**MCM-22 zeolite**	US5902917	Alkylaromatics production	Collins *et al*. (1999)
9.	**Y, Beta, ZSM-5, MCM-22, MCM-36, MCM-49, MCM-56 zeolite**	US6339179	Production of alkyl aromatics by passing transalkylation effluent to alkylation zone and to product recovery zone	Schulz *et al*. (2002)
10.	**Beta, Mor, Y Zeolite**	US6936744	Alkylaromatics production	Cheng *et al*. (2005)
11.	**X, Y, Mor, FAU, UZM-8, MCM-22, MCM-36, MCM-49**	US20080293986	Process for producing cumene	Schultz *et al*. (2008)
12.	**LZ-210 zeolite**	US20080171901	Aromatic transalkylation using LZ-210 zeolite	Jan *et al*. (2008,a)
13.	**Y-85 zeolite**	US20080171902	Aromatic transalkylation using Y-85 Zeolite	Jan *et al*., (2008,b)
14.	**Beta zeolite**	US7371910	Process for benzene alkylation and transalkylation of polyalkylated aromatics over improved zeolite beta catalyst	Cheun *et al*. (2008)
15.	**Beta , Y zeolite**	US20100292519	Aromatic alkylation process with reduced byproduct formation	Patrick *et al.* (2010)
16.	**MCM-22, MCM-36 zeolite**	US7951986	Process and catalyst for the transalkylation of aromatics	Clark *et al*. (2011)
17.	**ZSM, BEA, Y, MOR, MCM**	US20150183695	Process for producing cumene	Hwang *et al.* (2015)

To recapitulate, all the studies presented in literature for transalkylation of benzene with DIPB shows that large pore zeolite are effective for this reaction. Metal ion exchanged zeolites (Ca, La, Ni, Pt) gave better results in terms of conversion or selectivity than parent zeolite. Increase in temperature upto certain level improve conversion but further increase in temperature may cause many side reactions. Higher Benzene/DIPB ratio leads to higher yield of cumene.

2.2 VAPOR AND LIQUID PHASE TRANSALKYLATION

Transalkylation reactions can be carried out in both liquid and vapor phase. However, at relatively low temperature, liquid phase processes impose increased requirements of catalyst particularly in transalkylation reactions where the bulky polyalkylated species must be converted to additional monoalkylated product without producing unwanted by-products. This leads to a significant problem in case of transalkylation reactions [Clark *et al*., 2002].

Transalkylation reactions in liquid and vapor phase have been reported over a number of zeolites by different researchers. For example, in case of transalkylation of DIPB with benzene the equilibrium conversion of DIPB is 57% at lower temperature i.e. in liquid phase conditions (127 °C) and 65% at higher temperature i.e. in vapor phase conditions (527 °C) [Bozga *et al*., 2001]. Cheng *et al*. (2005) has reported 55% conversion under liquid phase conditions. The product yield is found to be increased in case of vapor phase reactions.

In the literature, higher conversion of reactant is reported in vapor phase conditions as compared to liquid phase reactions. Also, for liquid phase reactions high pressure (20-40 atm) operation is reported, whereas, vapor phase reactions were generally performed at atmospheric pressure. The following table 2.3 contains literature showing effect of parameters on reactant conversion and product yield.

Table 2.3- Comparison of liquid and vapour phase reactions

Sr. No	**Reaction**	**Zeolite**	**T (ºC)**	**P (atm)**	**Conversion of reactant / yield of product**	**Phase**	**Worker**
1.	**DIPB + BENZENE**	Y	130-250	10-20	C-83% Y-48%	Liquid	Kauffman (1968)
2.	**DIPB + BENZENE**	LaCaNiY	100	30	C – 30%	Liquid	Lishchiner *et al*. (1983)
4.	**DIPB + BENZENE**	Beta	121-232	20-40	Y- 24.5%	Liquid	Innens *et al*. (1990)
5.	**DIPB + BENZENE**	Y	37-315	20-40	Y- 19.2%	Liquid	Innens *et al*. (1992)
6.	**DIPB + BENZENE**	CaY	240	40 bar	C-24% Y-62%	Liquid	Bozga *et al*. (2001)
7.	**DIPB + BENZENE**	Beta	100-200	29	C-66%	Liquid	Cheng *et al*. (2005)
8.	**DIPB + BENZENE**	H-Mor	220-300	1	C-20%	Vapor	Maity *et al*., (2006)
9.	**DIPB + BENZENE**	SAPO-5	250	1	C-93%	Vapor	Kondamudi and Upadhyauy-ula (2008)
10.	**TMB + TOLUENE**	Faujasite	510	1.5	C- 57%	Vapor	Thomas *et al*. (1970)
11.	**TMB + TOLUENE**	Mordenite	420	35	C- 57%	Liquid	Mitche *et al*. (1972)
12.	**TMB + TOLUENE**	ZSM-35, ZSM-38	427	1	C-23%	Vapor	Haag and Olson (1979)
13.	**TMB + TOLUENE**	Na-H-Y	270-460	1	C- 65%	Vapor	Chao and leu (1989)
14.	**TMB + TOLUENE**	Beta	350	1	C- 70%	Vapor	Wang *et al*. (1990)
15.	**TMB + TOLUENE**	Beta, mordenite, omega	400	1	C- 68%	Vapor	Lee *et al*. (1998)
16.	**TMB + TOLUENE**	SSZ-35	287-482	200	C- 25%	Liquid	Nacamuli *et al*. (1999)
17.	**TMB + TOLUENE**	SSZ-35		400	C- 37%	Vapor	Nacamuli *et al*. (1999)
18.	**TMB + TOLUENE**	USY	250	1	C- 40%	Vapor	Khattaf *et al*. (2007)
19.	**TMB + TOLUENE**	ZSM-5, mordenite	400	1	C-59%	Vapor	Aitani *et al*. (2010)
20.	**TMB + TOLUENE**	Beta, mordenite, omega	300-450	1	C-52%	Vapor	Krejci *et al*. (2010)

2.3 ION EXCHANGE IN ZEOLITES

The most important technique used to modify zeolite is ion exchange. Metals ions belonging to groups like alkali and alkaline earth, transition, rare earth elements are often regarded as promoters for zeolite catalysts [Rahimi and Karimzadeh, 2011]. Modification by metal ions is reported to enhance the activity, selectivity and stability of zeolites. Metal modified zeolites are applied for a number of chemical reactions like hydrocarbon cracking [Lee *et al*., 2014], hydrocracking [Simon and Guillon, 2011; Park *et al*., 2013], ring opening [Kubicka *et al*., 2004], oxydehydrogenation [Nowinska *et al*., 2003], isomerisation reaction [Canizares *et al*., 2000; Villegas *et al*., 2006; Cheng *et al*., 2013; Arvela *et al*., 2013], transesterification [Srilatha *et al*., 2012], alkylation [Faramawy *et al*., 1999; Huang *et al*., 2007; Emana *et al*., 2015]. Metal modified zeolites are also extensively used for transalkylation reactions [Pradhan and Rao, 1993; Bozga *et al*., 2001; Kondamudi and Upadhyayula, 2008; Dumitriu *et al*., 2002; Serra *et al*., 2005; Kauffman *et al*., 1968].

To summarise, the product distribution of transalkylation reactions was found to be dependent on the catalyst chosen and its properties. Zeolite catalysts are found to possess high activity and selectivity for the transalkylation reactions which can further be enhanced by the incorporation of metal ions in the zeolite. Ion exchange technique is the most common method to modify zeolites. Metal modified zeolites have been extensively used for transalkylation reactions. Metal-ion type content of ion in zeolites and the feedstock composition were found to effect the product distribution of the transalkylation reactions. Large pore zeolite, low SiO_2:Al_2O_3 ratio, dealumination of catalyst, dual zeolite based catalyst gave better rate of transalkylation reaction and hence product yield. Reaction conditions like temperature, pressure, reactant ratio and space time play a crucial role in overall product distribution. It was found that increase in temperature leads to better conversion but after a certain temperature many side reactions may occur. Vapor phase conditions gave better reactant conversions and yields in comparison to liquid phase reactions.

2.4 JUSTIFICATION OF THE PRESENT WORK

Transalkylation reactions are of great importance in the chemical and petrochemical industries. These reactions are performed to convert low valued hydrocarbon to commercially important petrochemical products. Therefore, in past few decades these reactions have gained

attention on industrial scale. Development of effective catalyst is a key objective in this study and thus achieving high yield and selectivity of the product. From the thorough study of literature it has been seen that large pore zeolites are the potential catalysts for transalkylation reactions. Moreover, the metal ion exchange of parent zeolites leads to higher activity of the catalysts. Many metal ions exchanged zeolites have been applied for transalkylation reactions in the literature. The metal ions usually belong to alkali, alkaline and transition series. Use of rare earth metal ions modified zeolites for transalkylation reactions have not been explored much in the literature. It is seen that scarce literature is available on the use of rare earth metal ions (cerium, lanthanum and paraseodymium) modified Na-X and beta zeolites on the three reaction systems mentioned in section 1.1. Although, beta zeolite has been extensively studied for transalkylation reactions yet rare earth metal ions modified beta zeolite needs to be studied thoroughly. On the other hand, catalytic activity of NaX zeolite for catalyzing these reactions is very scarcely studied. The process of transalkylation undergoes a complex reaction scheme. For maximizing product selectivity and yield suitable catalysts of higher activity were focused to develop in the present investigation. The investigation of reaction mechanism and information of kinetic data may be helpful in further designing of reactor. A reaction rate model developed may be useful for scale up of reactor in industry for large scale production.

2.5 OBJECTIVES

The following objectives have been set for the proposed work:

(i) To modify and characterize the large pore (7-10 Å) zeolite modified with some rare earth metal ions.

(ii) To use these catalysts for transalkylation of toluene with TMB to produce xylene, and transalkylation of toluene with cumene to produce cymene, and similar reactions.

(iii) To study the kinetics and carry out parametric studies on these reactions.

(iv) To propose a suitable kinetic model for each reaction and carry out parametric estimation.

CHAPTER-3

Materials and Methods

This chapter presents a detailed description of the materials used, catalyst modification, catalyst characterization techniques, reactor system and experimental procedure for transalkylation reaction.

3.1 MATERIALS AND REAGENTS

Hbeta zeolite was obtained from Sud Chemie India Pvt. Ltd., Vadodra, Gujrat. It was in the form of extrudates (1.5 mm) having SiO_2/Al_2O_3 ratio 12.5 and surface area 633 m^2/g. NaX zeolite having surface area of 478 m^2/g and SiO_2/Al_2O_3 ratio 1.5 was procured from Fresia Chemicals, Mumbai, India.

All the chemicals used in the present study were of analytical reagent grade. Ceric ammonium nitrate (99% pure), Praseodymium ammonium nitrate (99% pure) and Lanthanum ammonium nitrate (99% pure), ammonium nitrate (99% pure) was procured from CDH Chemicals, India. Toluene was purchased from (> 99% pure) from M/s Merck, India. Benzene (> 99% pure), 1,4 DIPB(> 99% pure), cumene (> 99% pure), trimethylbenzene (> 99% pure) was obtained from Sigma Aldrich Pvt. Ltd., India. Nitrogen gas (used as carrier gas for experiments and GC analysis) of grade–I (99.999% pure), hydrogen gas of grade–I (99.999% pure), and helium gas of grade–I (99.999% pure), were obtained from Sigma gases and Services, India.

3.2 CATALYST MODIFICATION

Commercially available zeolites catalysts (Hbeta and NaX) were modified with rare earth metals such as lanthanum, cerium and praseodymium and used for the transalkylation reactions. The catalyst modification procedures are presented in the following sections.

3.2.1 Modification of NaX zeolite

The commercially available NaX zeolite was modified by exchanging its sodium ions with rare earth metal ions. The acidity was found to increase with the level of replacement of charge balancing cations [Ward and Hansford, 1969]. The underlying principle is to exchange cations by ammonium ions and then generate the hydrogen form (which is acidic form of zeolite) by thermal decomposition.

$$NaX + NH_4^+ \rightarrow NH_4X + Na^+ \xrightarrow{Heat} HX$$

where, X denotes zeolite. A convenient procedure is to reflux the zeolite with an aqueous ammonium salt solution for several hours. The zeolite is then filtered and washed to remove free excess of ammonium ions and displaced sodium ions. Higher degree of ion exchange can be obtained by repeating this batch exchange treatments. Cations that can be substituted for sodium cannot be introduced directly. This is due to high sensitivity of zeolite framework to the low pH value which may cause structural collapse of zeolite. For NaX zeolite, the critical pH is in the range of < 4.0. The calcination of NaX zeolite was done at 623 K for 3 h to remove moisture. The zeolite catalyst was then heated with 2% NH_4NO_3 solution at 363$\pm$10 K for 6 h, for three times; with subsequent calcining of the particles in between at 623 K. The sodium form of zeolite was thus converted to its protonic form (HX). The catalyst particles obtained after 18 h was boiled with a required percentage of rare earth ammonium nitrate solution for16 h which modified the HX zeolite [Plank *et al*., 1964]. This catalyst was then dried and calcined at 623 K and was kept for use in transalkylation reactions.

3.2.2 Modification of Hbeta zeolite

The commercially available Hbeta zeolite was modified by exchanging the H^+ ions with rare earth metal ions. At first, the zeolite extrudates were calcined for 3 h at 623 K. Calcined zeolite was then refluxed with required percentage of rare earth metal ammonium nitrate solution at 363 K for 24 h, thereby modifying Hbeta zeolite into rare earth metal ion beta form. The catalyst particles were then filtered and washed several times with deionized water and then dried at 393 K for 14 h. Finally, it was calcined for 4 h at 723 K to remove the excess ions. The apparatus used for carrying out refluxing is shown in Figure 3.1

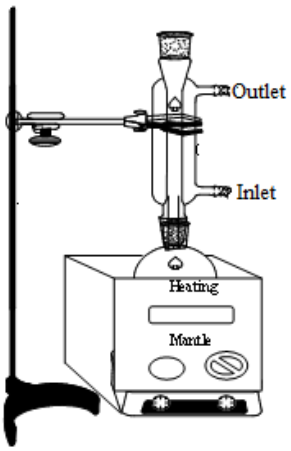

Figure 3.1: Refluxing apparatus setup for modification of zeolite

3.3 EXPERIMENTAL PROCEDURE

Vapor phase transalkylation reaction was carried out in a fixed-bed, continuous down-flow, stainless steel (SS 316) reactor. The reaction was carried out at atmospheric pressure. The reactor is equipped with a preheater in the upstream and a condenser in the downstream. The reaction temperature was measured using a thermowell extending from the top of the reactor to the centre of the bed. For, a typical kinetic run, 2 g of the catalyst supported on a wire mesh was loaded into the reactor. Before conducting the experiments, catalyst activation was done at a temperature 100 K higher than the reaction temperature (maintained according to reaction conditions), for 3 h under the nitrogen atmosphere. A dosing pump was used to introduce the reactant feed mixture into the reactor. Nitrogen gas was passed through the reactor at the rate of 0.565 l/h to activate the catalyst before the experimental run. During all experimental runs, nitrogen to feed flow ratio was kept constant at 0.2. The liquid feed vaporized in the preheater which was maintained at a temperature 30 K lower than the reaction temperature. The vaporized reactant feed mixture then passes through the catalyst bed in the reactor at proper reaction conditions. The effluent was condensed in the condenser maintained at 277-279 K. The liquid samples were collected and analyzed by using GC. The schematic of the experimental set up is represented in Figure 3.2.

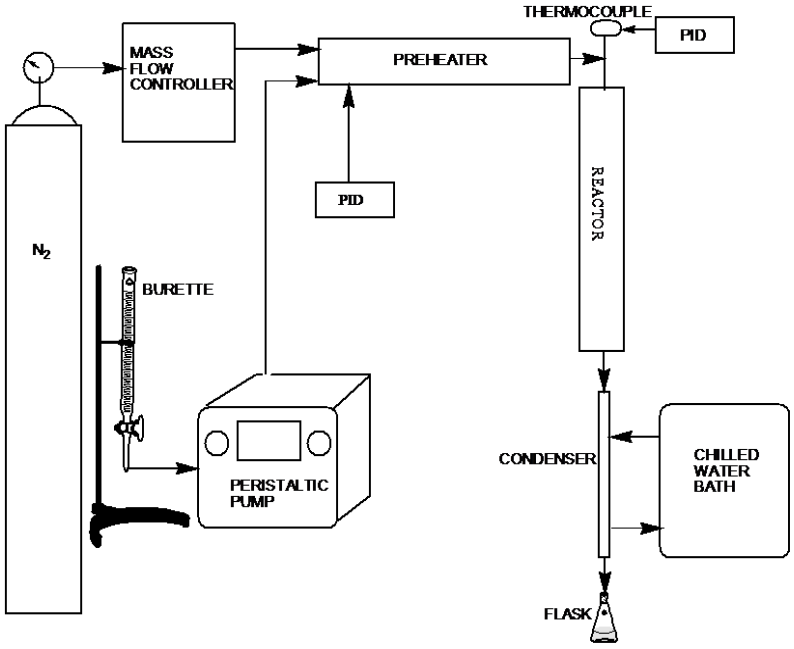

Figure 3.2: Schematic representation of reactor set up

3.4 PRODUCT ANALYSIS

GAS CHROMATOGRAPHY

The product samples were analyzed in a gas chromatograph (Bruker, Model: 436 GC Scion) using a fused silica capillary column having 10 m×0.53 mm×1.5 µm dimensions. The sample was introduced through a micro syringe. The temperature of injector was set at 230 °C during the analysis. The column temperature was initially set at 50 °C, and then increased to 250 °C at a rate of 10 °C /min. The flow rate of carrier gas (nitrogen) was maintained at 25 ml/min. A flame ionisation detector was used at 270 °C. Peaks were identified by matching the retention time with known standards.

3.5 CHARACTERIZATION TECHNIQUES

3.5.1 Energy Dispersive Spectra

The elemental compositions of small objects or surfaces are determined by EDS. The EDS works by detecting X-rays that are produced by a sample. The sample is placed in the path of an electric beam. The electric beam interacts with the sample exciting the atoms in the sample which produces X-rays to discharge the excess energy. The energy of the X-ray produced reflects the characteristic of the atoms of the sample and peaks are formed in the spectrum. A single element may have one or more peaks associated with them. EDS spectrum can be collected from a specific point on the sample which gives an analysis of a few cubic microns of the material. EDS is usually carried out in conjunction with a scanning electron microscope (SEM).

3.5.2 X-ray Diffraction

X-ray diffraction provides the characterization of the structure of a solid sample. It is commonly employed to identify the presence of amorphous or crystalline phases in the sample. Moreover, it is also used to determine the amount of crystalline sample present quantitavely. It helps in determining the unit cell parameters of the sample. This characterization technique is based on the elastic scattering theory. Powder XRD measurements use CuKα radiations to determine the crystallinity of the sample. The sample is subjected to an X-ray beam and the intensity of the emergent rays is recorded as a function of the deflection angle.

As zeolite materials are crystalline solids, they have a characteristic diffraction pattern used for identifying the structure and crystallinity of the sample. The X-ray diffractions produce a scattering pattern particular for the periodic arrangement of atoms or ions. Each zeolite has specific diffraction pattern used as reference for the determination of crystal phase and as a fingerprint. The principal equation used in the analysis of an X-ray powder pattern is the Bragg law :

$$n\lambda = 2\, dhkl \sin\theta \qquad (1)$$

where *n* is the order of diffraction ($n = 1, 2,\ldots$), θ is the Bragg angle between the incident Xray beam and the crystal planes, λ is the wavelength of the incident X-ray beam (λ= 1.54178 Å for Cu Kα) and *dhkl* is the interplanar distance on a set of planes.

Degree of crystallinity % = Peak Intensity of zeolite sample at peak 2θ / Peak intensity of reference sample at peak 2θ (2)

The powder X-ray diffraction patterns of the zeolite samples were recorded on a Bruker Angle X-Ray Scattering, Diffractometer D8, Germany with 2θ value in the range of 5°-60° at a scanning speed of 2° (2θ) per minute. The diffractometer was equipped with Ni-filtered Cu K-α radiation source. Sample preparation for the X-ray analysis involved grinding of the sample into a fine powder and placing 0.1-0.2 g of the sample into sample holder with light compression to make it flat and tight.

3.5.3 Scanning Electron microscopy

SEM is used to determine the morphology and crystal size of the sample. SEM consists of an electron gun, electron lenses, scan coils and detectors. A beam of electron is generated by the electron gun from a cathode or filament usually made of tungsten which escapes at high voltage from the filament. The electron lenses are use to control the final size of the beam. The electron beam is scanned over the sample or target with the help of scan coil. When the electrons hit the target, they collide with electrons in the inner atomic shells. Back scattered and secondary electrons that escape from the sample are detected. If there is no detection, the image will be black [Ohrman, 2000].

Scanning electron microscopy coupled with energy dispersive X-ray spectrometry was performed on JEOL JSM 6510LV instrument. For analysis, initially sample was

ultrasonicated in ethanol for required time. A drop of this suspension was put on a sample holder with the help of carbon tape. The sample was then coated with gold and visualized with instrument to assess the particle morphology.

3.5.4 Brunauer-Emmett-Teller (BET) surface area

This method was given by Stephen Brunauer, Paul Hugh Emmett, and Edward Teller in 1938. BET theory explains the phenomenon of physical adsorption of gas molecules on a solid surface. This theory serves as the basis for an important characterization technique for the measurement of the specific surface area of a material. The BET equation is expressed by

$$\frac{1}{X[(P_0/P)-1]} = \frac{1}{X_m C} + \frac{C-1}{X_m C}\left(\frac{P}{P_0}\right) \quad (3)$$

Where, P and P_0 are equilibrium and saturation pressure of adsorbates, X is the adsorbed gas quantity, and Xm is the monolayer adsorbed gas quantity, C is the BET constant, which is given by,

$$C = \exp\left(\frac{E_1 - E_L}{RT}\right) \quad (4)$$

E_1 and E_L are heat of adsorption for the first and higher layers respectively. This equation is an adsorption isotherm and can be plotted as a straight line with $1/X\,[(P_0/P) - 1]$ on the y-axis and P/P_0 on the x-axis according to experimental results.

The surface area of the catalysts was determined by BET method using micromeritics tristar - 3000 surface area analyzer. Prior to ananlysis, degassing of the samples were done at 473K for 2h under a nitrogen atmosphere to remove the physisorbed moisture from the catalysts.

3.5.5 Temperature Programmed Desorption of Ammonia

The temperature programmed ammonia desorption (TPD) was used to study the total surface acidity and the acid strength of the acidic zeolite catalysts. The temperature of the furnace was monitored by a multi-program contoller. Thermal conductivity detector was used to measure the desorbed ammonia. The NH_3-TPD thermogram profile obtained quantiitatively showed the amount of ammonia desorbed at increasing temperature intervals which corresponds to the distribution of acid strengths of the total surface acidity. The thermograms of the zeolites usually give two peaks at low and high temperatures (Figure 3.3). The

intensity of the high temperature desorption peak is related to the ammonia desorption from high acidic sites whereas the peak at low temperature characterized the desorption from weak acid sites [Tao *et al*., 1996; Camiloti *et al.*, 1999]. Physisorption occurs at low temperature whereas at higher region chemisorbtion prevails [Bagnasco, 1996, Hedge *et al.*, 1989].

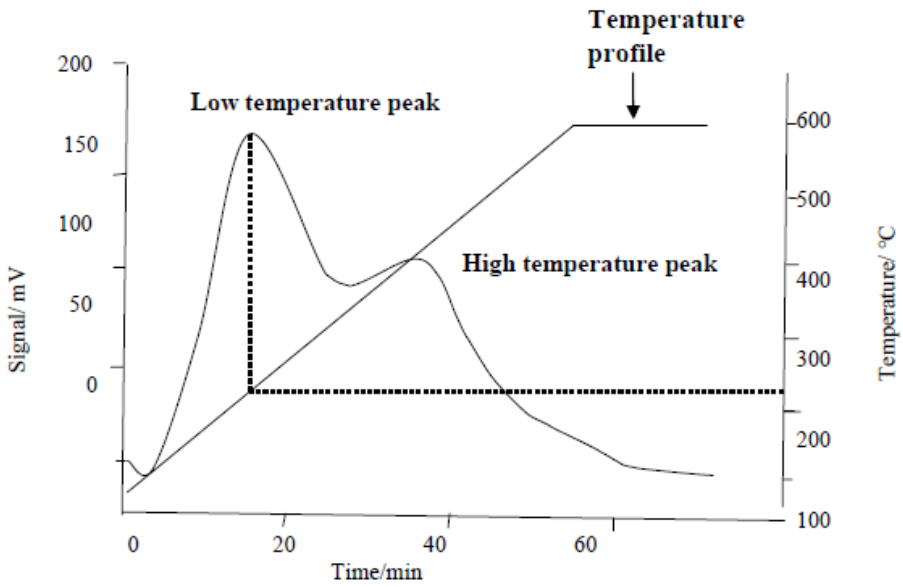

Figure 3.3: A general TPD graph of zeolite samples

Ammonia Temperature Program Desorption of the parent and modified catalysts were performed in a CHEM-BET 3000 instrument (Quantachrome). Catalyst sample (0.1 g) was first degassed at 723 K for 1 h with nitrogen followed by cooling to 273K temperature. Nitrogen-ammonia gas (1 mol%) mixture, was then passed through the sample for 1 h. The catalyst sample was heated to 372 K until the steady state was attained; thereafter the temperature of the sample was raised up to 1173 K at a heating rate of 10 K/min. The desorbed ammonia was detected by a Thermal Conductivity Detector analyzer.

CHAPTER- 4

Catalyst Characterization

This chapter deals with characterization of zeolite catalysts used in the present work. Commercially available Hbeta and NaX zeolites were modified with rare earth metal ions particularly lanthanum (La), cerium (Ce) and praseodymium (Pr) to improve their catalytic activity. These modified zeolites were then used as catalysts for transalkylation reactions. All the zeolites were characterized by various techniques (EDS, XRD, SEM, BET and TPD) to find the effect of loaded metal on various properties like crystallinity, acidity and surface area of the parent zeolite.

CHARACTERIZATION OF MODIFIED CATALYST

4.1 ENERGY DISPERSIVE SPECTRA

EDS of all the catalyst samples were done to determine whether exchange of metal ions have been taken place with Na^+, H^+ and to find the exchanged metal ion concentration (wt%) in Hbeta and NaX zeolite framework. The results obtained are shown respectively in Figure 4.1 and 4.2. These Figures show that ion exchange by the rare earth metals in Hbeta and NaX zeolite has been successfully carried out. The concentrations (wt%) of rare earth metal ions present (wt%) in the modified zeolites are reported in Table 1. Each metal cation was incorporated in zeolite Hbeta and NaX to negligible different extent (Table 4.1).

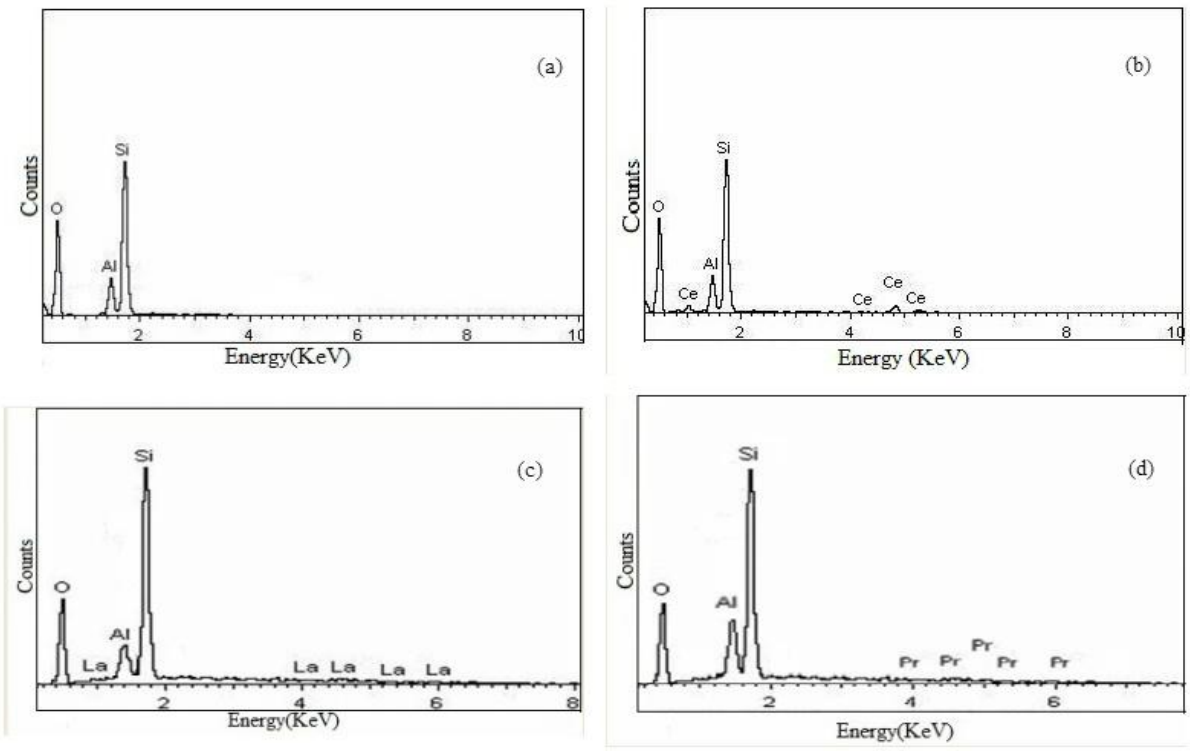

Figure 4.1: EDS of beta zeolite(a), CeB(b), LaB(c), PrB(d)

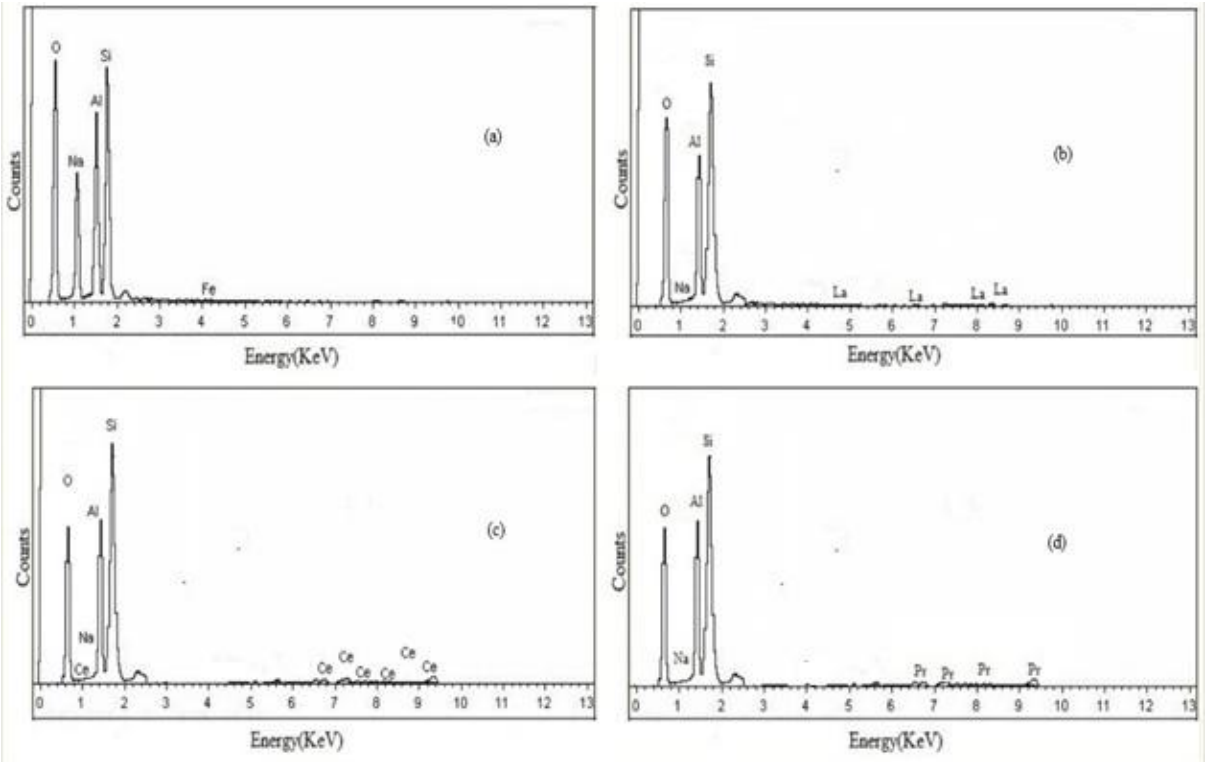

Figure 4.2: EDS of NaX zeolite(a), LaX(b), CeX(c), PrX(d)

4.2 X-RAY DIFFRACTION

Both parent and modified Hbeta zeolites were characterized by XRD and are shown in the Figures 4.3, 4.4, 4.5 and 4.6. In Figure 4.3, typical diffraction characteristics of BEA topology are observed for all the zeolites indicating the framework structure of all the modified zeolites was preserved during ion exchange procedure. The diffractogram of parent zeolite exhibited a high intensity reflection at 2θ value of 7.8° (101) and 21°-22° (302) which are typical characteristic peak of beta zeolite [Zhang *et al*., 2014]. Other peaks can be observed in 2θ ranging from 22.5°-30°. The intensity of the peaks are found to decrease in the cases of metal ion exchanged zeolites which shows that crystallanity of the Hbeta zeolite decreases on metal exchange. The crystallinity of modified samples of Hbeta zeolites were measured from the high intensity peaks at 7.8° and 21°-22° using eqn. 2.

At low loading of metal ions into zeolite framework, no diffraction lines corresponding to metal species were observed. At low loading, the rare earth metal ions replace the H^+ ions [Tang *et al*., 2014] and are highly dispersed in the zeolite framework [Garcia *et al*., 2011]. However, on increasing the metal loading, additional peaks of metal oxides present on the catalyst surface, may appear in XRD pattern [Amin and Anggoro, 2003; Siregar and Amin,

2006; Garcia *et al*., 2011] as shown in Figure 4.4. Similar observation was reported on high loading of cerium (16 wt%) into Hbeta zeolite framework [Wang and Zou, 2003].

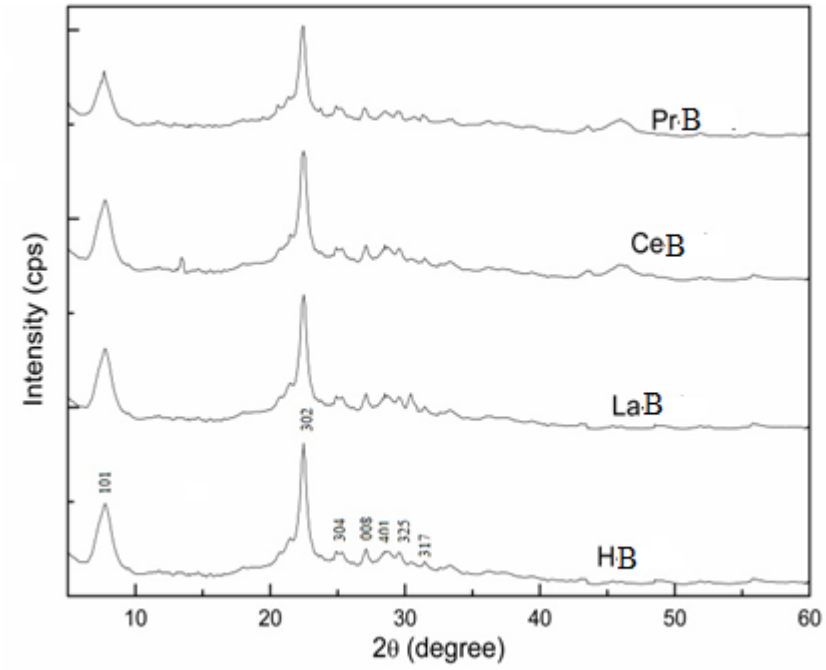

Figure 4.3: XRD of various rare earth metal modified beta zeolites

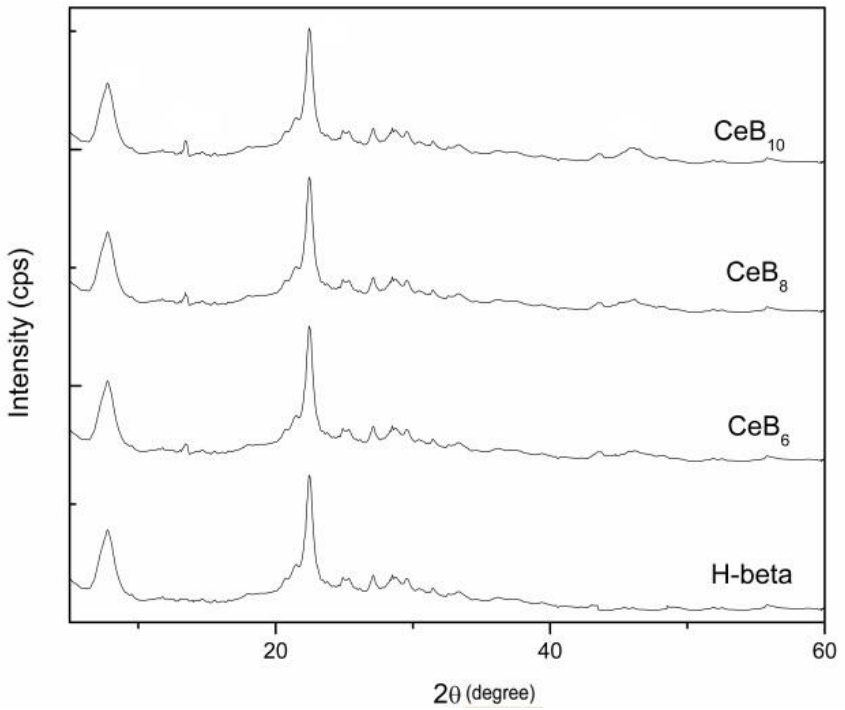

Figure 4.4: XRD of beta zeolite loaded with different concentration of metal ion

Both parent and modified NaX zeolites were also compared for their crystallinity. XRD patterns of parent and ion modified NaX zeolites are shown in Figure 4.5. The XRD patterns of NaX zeolite loaded with different concentration of metal ions are shown in Figure 4.6. The peaks at 2θ value at 6.19º (111), 11.6º (311), 18.6º (511), 20.3º (440) and 23.5º (533) correspond to NaX Faujasite zeolite topology. These peaks are well retained in rare earth metal ion exchanged NaX zeolite indicating no major structural change during metal exchange. However, the decrease in intensity of peaks was also observed in case of modified NaX zeolite. The degree of crystallinity of rare earth metal ionexchanged Hbeta and NaX samples was found in order of La>Ce>Pr which followed the order of electropositivity of the ions.

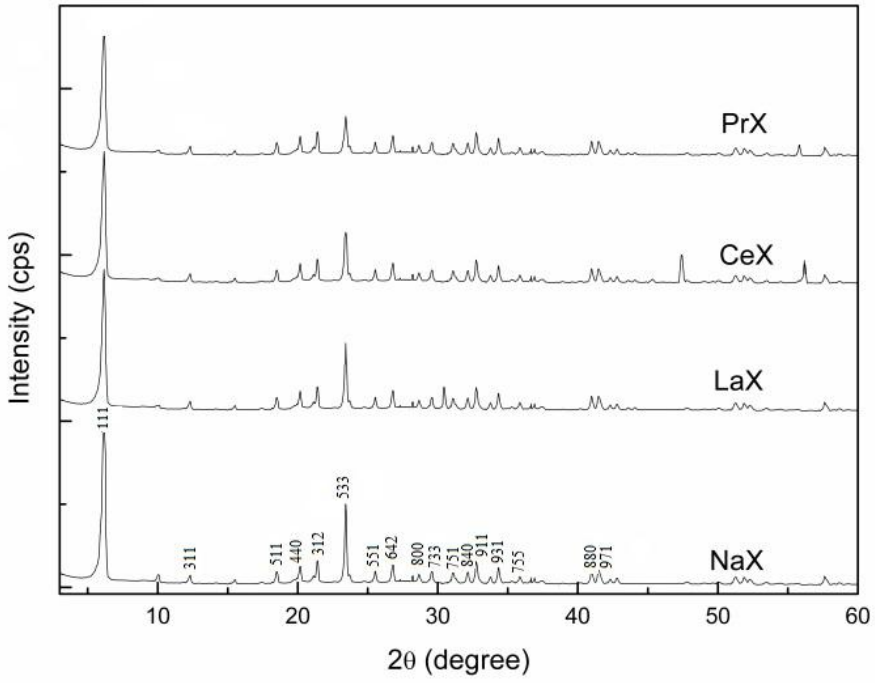

Figure 4.5: XRD of various rare earth metal modified NaX zeolites

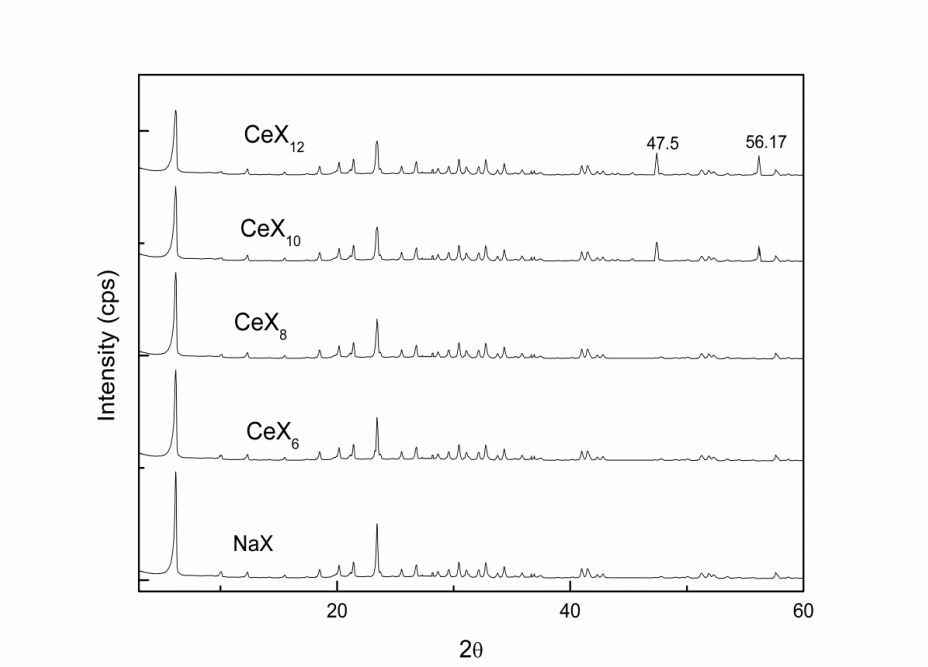

Figure 4.6: XRD of NaX zeolite loaded with different concentration of metal ion

4.3 SCANNING ELECTRON MICROSCOPY

SEM was used to find the surface morphology of the zeolites. Figure 4.7 shows the SEM images of zeolite Hbeta before and after ion exchange with rare earth metal ion. The SEM micrograph confirmed the phase purity of the crystal morphology. It is clear from the SEM images that both parent and modified Hbeta zeolite crystals are round in shape. Comparing the images of parent (Figure 4.7(a)) and modified zeolite beta (Figure 4.7 (b), (c) and (d)), no effect on zeolite morphology was observed after the ion exchange. However, the surface of metal modified zeolite. Metal modified zeolite is brighter than zeolite Hbeta due to the presence of oxide particles on its surface. The crystal sizes of all the catalysts were found to be around 0.5 μm. Similarly, Figure 4.8 shows the SEM images of NaX zeolites before and after ion exchange with rare earth metal ions. SEM micrograph of both parent and modified NaX zeolite showed octahedral crystals. The micrograph shows that the particles were of uniform size and structure suggesting that the loading of metal ions into the framework does not have much effect on the size of the zeolite particles. However, the crystal size in this case was found to be in range of 1.2-1.5 μm.

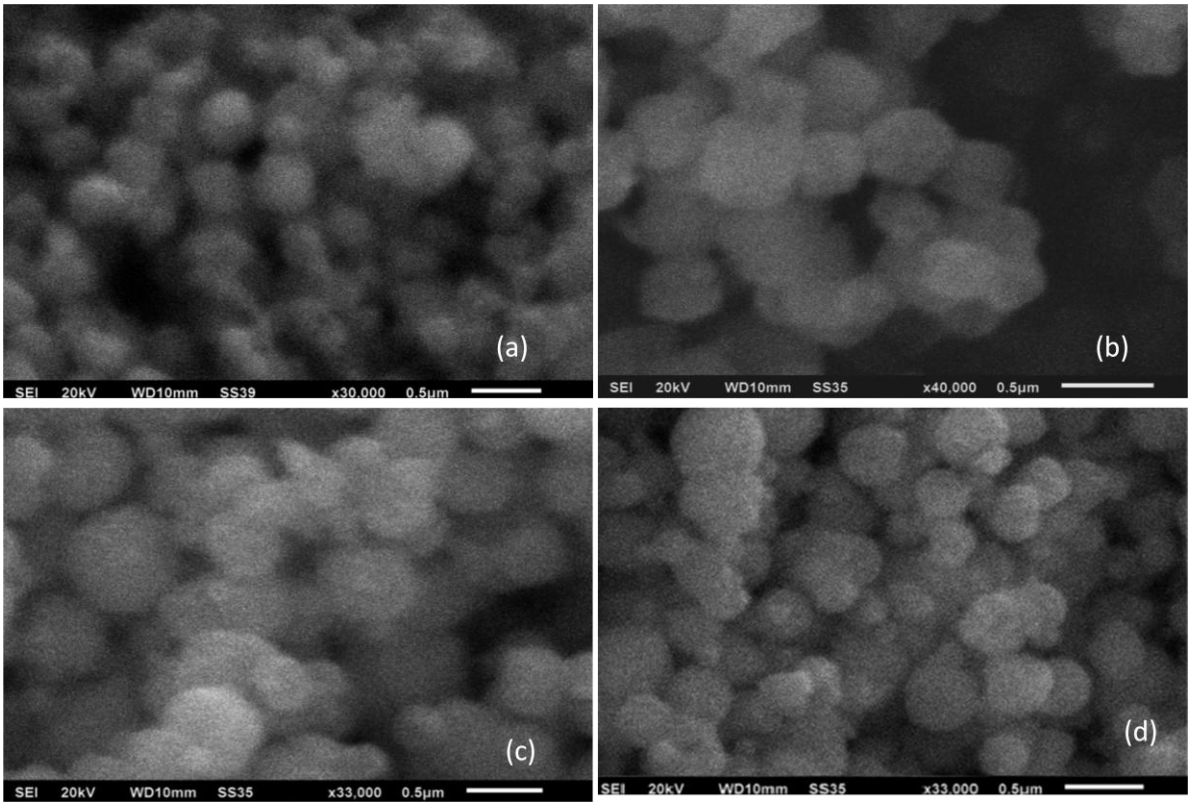

Figure 4.7: SEM of Hbeta zeolite(a), LaB(b), CeB(c), PrB(d)

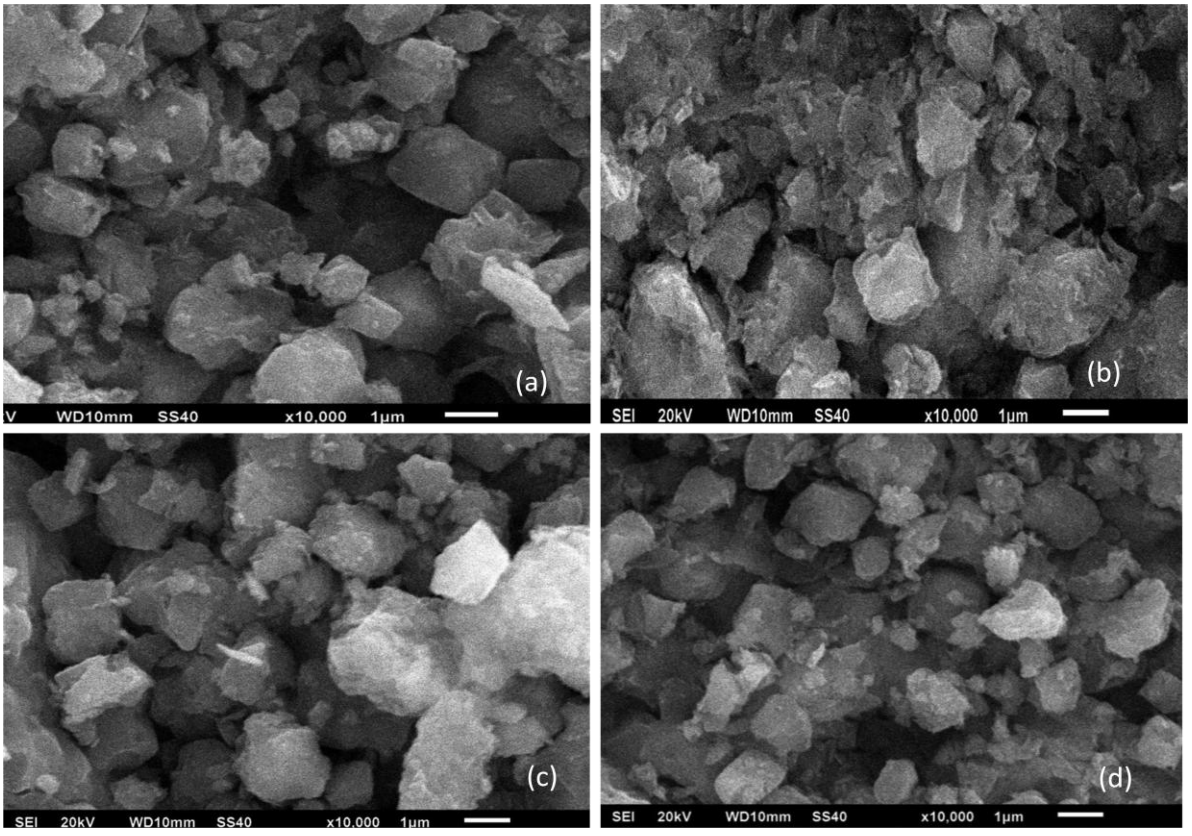

Figure 4.8: SEM of NaX zeolite(a), LaX(b), CeX(c), PrX(d)

4.4 TEMPERATURE PROGRAMMED DESORPTION OF AMMONIA

NH_3-TPD of all the zeolite catalyst was carried out to find the acidity. The TPD (Figure 4.9) profiles show that the parent and modified Hbeta zeolites contain mainly two types of acid sites of varying strengths. The peak at low temperature is due to ammonia desorption from the weak acid sites, whereas, the peak at high temperature is due to desorption of ammonia from strong acid sites. TPD profiles show that parent zeolites contain mainly weak acid sites. In metal modified Hbeta zeolites occurs an additional peak at higher temperature range (673-873 K) is observed which may be due to the presence of strong acid sites created by ions exchange. Moreover, the peak at low temperature shifted towards higher temperature with increase in exchange of metal ions. The number of acid sites also increases as the peak area increases with metal exchange. The profiles show that PrB is most acidic of all the modified beta zeolites. Acidity decreased in the order of PrB>CeB>LaB>Hbeta. This trend of acidity may be explained on the basis of combined effect of charge and size of metal ions, which determine the charge to size ratio and hence affects acidity.

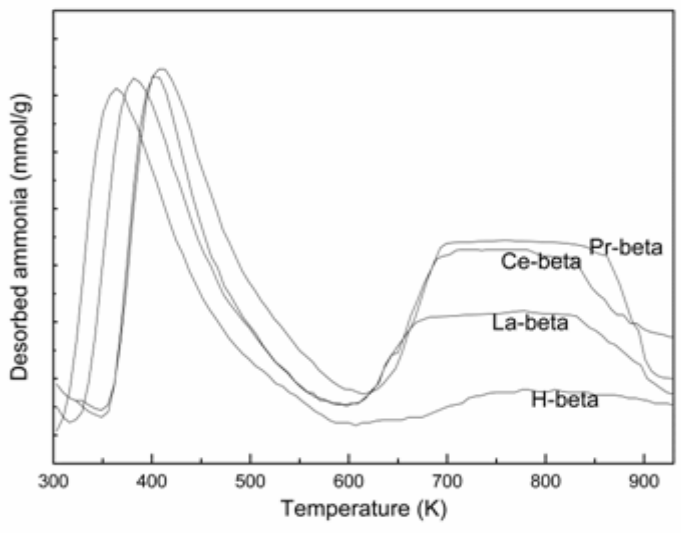

Figure 4.9: Ammonia-TPD profile of various rare earth metal modified beta zeolite

Similarly, for NaX zeolite the peak shifted towards higher temperature range in case of rare earth metal modified NaX zeolite as shown in Figure 4.10. Also, the acidic strength increased with increase in metal ion concentration in NaX zeolite. The trend of acidities of various metal modified zeolites was similar as observed in case of beta zeolite. Thus, it can be concluded that exchange with rare earth metals leads to increase in both quantity and strength of the acid sites in zeolite. From the TPD profiles (Figure 4.11) it was observed that

concentration of metal in zeolite also affects acidity of the catalyst. The acidity of various zeolites is reported in Table 1.

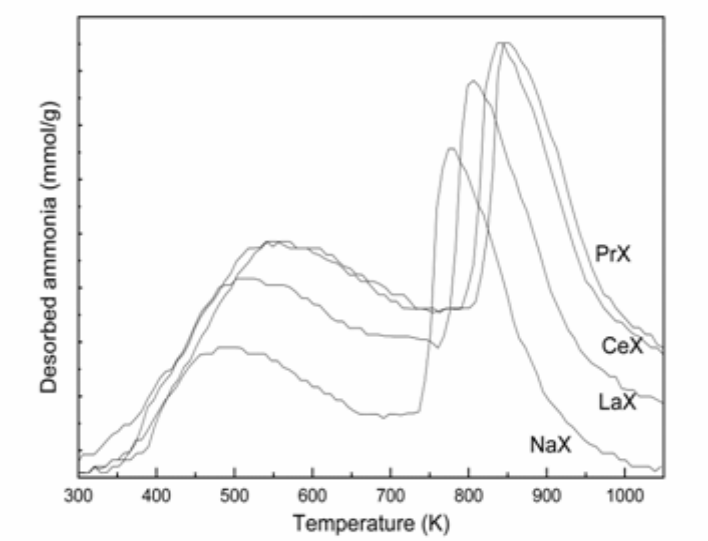

Figure 4.10: Ammonia-TPD profile of various rare earth metal modified NaX zeolite

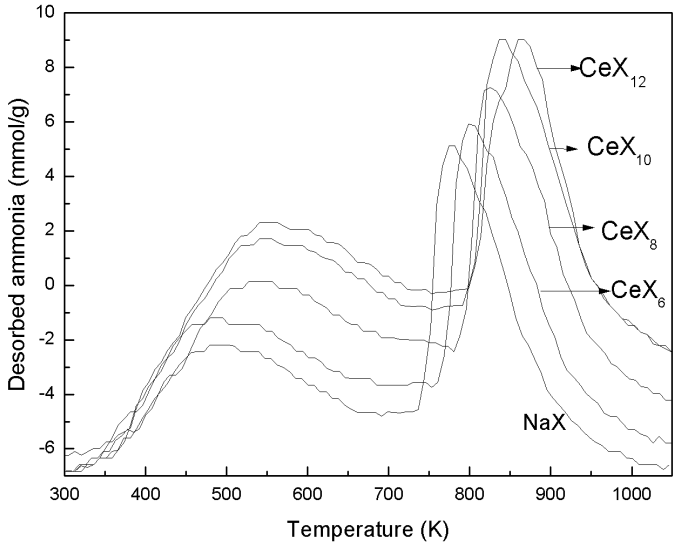

Figure 4.11: Ammonia-TPD of NaX zeolite loaded with different concentration of metal ion

4.5 BET ANALYSIS

The surface area of various zeolites, reported in Table 4.1, was obtained from nitrogen adsorption using BET technique. Incorporation of metal ions in zeolite pores reduces the total

surface area of the zeolite. It was observed that all modified samples showed a decrease in surface area. The estimated surface area shows that modified zeolite depends on the size of the metal ion involved in the exchange. Larger the size of the metal ion used for exchange; smaller is the surface area. In general, both microporous and mesoporous volumes were smaller for exchanged zeolites than the unmodified zeolites. However, the decrease in micropore volume is more pronounced because the exchanged cations preferentially locate in the zeolite micropores.

Table 4.1- Pysiochemical properties of various catalysts

Catalyst	**Metal (wt%)**	**Crystallinity (%)**	**Acidity (mmol/gm)**	**BET Surface area (m^2/g)**
Hbeta	NIL	100	0.88	633
LaB	8.02	89	1.39	526
CeB	8.10	91	1.79	545
PrB	7.99	92	1.91	554
NaX	NIL	100	0.25	478
LaX	7.94	89	0.72	352
CeX	7.8	90	1.27	370
PrX	7.72	92	1.33	384

To sum up, Energy dispersive spectrum confirmed that metal ion exchange has been carried out successfully. XRD studies shows that framework structure is well preserved after ion exchange. However the crystallinity of parent zeolites was found to decrease with metal ion content. SEM was done to find the particle mophology and average particle size. It was found that modified and parent beta zeolite particles were rounded in shape where as NaX (parent and modified) zeolite particles were octahedral in shape. Modified zeolite surface was bright due to oxide particles present on the surface. It was found that acidity of the metal modified zeolites were higher than the parent zeolite. PrB zeolite was most acidic among all the zeolites. All metal modified zeolites showed a decrease in the surface area which was due to decrease in both microporous and macroporous volume.

CHAPTER- 5

Transalkylation of Toluene with 1,2,4 Trimethylbenzene

This chapter deals with transalkylation of toluene and 1,2,4 TMB over modified Hbeta and NaX zeolite. Effect of various parameters like concentration of metal on catalyst, catalyst loading, time on stream, reaction temperature, reactant ratio and space time on reactant conversion and product yield were studied. The sections 5.1 and 5.2 present a detailed study of toluene-1,2,4TMB transalkylation over modified Hbeta and NaX zeolite respectively. The section 5.3 represents a study for the optimization of the transalkylation reaction system using RSM, a statistical tool, which helps in understanding the interactions among the model parameters.

INTRODUCTION

Global demand of p-xylene remains at a very high level and is growing sharply over the last decade. In the year 1999, the world consumption of mixed xylene was about 24 million tons and it will reach upto 70.5 million tons in 2020. Asia Pacific is expected to account for 81.5% of the global xylene demand in 2020. However, the net production coming from industries has not kept pace with steady increased demand of para xylene in the global market. As most plants are already operating at their full extent, further increase of demand may require some type of modification in the production system. The majority (> 90 percent) of mixed xylene isomers are used for blending into petrol as an octane additive [Das *et al*., 1994; Aitani *et al*., 2010; Dumitriu *et al*., 2002]. Xylene is used for the production of different industrially useful product. Terephthalic acid which is derived from xylene is the main component in the polyester industry, and is used in polyester terephthalate (PET) and polyester fibre manufacturing [Hanika *et al*., 2003]. By oxidation process of para-xylene, about 70% terephthalic acid is produced which is used in PET manufacturing [Das *et al*., 1994; Aitani *et al*., 2010]. Beside these, xylene has numerous applications as a key raw material for the production of films, resins, fibres, plasticizers and dimethylterephthalate in petrochemical industries [Dumitriu *et al*., 2002]. The transalkylation of toluene with TMB forms mixed xylene which consists of three isomers para-xylene, ortho-xylene and meta-xylene [Tsai *et al*., 2002; Hanika *et al*., 2003]. Transalkylation of toluene with trimethylbenzene (TMB) is often desirable and is considered as a promising catalytic process for the utilisation of these low valued by-products to commercially value added product like xylene [Tsai *et al*., 2002; Dumitriu *et al*., 2002; Hanika *et al*., 2003]. The industrial transalkylation process utilises protonic acids (HF, H_2SO_4), Lewis acids (BF_3, $AlCl_3$), silica alumina based catalyst, clays and zeolites [Pradhan *et al*., 1993; Das *et al*., 1994; Forni *et al*., 1995; Dumitriu *et al*., 1996; Bandyopadhyay *et al*., 1998; Lee *et al*., 1998; Tsai *et al*., 1999; Halgeri *et al*., 1999]. In

recent years, a variety of zeolite catalysts has been applied for transalkylation of toluene with trimethylbenzene [Aitani *et al*., 2010; Wang *et al*., 2010] However, it is remarkable that only molecular sieves with large pores are able to catalyze the reaction as large aromatic molecules (TMB) are involved in the transalkylation reaction [Wang and Tsai, 1990; Khattaf *et al*., 2007]. Mordenite, Faujasite Y, SAPO-5 are found to actively catalyze the transalkylation reaction due to their pore size and structure. Studies reveal that zeolite pore size, Si/Al ratio, and geometry affect the conversion of reactant and selectivity of product [Khattaf *et al*., 2007; Wang *et al*., 2010].

Available literature reveals that two categories of zeolite based catalysts have been used for transalkylation; one is the hydrogen or sodium form and other is metal exchanged zeolite. It is well known that substitution of noble, rare or transition metals in these aluminosilicates leads to significant changes in the catalytic properties. Higher the acidity of a zeolite higher is its activity [Pradhan *et al*., 1993]. The number and strength of the acid sites can be increased to a great extent by exchanging cations of the zeolite with some metal ions [Bandyopadhyay *et al*., 1998]. It is reported that replacement of sodium or hydrogen ions of zeolite with polyvalent cations (La, Ce, Cu, Ni, Pt etc.) imparts superior catalytic activity to the zeolites by increasing its acidity [Serra *et al*., 2005; Barman *et al*., 2005; Aitani *et al*., 2010]. This increased activity of modified zeolite is due to the exchange of monovalent cations with polyvalent cations which lead to formation of concentrated acidic sites rather than dispersed acidic sites. Out of various rare earth metals, cerium in its ionic state may lead to the formation of highly concentrated acidic sites formed by replacement of H^+ ions. Therefore, the aim of the present study is to investigate the effect of substitution of sodium with cerium ions in the large pore zeolite NaX and Hbeta zeolites on catalytic transalkylation of toluene and TMB to xylene.

The transalkylation reaction of toluene with trimethylbenzne is accompanied by a number of side reactions like isomerisation, disproportionation and dealkylation. The mechanism of transalkylation of toluene with trimethylbenzene is shown in Figure 5.1.

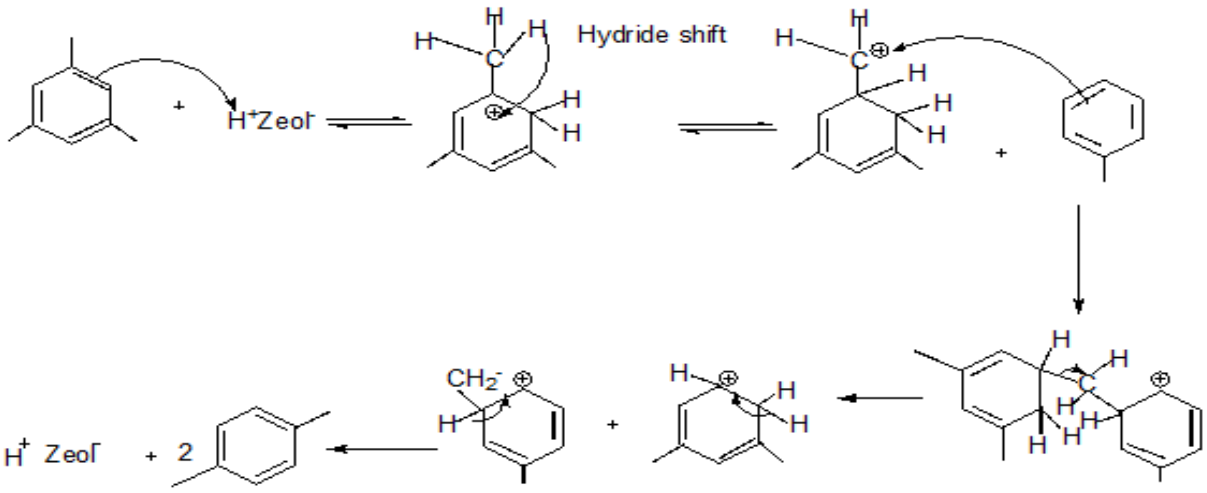

Figure 5.1: **Proposed Mechanism of transalkylation of toluene with trimethylbenzene**

According to the product distribution, the transalkylation of toluene with trimethylbenzene was accompanied with disproportionation and isomerisation. These reactions are as follows:

Primary reaction:

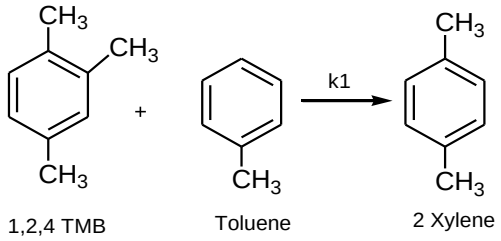

1,2,4 TMB Toluene 2 Xylene (i)

Secondary reactions:

i) Disproportionation reactions:

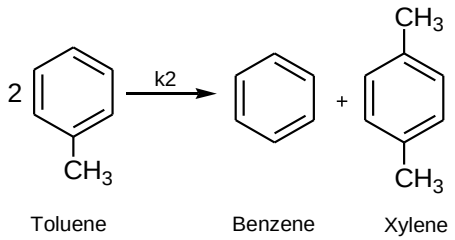

Toluene Benzene Xylene (ii)

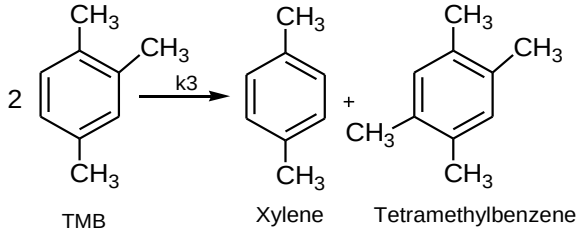

TMB Xylene Tetramethylbenzene (iii)

ii) Isomerisation reactions:

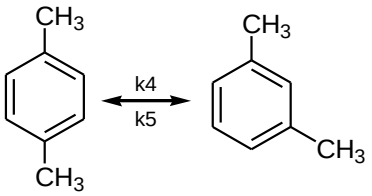

p-Xylene o-Xylene (iv)

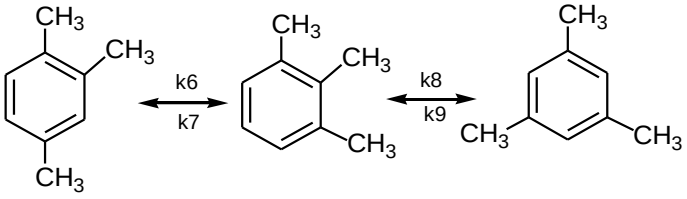

1,2,4 TMB 1,2,3 TMB 1,3,5 TMB

In this chemical reaction, **"xylene yield"** is the fraction of reactant converted to the xylene. The conversion of toluene and selectivity of xylene was calculated according to following formula:

$$Toluene\ conversion = \frac{(toluene\ in\ feed - toluene\ in\ product)}{toluene\ in\ feed} \times 100 \quad (5)$$

$$Xylene\ selectivity = \frac{Xylene\ in\ product\ mixture}{\begin{array}{c} aromatics\ \ in\ product \\ excluding\ toluene\ and\ trimethylbenzene \end{array}} \times 100 \quad (6)$$

5.1 Toluene and 1,2,4 Trimethylbenzene Transalkylation over Cerium modified Hbeta zeolite

5.1.1 EXPERIMENTAL

Cerium modified Hbeta zeolite was used as catalyst in the present study. The effect of cerium loading, temperature, catalyst loading, reactant mole ratio and space time on product distribution were studied. To investigate external diffusional effects, experiments were carried out over different weight of catalyst (2 g and 4 g) at constant space-time. To find the intraparticle diffusional effects, experiments were carried out at constant space-time with different particle size ranging from 0.5-1.5 mm.

From the catalyst characterization it was found that cerium ions have been incorporated into the Hbeta zeolite framework. Cerium modified beta zeolite was found to possess the same topology as of the parent zeolite which showed that the zeolite structure was preserved even after the ion exchange. From SEM studies it was found that average particle size and paticle morphology was similar in both modified and unmodified zeolite catalysts. TPD results showed that cerium modification of Hbeta zeolite enhanced its acidity from 0.88 mmol/gm to 1.79 mmol/gm which resulted into better activity of catalyst giving better reactant conversion, product yield and selectivity.

5.1.2 RESULT AND DISCUSSION

5.1.2.1 Effect of cerium loading and time-on-stream

The effect of cerium loading on toluene conversion and xylene selectivity is shown in Figure 5.2. The toluene conversion was found to increase with increase in cerium content. The toluene conversion over CeB_{12} (Hbeta modified with 12% ceric nitrate solution) was comparable with the conversion over CeB_{10} (Hbeta modified with 10% ceric nitrate solution) but the xylene selectivity decreased over CeB_{12} due to the formation of side products due to presence of the high acidic sites. The stability of modified Hbeta zeolites and unmodified Hbeta zeolite was tested for 3 h time-on-stream at 698 K and atmospheric pressure. The toluene conversion was found to remain constant during first 1 h as shown in Figure 5.3. It is seen from the figure that CeB_{10} zeolite gives much higher conversion than rest of the

catalysts. As the time processed, conversion of toluene decreased due to the deactivation of zeolite. Therefore, CeB_{10} was chosen for further studies.

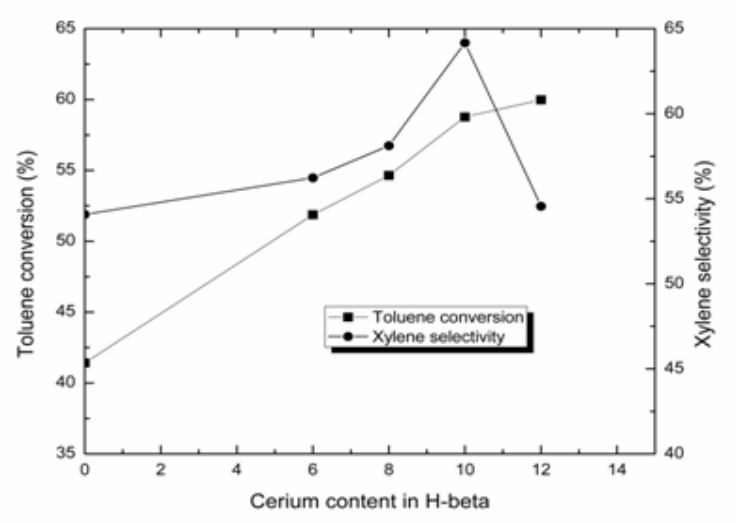

Figure 5.2: Effect of cerium content in Hbeta zeolite on toluene conversion and xylene selectivity. Reaction conditions: Pressure- 1 atm, catalyst- 2 g CeB_{10}, Temperature-698 K, TMB/toluene-3:1, space time–2.9 kg h/kmol, N_2 to feed rate-0.16.

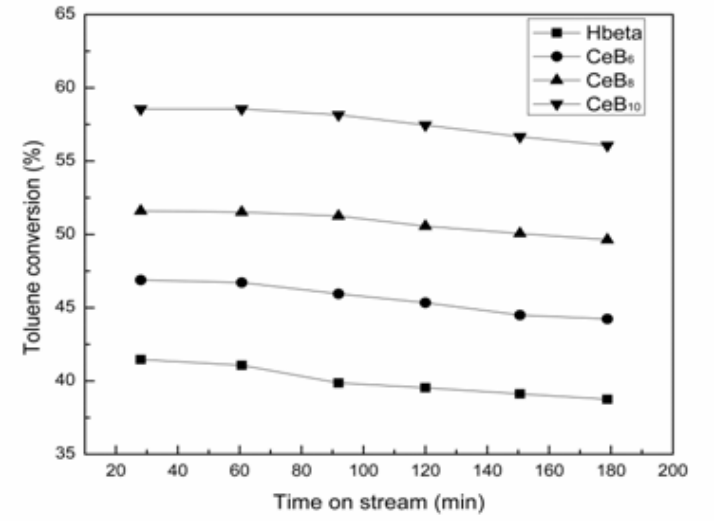

Figure 5.3: Effect of time on stream on toluene conversion and xylene yield over Hbeta and cerium modified beta zeolites. Reaction conditions: Pressure- 1 atm, catalyst-2 g CeB_{10}, Temperature-698 K, TMB/toluene-3:1, space time–2.9 kg h/kmol, N_2 to feed rate-0.16.

5.1.2.2 Effect of catalyst loading in the reactor

Catalyst loading was varied from 1.93-11.60% (w/w) of the reactants as shown in the Figure 5.4. The reactant conversion was found to increase with catalyst loading from 1.93% to 11.6%. It was observed that upto the catalyst loading of 7.73% conversion of toluene increases sharply due to the presence of large number of active sites available for the reactants. However, above catalyst loading of 7.73% although the surface area is provided for reaction, the increase in toluene conversion was negligible. The xylene yield and selectivity were also found to increase with increase in catalyst loading as shown in Figure 5.5.

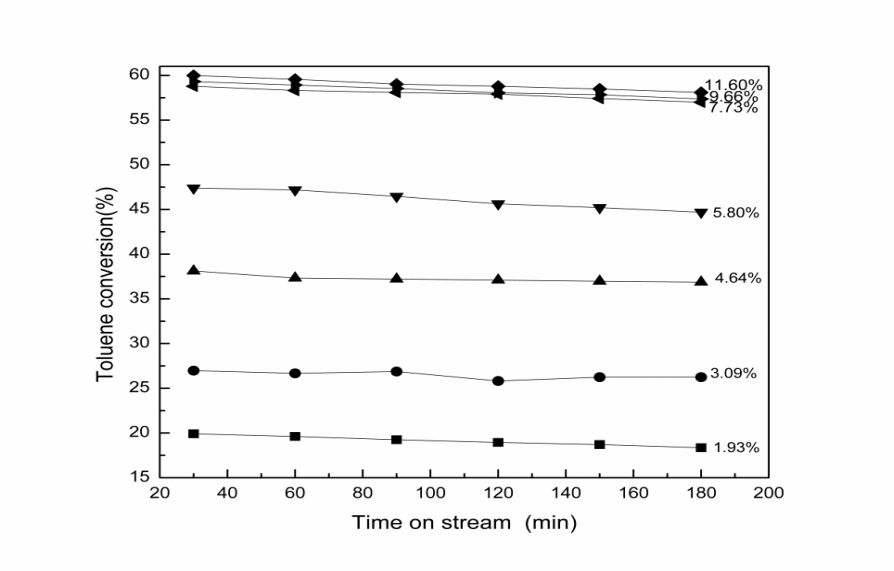

Figure 5.4: **Effect of catalyst loading (CeB_{10})on toluene conversion in 3h time on stream.**
Reaction conditions: Pressure- 1 atm, catalyst- 2 g CeB_{10}, Temperature-698 K, TMB/toluene-3:1, space time–2.9 kg h/kmol, N_2 to feed rate-0.16.

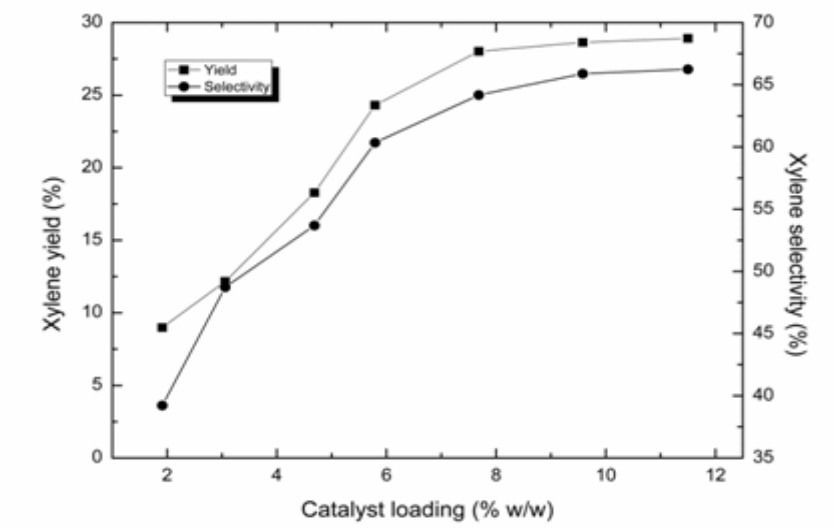

Figure 5.5: Effect of catalyst loading (CeB_{10}) on xylene yield and selectivity. Reaction conditions: Pressure- 1 atm, catalyst- 2 g CeB_{10}, Temperature-698 K, TMB/toluene-3:1, space time–2.9 kg h/kmol, N_2 to feed rate-0.16.

5.1.2.3 Effect of reaction temperature

The effect of temperature on product distribution was investigated at different temperatures in the range of 623-723 K over CeB_{10} catalyst. All the other parameters were kept unchanged. The product distribution varied with changing temperature as shown in Table 5.1. The conversion of toluene is maximum (58.77%) at 698 K and then decreases to 50% at temperature of 723 K. This decrease in conversion is due to deactivation of catalyst by coke formation on the catalyst surface. This is evident from the product distribution that with increase in temperature, formation of side products is increased; xylene selectivity is decreased but the xylene yield increased with increase in temperature.

Table 5.1- Product distribution of toluene-1,2,4 trimethylbenzene transalkylation at different temperatures over CeB_{10} zeolite catalyst

Product distribution (wt%)	**Temperature (K)**				
	623	**648**	**673**	**698**	**723**
Benzene	0.94	1.34	1.87	2.56	2.23
Toluene	14.28	11.33	9.07	8.41	10.2
Xylene					
Para	10.51	15.24	16.9	18.44	19.1
Ortho	1.84	4.79	6.66	9.58	10.07
TMB					
1,3,5-	5.01	4.28	4.94	5.01	5.71
1,2,4-	61.03	55.94	53.15	47.93	43.45
1,2,3-	3.41	3.72	3.86	3.96	4.53
TeMB	2.98	3.36	3.91	4.11	4.71
Toluene conv.(wt%)	30.01	44.46	55.53	58.77	50.00
TMB conv.(wt%)	23.32	29.72	33.28	39.78	45.41
Xylene yield (wt%)	15.21	21.03	23.56	28.02	29.17
Xylene selectivity(wt%)	50.02	60.09	61.77	64.17	62.94

Reaction conditions: Pressure, 1 atm, catalyst, 2 g CeB_{10}, TMB/toluene-3:1, space time–2.9 kg h/kmol, N_2 to feed rate-0.16.

5.1.2.4 Effect of TMB to toluene mole ratio

In the transalkylation reaction, the TMB to toluene mole ratio was varied from 0.5 to 4 at a reaction temperature of 698 K and space time of 2.9 kg h/kmol. From the Figure 5.6, it is seen that the maximum toluene conversion is obtained at a TMB to toluene ratio 3:1 above which conversion of toluene decreases. At higher mole ratio of TMB to toluene, all the active sites of the catalysts are blocked by the excess reactant. Less availability of toluene as limiting reactant decreases the conversion of toluene at higher mole ratio. The xylene yield is less when TMB is taken as limiting reactant due to less availability of number of alkyl groups in the system. However, at TMB to toluene mole ratio of 1:1, xylene yield is maximum but further increase of TMB in the reactant leads to the formation of more side products like TeMB.

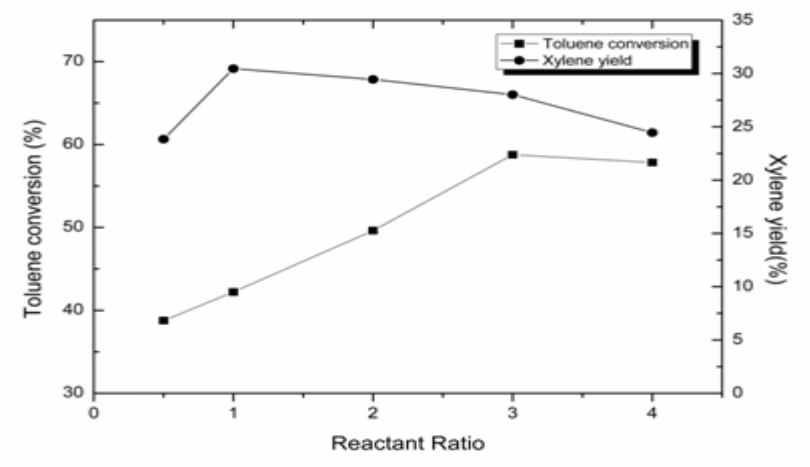

Figure 5.6: **Effect of reactant ratio on toluene conversion and xylene yield over CeB_{10} zeolite catalyst.** Reaction conditions: Pressure- 1 atm, catalyst- 2 g CeB_{10}, Temperature-698 K, space time–2.9 kg h/kmol, N_2 to feed rate-0.16.

5.1.2.5 Effect of space time

The effect of space-time was studied in the range of 0.88–2.9 kg h/kmol. The toluene conversion was increased with increase in space time as shown in Figure 5.7. This may be due to a higher contact time between the reactant and the catalyst which allows the reactants to remain in the vicinity of the catalyst for longer time thus, leading to higher conversion. Initially, xylene selectivity increased with space time, however, at much higher space time, xylene selectivity decreased due to the formation of undesired products.

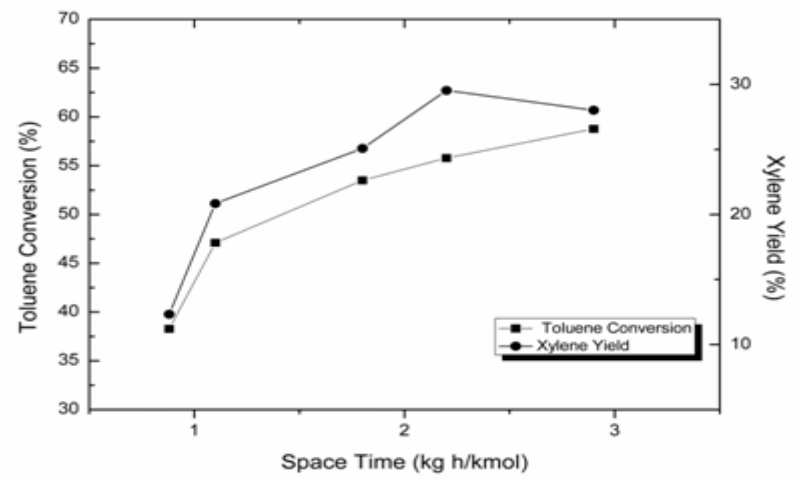

Figure 5.7: Effect of space time on toluene conversion and xylene yield over CeB_{10} zeolite catalyst. Reaction conditions: Pressure- 1 atm, catalyst- 2 g CeX_{10}, Temperature-698 K, TMB/toluene-3:1, N_2 to feed rate-0.16.

5.1.3 KINETIC STUDY

5.1.3.1 Mass transfer considerations

Any kinetic study must be done in presence of negligible mass transfer resistance during the reaction. Experiments were carried out at 598 K to investigate the external diffusional effects, with same catalyst size and constant space-time maintained by varying different feed rates. The results shown in Table 5.2, indicate that the conversion of toluene is same in both cases. Therefore, the external diffusional transfer resistance was found to be negligible**.**

Table 5.2- Effect of external diffusional resistances on toluene conversion over CeB_{10} zeolite catalyst

Space-time (kg h/kmol)	**Conversion of toluene (%)**	
	Catalyst weight = 0.002 kg	**Catalyst weight =0.004 kg**
1.1	14.56	14.11
1.8	20.13	20.01
2.2	24.19	23.98

Reaction conditions: Pressure- 1 atm, temperature- 598 K, reactant mole ratio-3:1, catalyst- 2 g, N_2: feed flow rate- 0.74

Experiments were also carried out to test the intraparticle diffusional resistance by varying the size of catalyst particle (Table 5.3). From the results, it is clear that toluene conversion is independent of the particle size, indicating that the particle sizes used in the present study were within the intraparticle diffusion free range.

Table 5.3- Effect of intraparticle diffusional resistance on toluene conversion over CeB_{10} zeolite catalyst

Particle size dp (mm)	**Conversion of toluene (%)**		
	space-time(kg h/kmol) =1.1	**space-time(kg h/kmol) = 1.8**	**space-time(kg h/kmol)= 2.2**
0.50	14.59	20.54	24.87
1.00	14.56	20.13	24.19
1.50	14.19	20.05	23.98

Reaction conditions: Pressure- 1 atm, temperature- 598 K, reactant mole ratio-3:1, catalyst- 2 g, N_2: feed flow rate- 0.74

5.1.3.2 Kinetic modeling

Langmuir-Hinshelwood-Hougen-Watson model

The experimental data was fitted in LHHW model to evaluate various rate constants of specific reaction scheme. The dual site, single site and stoichiometric models rate equations were derived as following.

Dual-site mechanism:

In dual site mechanism, both the reactants are assumed to be adsorbed on catalytic sites.

TMB-toluene transalkylation: TMB . C_v + Toluene . C_v ⟶ 2 Xylene . $2C_v$

Dispropotionation: 2 Toluene . $2C_v$ ⟶ Benzene . C_v + Xylene. C_v

A rate equation can be represented as,

$$Rate = k\, k_{ads} p_{reactant} C_v \quad (8)$$

Where, k is rate constant, k_{ads} is adsorption coefficient of any reactant, $p_{reactant}$ is partial pressure of any reactant, and C_v is concentration of vacant active sites available in the surface. In this reaction scheme,

$$\text{Total rate of disappearance of Toluene} = \text{Rate of Ist reaction} + \text{Rate of IInd reaction} \quad (9)$$

$$\text{Rate of Ist reaction} = k_1 k_T p_T k_{TMB} p_{TMB} C_v^2 \quad (10)$$

$$\text{Rate of IInd reaction} = k_2 k_T^2 p_T^2 C_v^2 \quad (11)$$

$$\text{Net rate} = k_1\, k_T\, p_T\ k_{TMB}\, p_{TMB}\, C_v^2 + k_2 k_T^2 p_T^2 C_v^2 \quad (12)$$

$$= C_v^2\, [k_1\, k_T\, p_T\ k_{TMB}\, p_{TMB} + k_2 k_T^2 p_T^2\,] \quad (13)$$

$$= (\tfrac{1}{Z})^2\, [k_1\, k_T\, p_T\ k_{TMB}\, p_{TMB} + k_2 k_T^2 p_T^2\,] \quad (14)$$

$$\text{Where, } C_v = \frac{1}{(1 + k_T\, p_T + k_{TMB}\, p_{TMB})} \quad (15)$$

Where, p_T p_{TMB} were calculated from the value of concentration of the reactants. The value of C_v was calculated as follows,

$$C_t = C_v + C_{T.S} + C_{TMB.S} \quad (16)$$

$$C_t = C_v + k_{T.}C_T C_v + k_{TMB.}C_{TMB}C_v \quad (17)$$

$$= C_v[\,1 + k_{T.}C_T + k_{TMB.}C_{TMB}] \quad (18)$$

$$C_v = \frac{C_t}{1+k_{T.}C_T+k_{TMB.}C_{TMB}} \quad (19)$$

As total number of sites are equal to 1,

$$C_v = \frac{1}{1+k_{T.}C_T+k_{TMB.}C_{TMB}} \quad (20)$$

$$C_v = \frac{1}{Z} \quad (21)$$

$$Z = 1 + k_{T.}C_T + k_{TMB.}C_{TMB} \quad (22)$$

Single-site mechanism:

In single site mechanism, only the limiting reactant is assumed to be adsorbed on catalytic sites.

TMB-toluene transalkylation: TMB + Toluene . C_v ⟶ 2 Xylene . $2C_v$

Dispropotionation: 2 Toluene . $2C_v$ ⟶ Benzene . C_v + Xylene. C_v

Total rate of disappearance of Toluene = Rate of Ist reaction + Rate of IInd reaction

Rate of Ist reaction = $k_1 k_T p_T p_{TMB} C_v$ (23)

Rate of IInd reaction = $k_2 k_T^2 p_T^2 C_v^2$ (24)

Net rate = $k_1\, k_T\, p_T\ \ p_{TMB}\, C_v + k_2 k_T^2 p_T^2 C_v^2$ (25)

$$= C_v[k_1\, k_T\, p_T\ \ p_{TMB} + k_2 k_T^2 p_T^2 C_v\,] \quad (26)$$

$$= (\tfrac{1}{Z})^2\,[k_1\, k_T\, p_T\ \ p_{TMB} + k_2 k_T^2 p_T^2 \tfrac{1}{Z}\,] \quad (27)$$

Where, $C_v = \frac{1}{(1 + k_T\, p_T\,)}$ (28)

And was calculated as follows,

$$C_t = C_v + C_{T.S} \quad (29)$$

$$C_t = C_v + k_{T.} C_T C_v \quad (30)$$

$$= C_v[\,1 + k_{T.} C_T] \quad (31)$$

$$C_v = \frac{C_t}{1+k_{T.} C_T} \quad (32)$$

As total number of sites are equal to 1,

$$C_v = \frac{1}{1+k_{T.} C_T} \quad (33)$$

$$C_v = \frac{1}{Z}$$

$$\text{Z}= 1 + k_{T.} C_T \quad (34)$$

Stoichiometricmodel:

In this model, rate of disappearance of toluene was considered to be independent of adsorption of any species.

$$\text{Net rate} = k_1\, p_T\, p_{TMB} + k_2\, p_{TMB} \quad (35)$$

The following rate expression using L-H-H-W model with surface reaction as a rate controlling step and dual site (both reactant adsorbed on catalyst) mechanism was found to fit the kinetic data significantly better than the other models.

$$-r_T = dX_T\,/d\tau = (\,k_1\, K_T K_{TMB} p_T p_{TMB} + k_2 K_T^2 p_T^2)/Z^2$$

where Z = 1+ $K_{TMB} p_{TMB}$ + $K_T p_T$

The partial pressures in the above equations were calculated using the fractional conversions and total pressure P as given by following expressions.

$$p_T = (\,1 - X_T\,)P/\ 4.64 \quad (36)$$

$$p_{Tmb} = (\,2.5 - X_{Tmb}\,)P/\ 4.64 \quad (37)$$

$$p_{p-xyl} = \left(X_{p-xyl}\right)P/\ 4.64 \quad (38)$$

$$p_{o-xyl} = \left(X_{o-xyl}\right)P/\ 4.64 \quad (39)$$

$$p_{1,3,5TMB} = \left(X_{1,3,5TMB}\right)P/\ 4.64 \quad (40)$$

$$p_{1,2,3TMB} = \left(X_{1,2,3TMB}\right)P/\ 4.64 \quad (41)$$

$$p_{TeMB} = (X_{TeMB})P/\ 4.64 \quad (42)$$

Where, k_1, k_2 are the reaction rate constants, K_T and K_{TMB} are adsorption constants, p_T and p_{TMB} are partial pressures of toluene and TMB respectively. In the reaction system, the total number of moles of different components was found to be 4.64. A non-linear regression was used for model parameter estimation. The optimum value of the parameters was estimated by minimizing the objective function given by equation (43).

$$f = \sum_{i=1}^{n}[(\ Rate\ predicted)i - (rate\ experimental)i]^2 \quad (43)$$

Model selection

The kinetic and adsorption constants evaluated by nonlinear regression are tabulated in Tables 5.4-5.6. For dual site model, estimated parametes are calculated and reported in Table 5.4 and the estimated error was 8.35×10^{-4}. For single site model, estimated parametes are calculated and reported in Table 5.5, error estimate was 6.4×10^{-3}. For stoichiometric model with the values of the constants from Table 5.6, the error was 4.7×10^{-3}. By comparing the standard errors, model followed by dual site mechanism was found to be the best. The experimental and the predicted toluene conversions for this model, at different temperatures, are plotted in Figure 5.8. The plot shows a good correlation between experimental and predicted rates having an R^2 value of 0.96.

Table 5.4- Kinetic and adsorption parameters for dual site mechanism for toluene-1,2,4 trimethylbenzene transalkylation over CeB_{10} zeolite catalyst

Kinetic and adsorption parameters	**Temperature (K)**			
	623	**648**	**673**	**698**
$\mathbf{k_1}$ (kmol/kg h)	1.42	3.20	8.93	16.58
$\mathbf{k_2}$ (kmol/kg h)	0.79	1.81	4.64	13.07
$\mathbf{K_T}$ (atm^{-1})	2.24	2.01	1.40	1.23
$\mathbf{K_{TMB}}$ (atm^{-1})	0.94	0.88	0.55	0.23

Table 5.5- Kinetic and adsorption parameters for single site mechanism for toluene-1,2,4 trimethylbenzene transalkylation over CeB_{10} zeolite catalyst

Kinetic and adsorption parameters	**Temperature (K)**			
	623	**648**	**673**	**698**
$\mathbf{k_1}$ (kmol/kg h)	0.50	1.77	3.65	4.5
$\mathbf{k_2}$ (kmol/kg h)	0.01	1.04	2.52	3.04
$\mathbf{K_T}$ (atm^{-1})	2.30	1.24	1.18	1.15

Table 5.6- Kinetic and adsorption parameters for stoichiometric model for toluene-1,2,4 trimethylbenzene transalkylation over CeB_{10} zeolite catalyst

Kinetic and adsorption parameters	**Temperature**			
	623	**648**	**673**	**698**
$\mathbf{k_1}$ (kmol/kg h)	1.06	2.12	3.28	4.95
$\mathbf{k_2}$ (kmol/kg h)	0.65	1.12	1.37	1.92

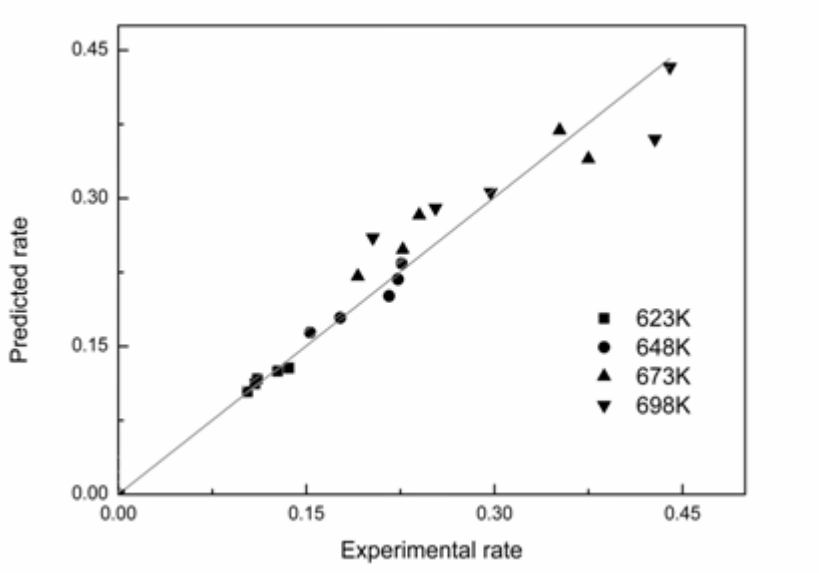

Figure 5.8- Experimental versus predicted rate of toluene conversion for xylene production over CeB_{10} zeolite catalyst

The kinetic constants derived from equation (14), were used to find the activation energy, using the Arrhenius equation (44). Activation energy for transalkylation reaction was estimated to be 122.4kJ/mol. Activation energy of 130.2 kJ/mol was reported for DIPB-

benzene transalkylation reaction over SAPO-5 catalyst [Kondamudi and Upadhyayula, 2008]. Activation energy and pre-exponential factors of different reactions are reported in Table 5.7.

$$\ln K = \ln A - E_a / RT \quad (44)$$

Table 5.7: Activation energy and pre-exponential factors for different reactions over CeB_{10} zeolite catalyst

Reaction	E_a (kJ/mol)	Pre-exponential factor
Transalkylation reaction	122.4	2.4×10^{10}
Toluene dispropotionation	135.7	2.1×10^{11}

Another important thermodynamic adsorption parameters (enthalpy and entropy of adsorption) were calculated using equation (45). The values of enthalpy and entropy change are reported in Table 5.8. The adsorption equilibrium constants are plotted in Figure 5.9 which shows a satisfactory trend.

$$\ln k = \frac{-\Delta H}{RT} + \frac{\Delta S}{R} \quad (45)$$

Table 5.8- Thermodynamic adsorption parameters for toluene-1,2,4 trimethylbenzene transalkylation over CeB_{10} zeolite catalyst

Reactants	ΔH_{ads}(kJ/mol)	ΔS_{ads}(J/mol K)
Toluene	-31.75	-43.89
1,2,4 TMB	-66.51	-105.83

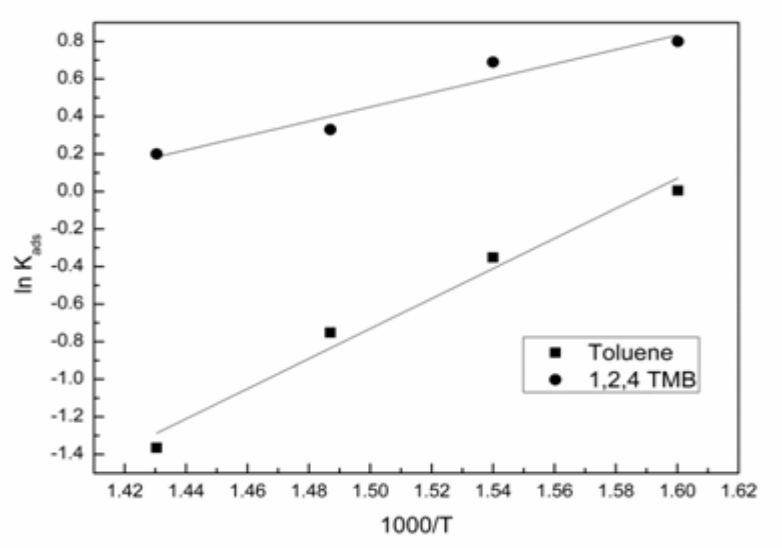

Figure 5.9: Arrhenius plot for adsorption equilibrium constants for toluene-1,2,4 trimethylbenzene over CeB_{10} zeolite catalyst

5.1.3.3 Deactivation kinetics

For a differential reactor, the deactivation constant may be assumed to be independent of reaction concentration. For a batch of solid (catalyst) and plug flow of fluid the following equation (46) may be used for determining the deactivation constant. A plot of ln[ln(C_{A0}/C_A)] vs t at four temperatures using CeB_{10} catalyst is shown in Figure 5.10; the slopes of the lines at different temperatures represent k_d (deactivation constant). The deactivation constant was found to be lower than the reaction constants. A graph of ln K_d vs 1/T was plotted to find the apparent activation energy for deactivation (Figure 5.11). The apparent activation energy for deactivation of catalyst was found to be 27.85 kJ/kmol. In case of alkylation and transalkylation reactions, the coke formed is olefinic in nature which forms fast; hence, catalyst is more susceptible to pore blockage at low temperatures [Sridevi *et al*., 2001].

$$\ln\left[\ln\left(\frac{C_{A0}}{C_A}\right)\right] = \ln(k\tau') - k_d t \qquad (46)$$

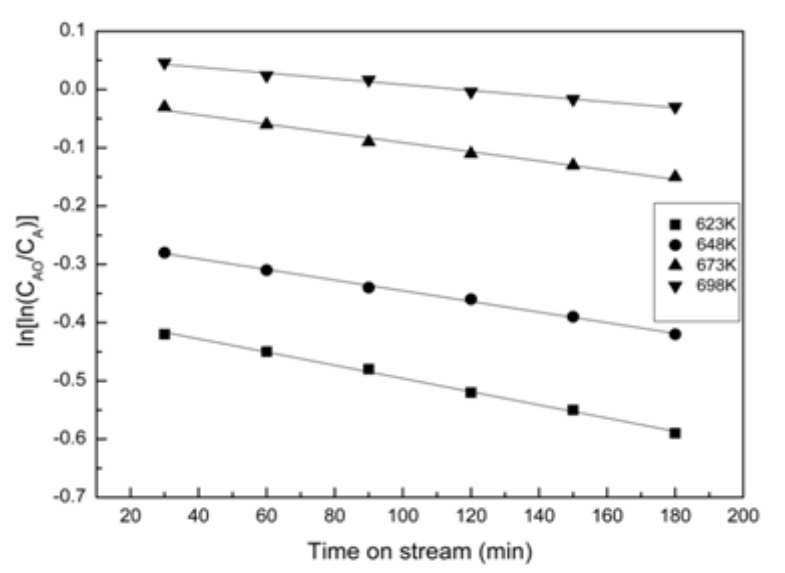

Figure 5.10: Plots of ln[ln(C_{AO}/C_A)] *vs* time at different temperatures for toluene-1,2,4 trimethylbenzene over CeB_{10} zeolite catalyst

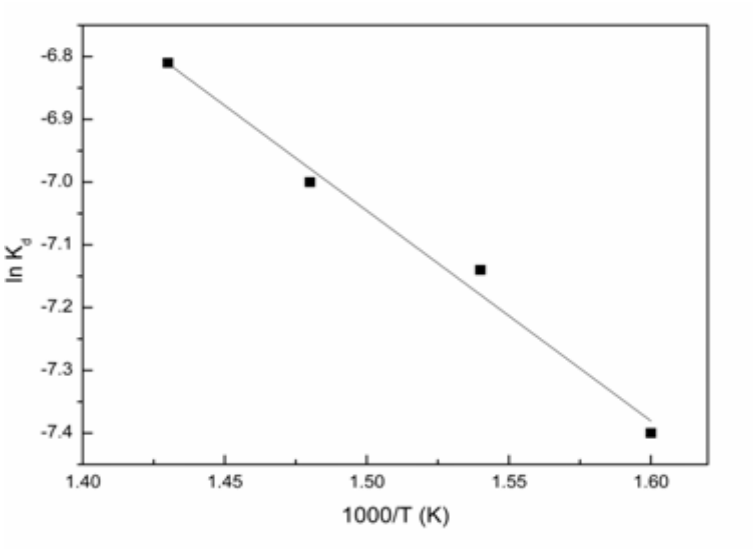

Figure 5.11: Arrhenius Plot for deactivation kinetics for toluene-1,2,4 trimethylbenzene over CeB_{10} zeolite catalyst

5.1.4 CONCLUSION

Transalkylation of toluene with TMB was carried out over Hbeta and CeB zeolite catalysts. Modification of zeolite with cerium increased the activity of catalyst and selectivity of the product. A time on stream study showed that the catalyst was quite stable at an operating temperature of about 700 K. Maximum toluene conversion and xylene selectivity obtained over Hbeta zeolite were 41.42% and 54.08% respectively, whereas cerium modified zeolite lead to substantial improvement in both toluene conversion (58.77%) and xylene selectivity (64.17%) at a temperature-698 K, reactant ratio-3, space time-2.9 kg h/kmol. A reaction mechanism was proposed with a rate expression for the disappearance of toluene. The kinetic and adsorption constants of the rate equation were estimated. The activation energy for transalkylation reaction was determined to be 122.4 kJ/mol which is comparable with the data reported in the literature for transalkylation reactions.

5.2 Toluene and 1,2,4 Trimethylbenzene Transalkylation over Cerium modified NaX zeolite

5.2.1 EXPERIMENTAL

The study was conducted at temperatures ranging from 573-773 K. Cerium modified NaX zeolite was used as a catalyst. Cerium loading on zeolite catalyst was varied from 6-12 wt%, whereas catalyst loading in the reactor was varied from 1.91-11.50% (w/w) of the reactants. The 1,2,4 TMB to toluene ratio was varied from 0.45 to 3.1. The range chosen for space time in the present study was 1.19 – 4.44 kg h/kmol. Kinetics studies were done to find out various kinetic and thermodynamic parameters.

From the catalyst characterization it was found that cerium ions have been incorporated into the NaX zeolite framework. Cerium modified NaX zeolite was found to possess the same topology as of the parent zeolite which showed that the zeolite structure was preserved even after ion exchange. From SEM studies it was found that average particle size and paticle morphology was similar in both modified and unmodified zeolite catalysts. TPD results showed that cerium modification of NaX zeolite enhanced its acidity which was 1.27 mmol/gm in comparison to NaX (0.25 mmol/gm) which resulted into better activity reflected in terms of better reactant conversion, product yield and selectivity.

5.2.2 RESULTS AND DISCUSSION

5.2.2.1 Effect of cerium loading and time-on-stream

Effect of cerium loading on NaX zeolite catalyst on product distribution is shown in Table 5.9. The results show that modified zeolite shows better results for toluene conversion, xylene yield and xylene selectivity than NaX zeolite. From the product distribution, it is seen that disproportionation of toluene is less favorable than disproportionation of TMB which produces TeMB. Further, isomerisation of TMB yields 1,3,5 TMB as major product rather than 1,2,3 TMB. Due to steric hindrance of the alkyl groups 1,2,3 TMB is not stable at all as a product. Similar results are obtained in case of xylene isomers as para-xylene isomer being produced in larger amount than ortho isomer which is sterically favoured product.

Figure 5.12 shows that xylene yield and toluene conversion increase with increase in cerium loading in the catalyst. However, the xylene selectivity and yield both decreased for cerium

loading above 10% of ceric ammonium nitrate solution. This may be due to the fact that generated acid sites are very strong to initiate disproportionation and isomerisation reactions thereby lead to increase the formation of side product thus decreasing the yield and selectivity of xylene. Therefore, further study was done using CeX_{10} catalyst.

Table 5.9- Product distribution of toluene-1,2,4 trimethylbenzene transalkylation over various NaX zeolite catalysts

Product Distribution(wt%)	**Catalyst**				
	NaX	**CeX_6**	**CeX_8**	**CeX_{10}**	**CeX_{12}**
Benzene	1.79	1.81	1.86	1.88	1.93
Toluene	18.45	15.5	14.7	12.90	11.97
Xylene					
Para	7.54	9.92	11.53	15.28	13.97
Ortho	2.75	4.95	5.45	5.78	5.46
TMB					
1,3,5-	8.21	8.01	7.95	7.66	7.41
1,2,4-	54.31	52.38	51.83	48.9	48.23
1,2,3-	3.27	3.79	4.01	4.97	6.25
TeMB	3.68	3.64	2.67	2.63	3.85
Toluene conv. (wt%)	21.28	33.90	37.28	44.96	48.95
Xylene yield (wt%)	10.29	14.87	16.98	21.06	20.43
Xylene selectivity(wt%)	37.77	46.29	50.73	55.13	52.55
1,2,3 and 1,3,5 TMB isomers yield (wt%)	11.48	11.80	11.96	12.63	13.66
1,3,5 TMB/1,2,3 TMB (wt%)	2.51	2.20	1.98	1.54	1.18
Para/ortho Xylene (wt%)	2.74	2.00	2.11	2.64	2.55

Reaction conditions: Pressure, 1 atm; temperature, 723 K; reactant mole ratio, 2.5; space time, 4.44 kg h/kmol; catalyst, 2 g CeX_{10}; N_2: feed flow rate,0.74.

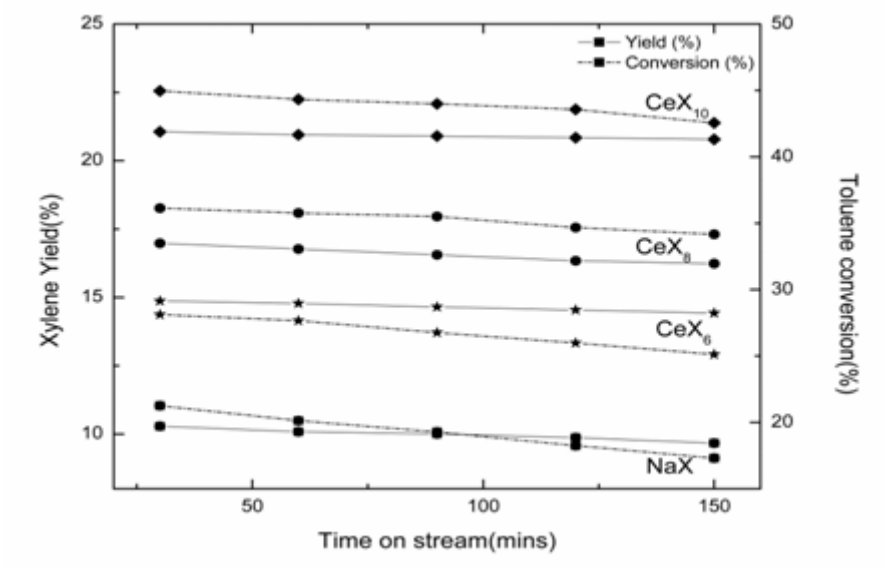

Figure 5.12: **Effect of time on stream and cerium modification on toluene conversion and xylene yield over NaX and cerium modified NaX zeolites.** Reaction conditions: Pressure- 1 atm, temperature- 723K, reactant mole ratio- 2.5, space time- 4.44 kg h/kmol, catalyst- 2 g, N_2: feed flow rate- 0.74.

5.2.2.2 Effect of catalyst loading in the reactor

Catalyst loading was varied from 1.91-11.50% (w/w) of the reactants as shown in the Figure 5.13. The conversion of reactant is found to increase with increase in catalyst loading from 1.91% to 11.5%. It was observed that up to the catalyst loading of 7.66% conversion of toluene increases sharply due to the presence of large number of active sites available for the reactants. However, catalyst loading above 7.66%, toluene conversion increases slowly. The xylene yield and selectivity are also found to increase with increase in catalyst loading as shown in Figure 5.14.

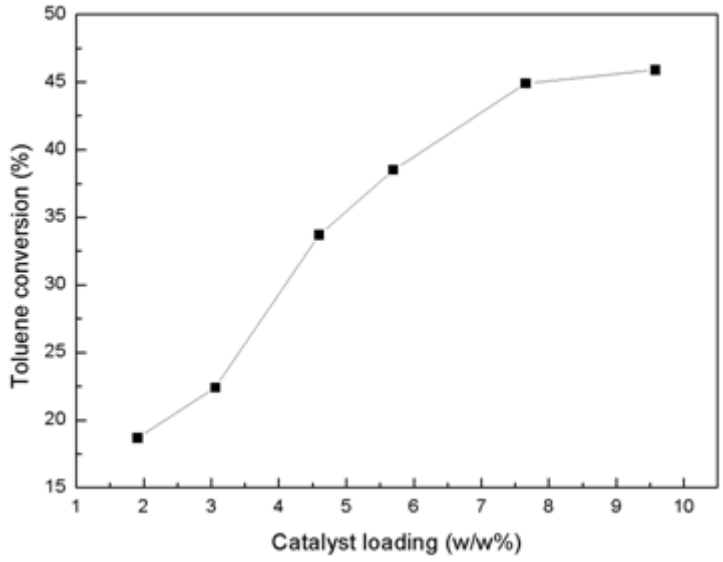

Figure 5.13: **Effect of catalyst loading (CeX_{10}) on toluene conversion in 3h time on stream.** Reaction conditions: Pressure- 1 atm, temperature- 723 K, reactant mole ratio- 2.5, space time- 4.44 kg h/kmol, catalyst- 2 g CeX_{10}, N_2: feed flow rate- 0.74.

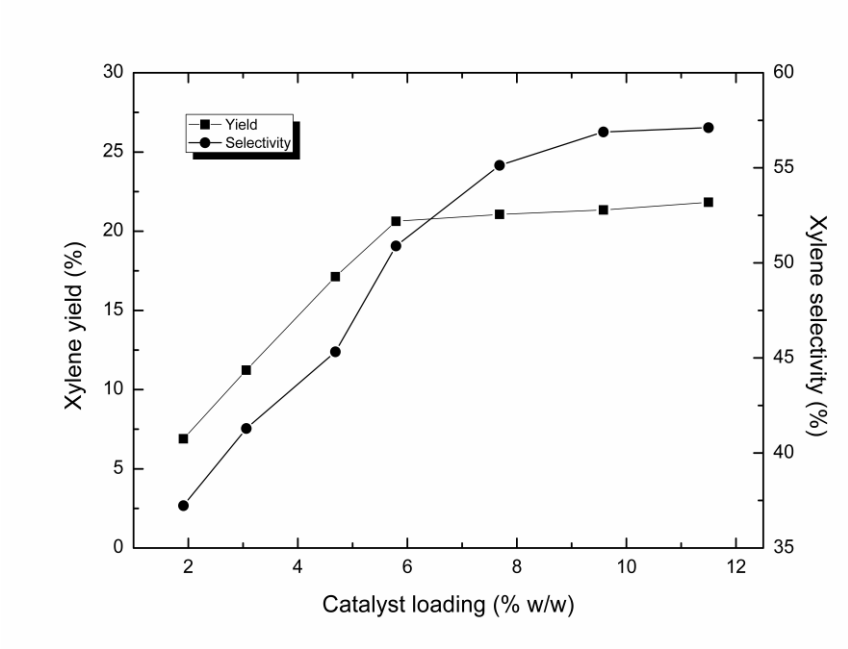

Figure 5.14: **Effect of catalyst loading (CeX_{10}) on xylene yield and selectivity.** Reaction conditions: Pressure- 1 atm, temperature- 723 K, reactant mole ratio- 2.5, space time- 4.44 kg h/kmol, catalyst- 2 g CeX_{10}, N_2: feed flow rate- 0.74.

5.2.2.3 Effect of reaction temperature

The reaction temperature can strongly influence the rate of reaction and yield of products as intrinsic rate constants are the function of reaction temperature. In order to find the optimum condition for maximum conversion and product selectivity, reactions were carried out at different temperatures (573-773 K) over 2 g of CeX_{10} zeolite catalyst. The product distribution at different temperature is summarized in Table 5.10 which shows that the reaction temperature has a significant effect on product distribution. The toluene conversion increases with rise in temperature and reach a maxima of 45% at 723 K. On the other hand, TMB conversion still shows an increase at higher temperature. Xylene selectivity is found to increase as temperature is raised from 573 K to 673 K decreasing the selectivity of other side products. As higher temperature, benzene and TeMB yield increases due to favoured disproportionation and isomerisation reaction. 1,3,5TMB/1,2,3TMB ratio decreases at higher temperature as shown in the Figure 5.15. In case of isomerisation of 1,2,4TMB, low temperature favors sterically stable products whereas high temperature provides sufficient activation energy to the reactant to overcome steric hindrance which leads to formation of 1,2,3TMB.

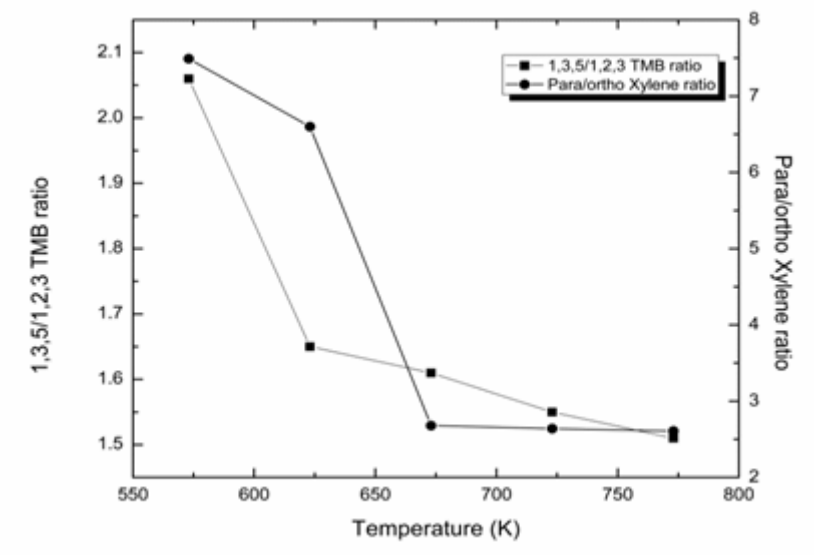

Figure 5.15: **Effect of temperature on isomers distribution over CeX_{10} zeolite catalyst.** Reaction conditions: Pressure- 1 atm, reactant mole ratio- 2.5, space time- 4.44 kg h/kmol, catalyst- 2 g CeX_{10}, N_2: feed flow rate- 0.74.

Table 5.10- Product distribution of toluene and 1,2,4 trimethylbenzene transalkylation over different temperatures over CeX_{10} zeolite catalyst

Product distribution (wt %)	Temperature(K)				
	573	**623**	**673**	**723**	**773**
Benzene	0.90	1.21	1.39	1.88	1.91
Toluene	19.24	15.21	14.32	12.90	13.39
Xylene					
Para	9.97	14.00	13.97	15.28	16.56
Ortho	1.33	2.12	5.21	5.78	6.34
TMB					
1,3,5-	6.23	6.31	6.46	7.66	7.73
1,2,4-	57.91	55.26	52.45	48.9	46.26
1,2,3-	3.02	3.83	4.01	4.97	5.11
TeMB	1.40	1.97	2.19	2.63	2.7
Toluene conv. (wt%)	18.00	35.11	38.90	44.96	42.87
TMB conv. (wt%)	24.37	27.83	31.49	36.12	39.57
Xylene yield (wt%)	11.30	16.12	19.18	21.06	22.90
Xylene selectivity(wt%)	49.45	54.75	57.71	55.13	57.96
1,2,3 and 1,3,5 TMB isomers yield (wt%)	9.22	10.14	10.47	12.63	12.84

Reaction conditions: Pressure, 1 atm; reactant mole ratio,2.5; space time,4.44 kg h/kmol; catalyst,2 g CeX_{10}; N_2: feed flow rate,0.74.

5.2.2.4 Effect of TMB to toluene mole ratio

The transalkylation reactions were carried out by varying TMB to toluene mole ratio from 0.45 to 3.1 at a reaction temperature of 723K and space time of 4.44 kg.h/k mol. As shown in Figure 5.16, the toluene conversion passes through a maximum at a reactant mole ratio of 2.5. Above this mole ratio of TMB to toluene, excess reactant covers the maximum number of the active sites of the catalysts. Toluene being a limiting reactant is less available at catalytic sites which lead to a decrease in the conversion of toluene at higher mole ratio. Xylene selectivity and yield were found to be maximum around equimolar TMB to toluene ratio. This shows that xylene yield is due to transalkylation of toluene and trimethylbenzene rather than

disproportionation of TMB. The number of alkyl groups increases in the reaction system with higher amount of TMB in the reaction feed stock which leads to the formation of more side products like TeMB. Also, increase in 1,2,4 TMB molecules causes an increase in isomerisation product (1,3,5 TMB and1,2,3 TMB) which leads to decrease in xylene selectivity and yield. 1,3,5/1,2,3 TMB and para/ortho xylene ratio is found to decrease with increase in TMB in the feed stock. It is observed that transalkylation is favoured at lower or equimolar reactant ratio while an increase in reactant ratio results in disproportionation and isomerisation.

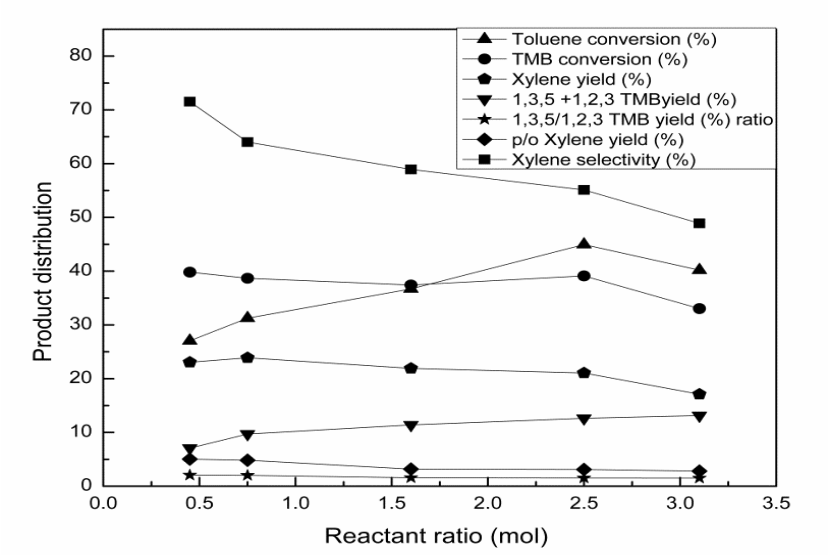

Figure 5.16: Effect of reactant ratio on product distribution over CeX_{10} zeolite catalyst. Reaction conditions: Pressure- 1 atm, temperature- 723K, space time- 4.44 kg h/kmol, catalyst- 2 g CeX_{10}, N_2: feed flow rate- 0.74.

5.2.2.5 Effect of space time

The effect of space time was studied by varying the flow rate of the reactant feed mixture. The range chosen for study was 1.19 – 4.44 kg h/kmol at a temperature of 723K and reactant ratio of 2.5. Toluene conversion is found to increase with increase in space time. The higher contact time allows the reactant molecules to stay over the catalyst for long time which favors the reactants to get enough time to react with each other resulting in higher yield of products at higher space time. The product distribution is given in Table 5.11. With increase in space time, the product yield from isomerisation and disproportionation reactions increases which is evidence from the increase in yield of TMB isomers and benzene. As xylene is produced by disproportionation of TMB in addition to transalkylation with toluene, thus xylene yield and

selectivity both are increased with increase in contact time. Effect of space time on toluene conversion at various temperatures were also studied and is represented in Figure 5.17.

Table 5.11- Product distribution of toluene-1,2,4 trimethylbenzene transalkylation at different space time at 723K over CeX_{10} zeolite catalyst

Product distribution (wt%)	**Space time (kg h/kmol)**				
	1.19	2.70	3.47	4.16	4.44
Benzene	1.12	1.23	1.45	1.69	1.88
Toluene	17.83	16.50	14.80	13.7	12.90
Xylene					
Para	6.79	9.82	10.9	12.47	15.94
Ortho	1.23	2.19	3.54	4.53	5.12
TMB					
1,3,5-	5.67	6.14	6.90	7.23	7.66
1,2,4-	62.54	58.46	56.13	53.47	48.9
1,2,3-	2.93	3.56	3.98	4.42	4.97
TeMB	1.89	2.10	2.30	2.49	2.63
Toluene conv. (wt%)	23.90	29.6	36.86	41.76	44.96
TMB conv. (wt%)	18.31	23.64	26.68	30.15	36.12
Xylene yield (wt%)	8.02	12.01	14.44	17.00	21.06
Xylene selectivity (wt%)	40.85	47.96	49.67	51.78	55.13

Reaction conditions: Pressure, 1 atm; temperature, 723 K; reactant mole ratio, 2.5; catalyst, 2 g CeX_{10}; N_2: feed flow rate,0.74.

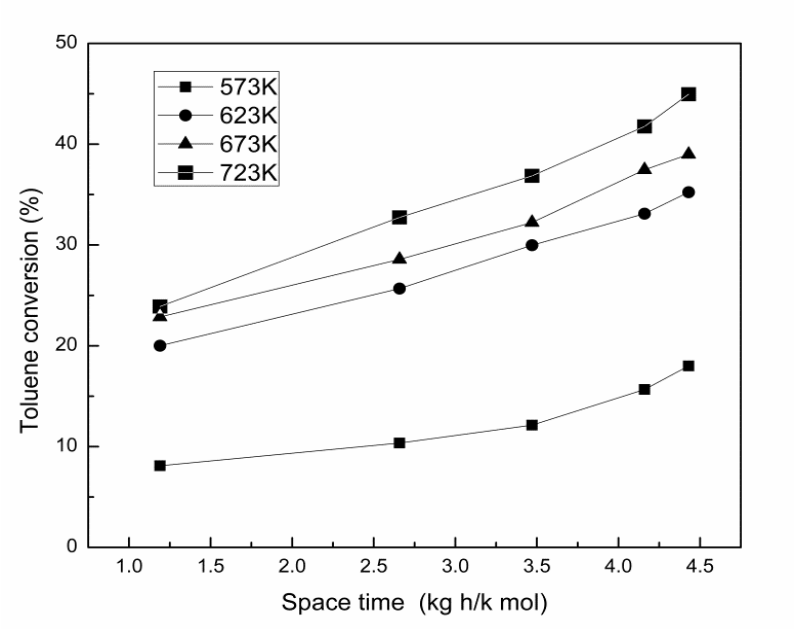

Figure 5.17: **Effect of space time on toluene conversion at various temperatures over CeX_{10} zeolite catalyst.** Reaction conditions: Pressure- 1 atm, temperature- 723 K, reactant mole ratio- 2.5, catalyst- 2 g CeX_{10}, N_2: feed flow rate- 0.74.

5.2.3. KINETIC STUDY

5.2.3.1 Mass transfer considerations

To investigate external diffusional effects, experiments were carried out over the different weight of the catalyst (2 g and 4 g) at constant space-time. Feed rates were varied during the reaction so as to keep the space time constant. The results are represented in Figure 5.18. The results show that toluene conversion remains almost same in both the cases which confirm complete absence of external diffusional resistance.

To find the intraparticle diffusional effects, experiments were carried with catalyst having different particle size. Toluene conversion was found to remain same over different catalyst size (Figure 5.19). This determines that the particle sizes employed in the kinetic study were within the intraparticle diffusion free range.

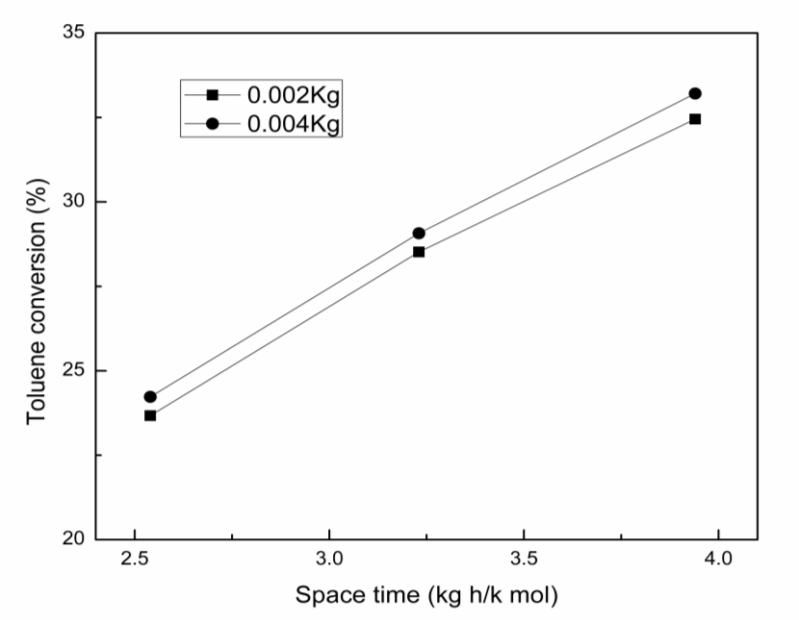

Figure 5.18: **Effect of External diffusion.** Reaction condition: Reaction temperature- 623 K, reactant mole ratio- 2.5:1, catalyst- CeX_{10}, N_2 to feed ratio- 0.74.

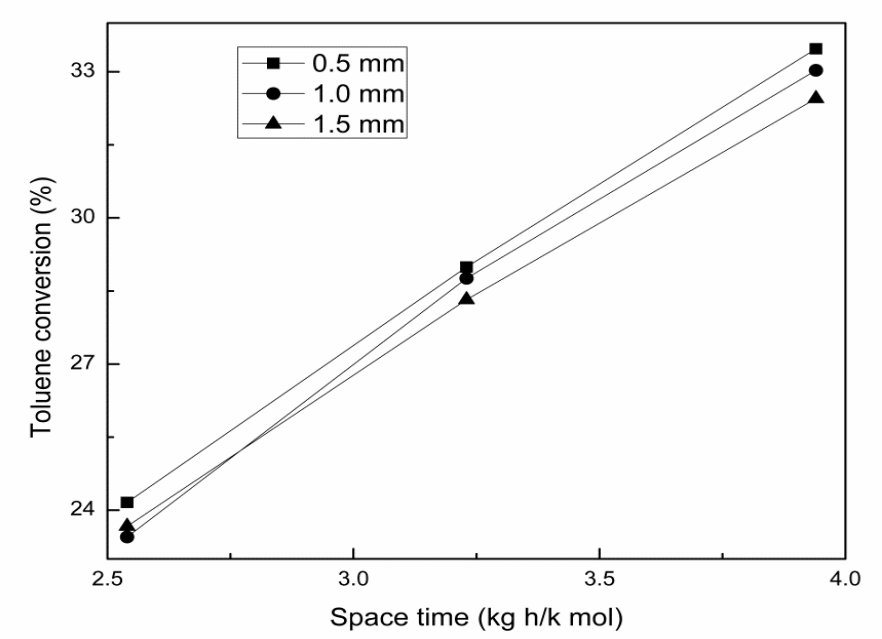

Figure 5.19: **Effect of internal diffusion.** Reaction conditions: Pressure- 1 atm, temperature- 623 K, reactant mole ratio- 2.5, catalyst- 2 g CeX_{10}, N_2: feed flow rate- 0.74.

5.2.3.2 Kinetic study

To study the reaction kinetics, transalkylation reaction was performed in the presence of CeX_{10} catalyst at different reaction temperatures (573-748K). For all kinetic runs, TMB to

toluene molar ratio was kept constant at 2.5, whereas nitrogen to $Feed_{Tol}$ ratio was maintained at 0.74. For each temperature, $W/F_{Tol,}$ (space time) was varied by keeping the weight of the catalyst constant and changing the flow rate of the feed. As seen from the Figure 5.20, toluene conversion increases with W/F_{Tol} at all four temperatures. In the first attempt, the simplest available correlation for rate expression was obtained by choosing the n^{th} order kinetics to represent the surface kinetics. In the present case, since trimethylbenzene in the feed is in excess, irreversible pseudo-first order reaction was assumed on the basis of toluene. Following the pseudo-first order kinetics, graph of $-ln(1-X_T)$ *vs t* was plotted and is shown in Figure 5.20. The linear nature of these plots supported that the (pseudo) first order kinetics fits the data reasonably well. From the slope of each line data value of rate constant was calculated at different temperatures. The kinetic constants derived were used to found the activation energy, using the following Arrhenius equation (44). Activation energy (E_a) was evaluated from the slope of the graph between lnk *vs* 1/T (Figure 5.21). The values of E_a and A (Frequency factor) from the plot was found to be 59.22 kJ/mol and 2.1×10^7.

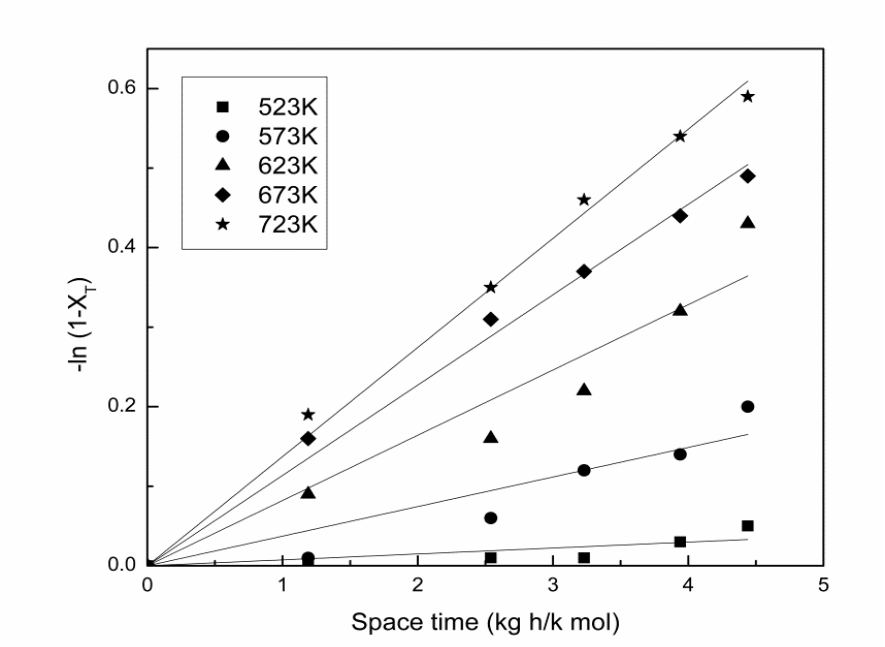

Figure 5.20: Plots of $-ln(1-X_T)$ *vs* time for toluene-1,2,4 trimethylbenzene transalkylation at different temperatures over CeX_{10} zeolite catalyst

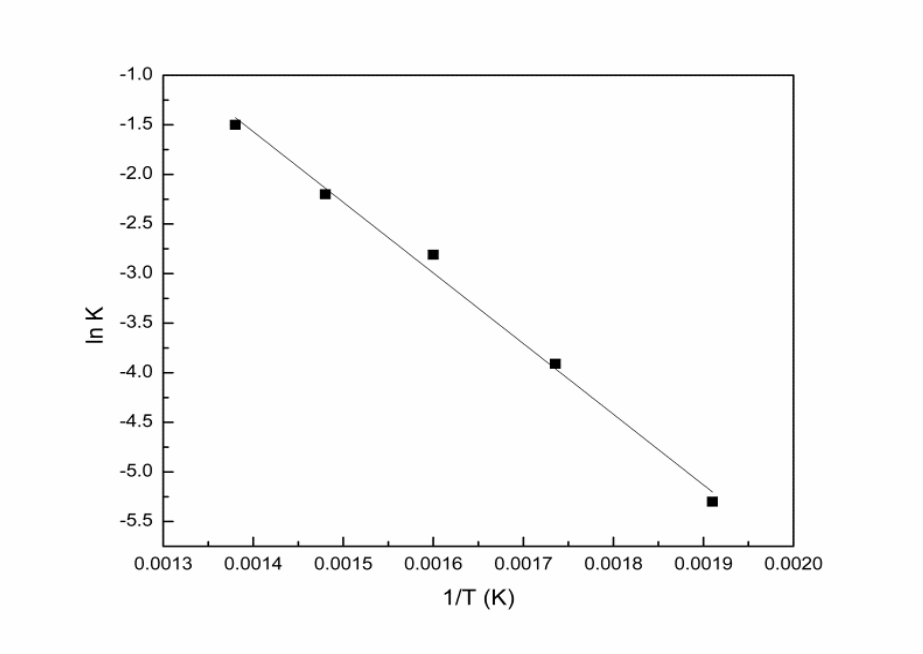

Figure 5.21: **Arrehenius Plot for toluene-1,2,4 trimethylbenzene over CeX_{10} zeolite catalyst**

5.2.3.3 Kinetic modeling

Langmuir-Hinshelwood-Hougen-Watson model

LHHW model was fitted to evaluate various rate constants of different reactions. LHHW model with surface reaction following dual site mechanism (derived in 5.1.3.2) was found to fit the kinetic data significantly better than the other models.

Net rate of disappearance of Toluene $= C_v^2\,[k_1\,k_T\,p_T\;\;k_{TMB}\,p_{TMB}\;+\;k_2 k_T^2 p_T^2\,]$

The partial pressures in the equations were calculated using the fractional conversions and total pressure P as given by following expressions.

$$p_T = (\,1 - X_T\,)P/\;6.09 \tag{47}$$

$$p_{Tmb} = (\,2.5 - X_{Tmb}\,)P/\;6.09 \tag{48}$$

$$p_{p-xyl} = \left(X_{p-xyl}\right)P/\;6.09 \tag{49}$$

$$p_{o-xyl} = \left(X_{o-xyl}\right)P/\;6.09 \tag{50}$$

$$p_{1,3,5TMB} = \left(X_{1,3,5TMB}\right)P/\ 6.09 \quad (51)$$

$$p_{1,2,3TMB} = \left(X_{1,2,3TMB}\right)P/\ 6.09 \quad (52)$$

$$p_{TeMB} = \left(X_{TeMB}\right)P/\ 6.09 \quad (53)$$

The total number of moles of different components present in the reaction system was found to be 6.09. A non-linear regression method was used for model parameter estimation. The optimum value of the parameters was estimated by minimizing the objective function given by equation (43).

For model equation, the standard error of estimate for the rate of disappearance of toluene was 3.02×10^{-4} which was calculated using the values of constants from Table 5.12. Figure 5.22 shows experimental and predicted rate are quite comparable having an R^2 value of 0.96.

Table 5.12- Kinetic and adsorption parameters for dual site mechanism for toluene-1,2,4 trimethylbenzene transalkylation over CeX_{10} zeolite catalyst

Kinetic and adsorption parameters	**Temperature(K)**			
	573	**623**	**673**	**723**
k_1 ((kmol/kg h)	1.50	6.93	10.54	25.99
k_2 (kmol/kg h)	0.81	4.54	7.12	17.48
K_T (atm^{-1})	1.04	0.92	0.81	0.769
K_{TMB} (atm^{-1})	0.57	0.20	0.09	0.034

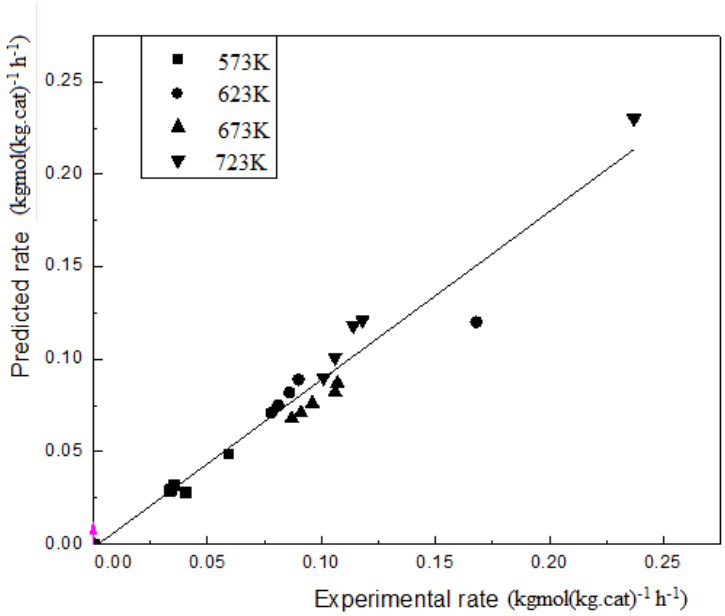

Figure 5.22: Experimental vs predicted values of reaction rate of toluene conversion for xylene production over CeX_{10} zeolite catalyst

Table 5.13- Activation energy and pre-exponential factors for different reactions over CeX_{10} zeolite catalyst

Reaction	E_a (kJ/mol)	Pre exponential factor
Transalkylation reaction	62.345	0.81×10^6
Toluene disproportionation	67.71	1.5×10^6

Activation energy for transalkylation reaction and disproportionation reaction over CeX_{10} catalyst are reported in Table 5.13. The value of activation energy varying from 46 to 104.6 kJ/mol in the temperature range 483–543 K for the transalkylation of *m*-diethylbenzene over beta zeolite are reported [Forni *et al*., 1995]. Thermodynamic adsorption parameters like enthalpy and entropy of adsorption were calculated using the eqiation (45). The values of enthalpy and entropy change are reported in Table 5.14. The adsorption equilibrium constants are plotted in Figure 5.23 which shows a satisfactory trend.

Table 5.14- Thermodynamic adsorption parameters for toluene-1,2,4 trimethylbenzene transalkylation over CeX_{10} zeolite catalyst

Reactants	ΔHads (kJ/mol)	ΔSads (J/mol K)
Toluene	-7.019	-11.97
1,2,4 TMB	-13.88	-28.18

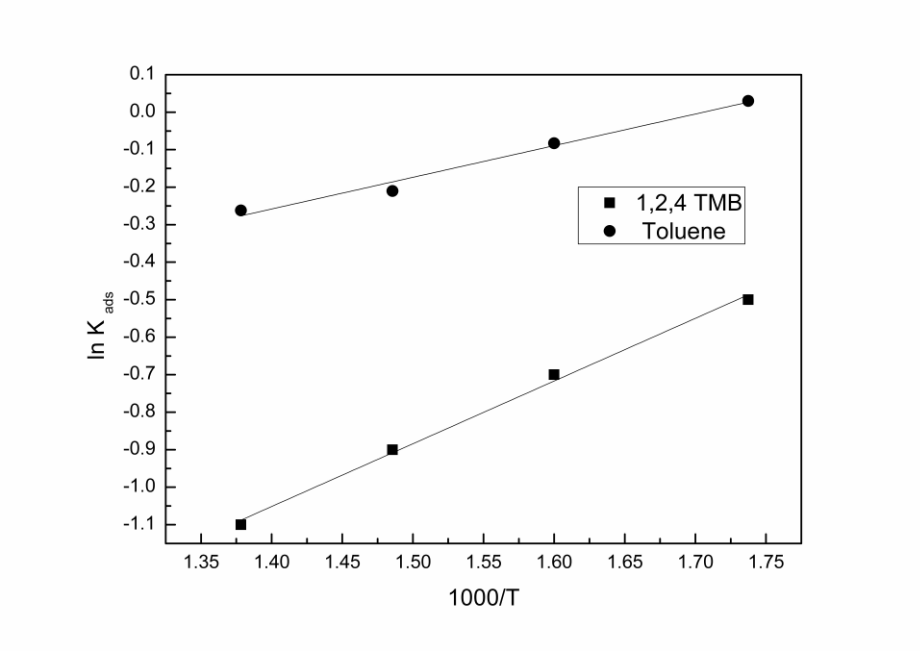

Figure 5.23: **Arrhenius plot for adsorption equilibrium constants for toluene-1,2,4 trimethylbenzene over CeX_{10} zeolite catalyst**

5.2.3.4 Deactivation kinetics

To study the deactivation kinetics similar method was followed as described in section 5.1.3.3. The deactivation constant was determined using equation (46). A plot of $\ln[\ln(C_{A0}/C_A)]$ vs t using CeX_{10} catalyst at four temperatures is shown in Figure 5.24; the slopes of the lines at different temperatures represent the deactivation constant k_d. The apparent activation energy for deactivation of catalyst which was found to be 14.3 kJ/kmol.

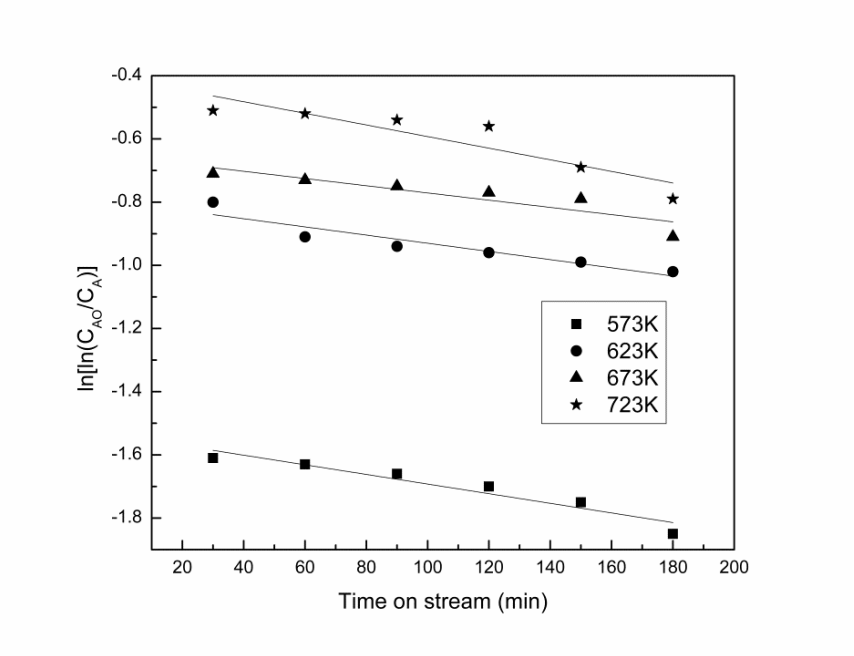

Figure 5.24: Plots of ln[ln(C_{AO}/C_A) *vs* time at different temperatures for toluene-1,2,4 trimethylbenzene over CeX_{10} zeolite catalyst

5.2.4 CONCLUSION

Trimethylbenzene transalkylation with toluene was carried out over cerium modified large-pore NaX zeolite. Differences in catalytic activity of parent zeolite and modified zeolite were pronounced with time on stream study. Maximum toluene conversion over modified zeolite was found to be 45% which was much higher than parent zeolite (21.28%). Modification of zeolite with cerium brings significant improvement in the activity of catalyst and selectivity of the product. Zeolite modified with cerium possesses higher reactant conversion (45%), product yield (21%) and selectivity (55%) compared to unmodified zeolite. Cerium modified large pore zeolite show higher activity and less deactivation at temperature range of 623-723 K as compared with 773 K. At high reaction temperature of 773 K isomerisation and disproportionation of TMB is favoured. Low reactant ratio favours high xylene yield and selectivity. Based on the product distribution, a reaction mechanism was proposed together with a rate expression for the disappearance of toluene using LHHW approach. The kinetic and the adsorption constants of the rate equation during their various transformation reactions were estimated by the best fit. The activation energy for the xylene synthesis reaction was determined to be around 60 kJ/mol. Catalyst deactivation constant based on time on stream was also found which was much lower than the reaction constants.

In transalkylation of toluene with TMB, metal exchanged Hbeta and NaX zeolites were found to be highly active than the parent zeolites. Catalytic performance of cerium modified beta zeolite was found superior than cerium modified NaX zeolite. Cerium modified large pore beta zeolite shows highest activity at 698 K giving a maximum toluene conversion of 58.7% compare to CeX (45%) at 723 K. Maximum xylene yield (29.02%) and xylene selectivity (64.17%) were achieved at 698 K, TMB/toluene mole ratio of 3:1, 2.91 kg h/kmol space time, over CeB which were higher than xylene yield (21.06%) and xylene selectivity (55.13%) over CeX zeolite at 723 K, TMB/toluene mole ratio of 2.5:1, 4.44 kg h/kmol space time. The activation energy for the xylene synthesis reaction over CeB and CeX zeolite was estimated to be 122.4 kJ/mol and 62.3 kJ/mol respectively, whereas the value of deactivation energy was 27.85 kJ/mol and 14.3 kJ/mol respectively.

5.3 Optimization of Process Parameters for Transalkylation of Toluene to Xylene using Response Surface Methodology

5.3.1 INTRODUCTION

Transalkylation of TMB and toluene is a complex reaction including disproportionation, dealkylation and isomerisation reactions. The outcome of this process depends on a number of parameters (factors) like time, temperature, pressure, reactant concentration, and catalyst properties. Many investigators have studied this transalkylation reaction over various kinds of catalysts through conventional optimization by varying one parameter at a time and maintaining other factors constant [Dumitriu *et al*., 2002; Tsai *et al*., 2002; Khattaf *et al*., 2007; Krejci *et al*., 2010]. Response surface methodology (RSM) is a statistical technique for modeling and optimization of multiple variables by combining experimental design with interpolation by first- or second-order polynomial equations [Fang *et al*., 2010]. The main advantage of RSM is evaluation of multiple parameters and their interactions. RSM has been successfully applied for the optimization of many bioprocesses [Canattieri *et al*., 2007; Anupama *et al*., 2010; Fang *et al*., 2010], physical processes like adsorption [Gottipati and Susmita, 2012], chemical processes like alkylation [Hafizi *et al*., 2012; Elavarasan *et al*., 2009] and synthesis of carbon nanotubes [Angulakshmi *et al*., 2012].

There is no study available in the literature for the optimization of the transalkylation reaction system using a statistical tool like RSM which helps in understanding the interactions among the parameters. RSM is used to predict the optimum conditions giving maximum reactant (toluene) conversion and product (xylene) selectivity. The Box-Behnken design is used for fitting of the response surfaces. The Box-Behnkehn design generates a second degree polynomial for optimizing a process using a small number of experimental runs. In general, the number of experimental points is given by $2k\ (k-1) + C_0$, where, k is the factor number and C_0 is the number of replications at the centre points [Ferreira *et al*., 2007]. The experimental data was analyzed by the response surface technique of Design Expert to fit the following second-order polynomial equation:

$$Y = a_0 + a_1x_1 + a_2x_2 + a_3x_3 + a_{12}x_1x_2 + a_{13}x_1x_3 + a_{23}x_2x_3 + a_{11}x_1^2 + a_{22}x_2^2 + a_{33}x_3^2 \quad (54)$$

where, Y denotes the predicted response (percent conversion and selectivity), x_1, x_2, x_3 are independent variables, a_0 is offset term, coefficients a_1, a_2, a_3 are for linear effects, a_{12}, a_{13}, a_{23}

are interaction coefficients, and a_{11}, a_{22}, a_{33} are quadratic interaction coefficients. Statistical analysis of the model was performed to carry out the analysis of variance.

5.3.2 EXPERIMENTAL

Cerium modified beta zeolite was used as catalyst for transalkylation reaction. The range of variables (temperature: 300-500 ºC, reactant ratio: 0.5-3.5, space time 2.7-5.2 kg h/kmol) were selected on the basis of values given in the literature for transalkylation of toluene with 1,2,4 TMB using similar catalysts [Dumitriu *et al*., 2002; Khattaf *et al*., 2007; Krejci *et al*., 2010].

Design of Experiment and Statistical Analysis

A 3-level-3-factor Box- Behnken design of Design expert 6.0.8 software with three replicates at the centre point was employed in this study. The design expert software generated a set of 15 experiments using different combinations of variables values. The experimental runs were conducted at these conditions. The results were used to estimate the relationship of toluene conversion and xylene selectivity with the combined effect of temperature, reactant ratio and space time. To avoid any bias, all the experiments were run in a random manner.

5.3.3 RESULTS AND DISCUSSION

5.3.3.1 Optimization of reaction conditions and data analysis

The codes of various variables and the ranges chosen for study are given in Table 5.15. The results of 15 experiments carried out for different reaction conditions are summarized in Table 5.16. The above mentioned second degree polynomial (equation 54) was fitted to the data using DOE software to determine the optimum conditions that resulted in the maximum toluene conversion and xylene selectivity.

Table 5.15- Parameter levels and coded values used for DOE

Factor	**Symbol**	**Range and level**		
		-1	0	+1
Temperature (°C)	x_1	300	400	500
Reactant ratio	x_2	0.5	2	3.5
Spacetime (Kg h/Kmol)	x_3	2.7	3.95	5.2

Table 5.16- Experimental design and response values

Run no.	x_1	x_2	x_3	Toluene conversion	Predicted conversion	Xylene selectivity	Predicted selectivity
1.	-1	0	+1	57.87	57.31	57.56	57.64
2.	0	0	0	76.45	75.54	76.87	75.39
3.	-1	0	-1	45.55	44.99	41.45	41.53
4.	+1	0	-1	56.42	56.98	45.34	45.26
5.	0	+1	-1	61.13	61.13	31.22	30.63
6.	+1	-1	0	54.22	53.66	60.01	59.50
7.	0	-1	+1	61.22	61.22	78.98	79.57
8.	0	0	0	75.15	75.54	76.65	75.39
9.	-1	-1	0	38.11	38.67	59.87	59.20
10.	0	0	0	75.01	75.54	72.65	75.29
11.	-1	+1	0	58.44	59.00	39.99	40.5
12.	+1	0	+1	67.87	68.43	54.34	54.26
13.	0	+1	+1	67.12	67.12	58.78	58.19
14.	0	-1	-1	52.12	52.12	46.31	46.90
15.	+1	+1	0	67.66	68.03	39.87	40.54

By applying multiple regression analysis on the experimental data, the following second degree polynomial was found to represent the relationship between response variables (toluene conversion and xylene selectivity) and process variables.

For toluene conversion

$$Y = 75.54 + 5.77x_1 + 6.08x_2 + 4.86x_3 - 1.72x_1x_2 - 0.22x_1x_3 - 0.78x_2x_3 - 12.20x_1^2 - 8.73x_2^2 - 6.41x_3^2 \quad (55)$$

For xylene selectivity

$$Y = 75.39 + 0.086x_1 - 9.41x_2 + 10.67x_3 - 0.065x_1x_2 - 1.78x_3 - 1.28x_2x_3 - 14.80x_1^2 - 10.65x_2^2 - 10.92x_3^2 \quad (56)$$

The adequacy of the model was checked using analysis of variance (ANOVA). ANOVA tests the significance of the ratio of mean due to regression and mean square due to residual error.

Various statistical data were examined, including F statistics, R^2, p value, sum of squares, mean square and degree of freedom.

R^2 for toluene conversion and xylene selectivity was found to be 0.966 and 0.948 respectively, which measures goodness of fit of linear regression. The model F values for toluene conversion was 15.73 and for xylene selectivity was 10.21. These values indicate that the model is significant. The statistically significant p-values for model and various terms involved should be less than 0.05. The "Lack of fit" p-values (Prob>F) for toluene conversion and xylene selectivity were 0.0326 and 0.0989 respectively. Although the model F-values were significant but the response (toluene conversion) had a significant "Lack of fit". Therefore in order to improve the model fit, quadratic by linear terms were added to model equations. By adding the terms $x_1^2\ x_2$ and $x_1^2\ x_3$ to equation (55) and the term $x_1^2\ x_3$ to equation (56) an acceptable model was obtained. The resulting model equations are

For toluene conversion

$$Y = 75.54 + 5.77x_1 + 3.73x_2 + 3.77x_3 - 1.72x_1x_2 - 0.22x_1x_3 - 0.78x_2x_3 - 12.20x_1^2 - 8.73x_2^2 - 6.41x_3^2 + 4.71x_1^2x_2 + 2.71x_1^2x_3 \quad (57)$$

For xylene selectivity

$$Y = 75.39 + 0.086x_1 - 9.41x_2 + 15.06x_3 - 0.065x_1x_2 - 1.78x_3 - 1.28x_2x_3 - 14.80x_1^2 - 10.65x_2^2 - 10.92x_3^2 - 8.78x_1^2x_3 \quad (58)$$

ANOVA for toluene conversion and xylene selectivity is represented in Table 5.17 and 5.18 respectively. The model F values of 122.65 for toluene conversion and 91.88 for xylene selectivity, p-values of 0.0011 for toulene conversion and 0.0003 for xylene selectivity shows that the model is significant. From the data it is clear that, in case of toluene conversion all the selected factors and their interaction terms have significant effect on toluene conversion. However, in case of the xylene selectivity temperature having p-value more than 0.05 has no significant effect.

Table 5.17- ANOVA for quadratic model of toluene conversion

Sources	**Df**	**Sum of Squares**	**Mean Square**	**F value**	**P-value**	
Model	11	1685.31	153.21	122.65	0.0011	Significant
X_1	1	266.80	266.80	213.59	0.0007	
X_2	1	55.58	55.58	44.49	0.0069	
X_3	1	56.93	56.93	45.57	0.0066	
$X_1 X_2$	1	11.87	11.87	9.50	0.0540	
$X_1 X_3$	1	0.19	0.19	0.15	0.7231	
$X_2 X_3$	1	2.42	2.42	1.94	0.2584	
X_1^2	1	549.53	549.53	439.91	0.0002	
X_2^2	1	281.37	281.37	225.25	0.0006	
X_3^2	1	151.69	151.69	121.43	0.0016	
$X_1^2 X_2$	1	44.46	44.46	35.59	0.0094	
$X_1^2 X_3$	1	9.42	9.42	7.54	0.0710	
Residual	3	3.75	1.25			
Lack of Fit	1	2.49	2.49	3.94	0.1854	not significant
Pure Error	2	1.26	0.63			
Cor Total	14	1689.05				
Std. Dev.	1.12					
C.V. %	1.83					
R^2	0.9978					
Adj R^2	0.9896					
Adeq precision	36.88					

Table 5.18- ANOVA for quadratic model of xylene selectivity

Sources	**Df**	**Sum of Squares**	**Mean Square**	**F value**	**P value**	
Model	10	3246.90	324.69	91.88	0.0003	Significant
X_1	1	0.060	0.060	0.017	0.9030	
X_2	1	708.95	708.95	200.62	0.0001	
X_3	1	906.91	906.91	256.64	< 0.0001	
$X_1 X_2$	1	0.017	0.017	0.0047	0.9482	
$X_1 X_3$	1	12.64	12.64	3.58	0.1316	
$X_2 X_3$	1	6.53	6.53	1.85	0.2457	
X_1^2	1	809.04	809.04	228.95	0.0001	
X_2^2	1	418.99	418.99	118.57	0.0004	
X_3^2	1	439.89	439.89	124.48	0.0004	
$X_1^2 X_3$	1	154.18	154.18	43.63	0.0027	
Residual	4	14.14	3.53			
Lack of Fit	2	2.85	1.42	0.25	0.7984	non significant
Pure Error	2	11.29	5.64			
Cor Total	14	3261.04				
Std. Dev.	1.88					
C.V.%	3.36					
R^2	0.9957					
Adj R^2	0.9848					
Adeq precision	30.40					

R^2 values respectively for toluene conversion and xylene selectivity were found to be 0.997 and 0.995. Figures 5.25 and 5.26 show the relation between the experimental and predicted values for toluene conversion and xylene selectivity. The experimental values in these Figures are the measured response values for the experimental runs designed by Box-Behnken method whereas the predicted values are calculated by the proposed model equation. It is clear from these Figures that there is a good correlation between the experimental and predicted values of the responses.

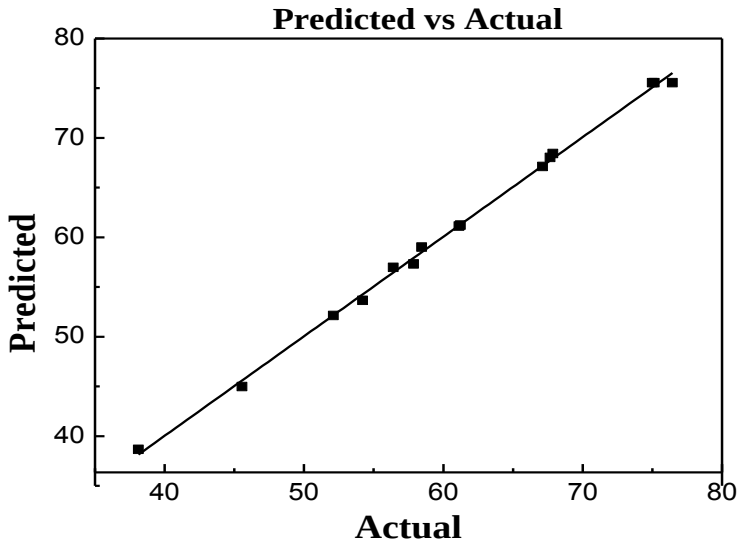

Figure 5.25: Comparison of experimental and predicted values for toluene conversion using RSM

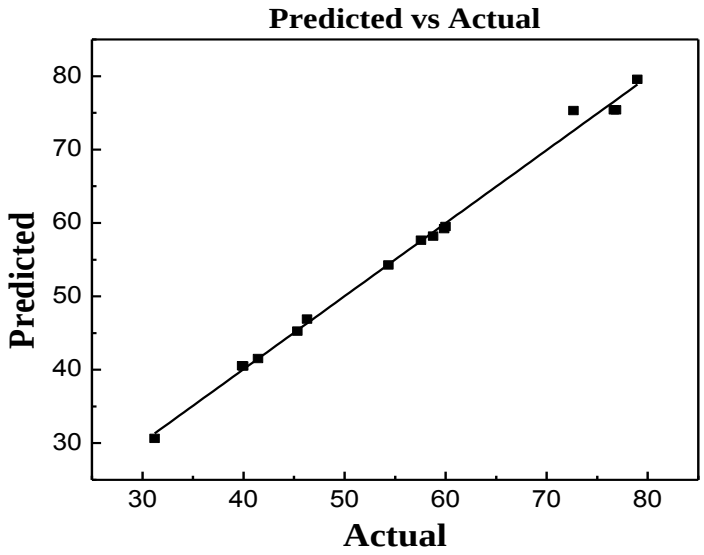

Figure 5.26: Comparison of experimental and predicted values for xylene selectivity using RSM

The lack of fit p-values (Prob>F) for toluene conversion and xylene selectivity are 0.1854 and 0.7984 respectively, show that the lack of fit is not significant. Adequate precision value is another criterion to check the accuracy of the model. It measures the signal to noise ratio and its value should be more than 4. Adequate precision values for toluene conversion and xylene selectivity are 36.88 and 30.40 respectively show adequate signal. The coefficients of

variance respectively for toluene conversion and xylene selectivity were 1.83 and 3.36. The low value of coefficient of variance shows the results were reliable and reproducible and the model was precise.

The response surface plot is a three dimensional plot which shows interaction effects of two variables within the selected range while keeping the third variable constant at the centre point. Figures 5.27 (a,b,c) and 5.28 (a,b,c) show response surface plots respectively for toluene conversion and xylene selectivity From these plots it is clear that each response surface has a clear peak and each contour plot is elliptical in shape with a clear highest point in the smallest curve of the plot depicting the optimum for the response variables lay in the design boundary. Figures 5.27 (a,b) show the response surface and contour plots for toluene conversion as a function of temperature. From these plots it is clear that moderate values of temperature favors high toluene conversion. The toluene conversion first increases with increase in temperature and after attaining maxima it decreases with further increase in temperature. The decline in conversion may be attributed to increased desorption rate of reactants from the catalyst surface at high temperature. Similar observation for this reaction system is reported in literature [Krejci *et al*., 2010]. Figures 5.27 (b,c) show that the conversion increases initially with increase in reactant ratio. Further increase in reactant ratio causes the conversion to decrease. This may be due to the fact that at high reactant ratio, most of the catalytic sites are occupied by TMB which lowers the availability of toluene at the catalytic sites; thus causing a decline in conversion. Similarly, Figures 5.27 (c,a) show that conversion is maximum at near higher values of space time. At low values of space time, conversion increases with increase in space time as the reactants remain in the reaction environment for more time.

The maximum toluene conversion of 76.58% is obtained at a temperature of 424 °C and reactant ratio of 2.30 (Figure 5.27 a). The maximum toluene conversion of about 76.79% is obtained at temperature of 425 °C and space time of 4.33 kg h/kmol (Figure 5.27 b). The maximum toluene conversion of about 76.44% is obtained at space time of 4.31 kg h/kmol and reactant ratio of 2.30 (Figure 5.27 c).

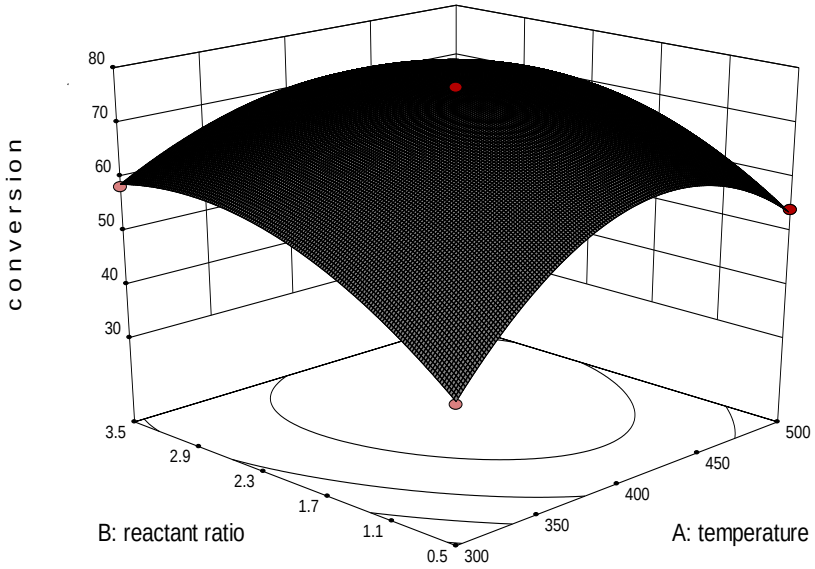
conversion
80
70
60
50
40
30
3.5
2.9
2.3
1.7
1.1
0.5
B: reactant ratio
300
350
400
450
500
A: temperature

(a)

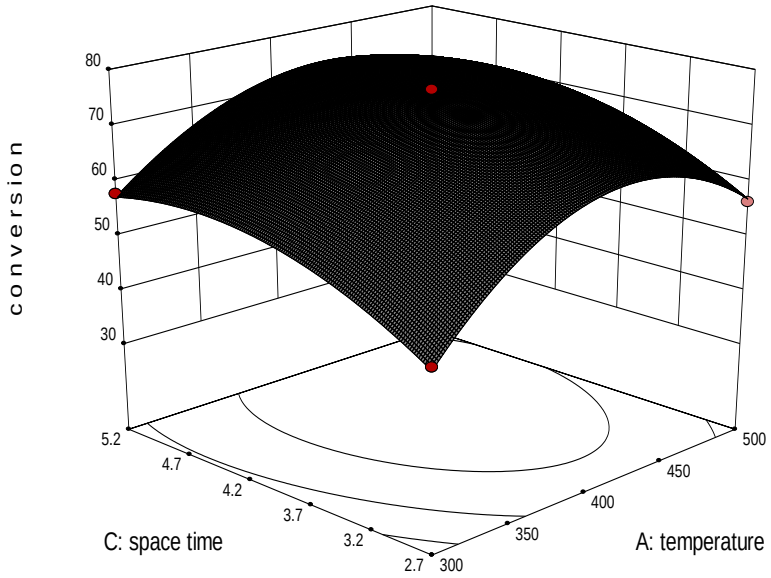
conversion
80
70
60
50
40
30
5.2
4.7
4.2
3.7
3.2
2.7
C: space time
300
350
400
450
500
A: temperature

(b)

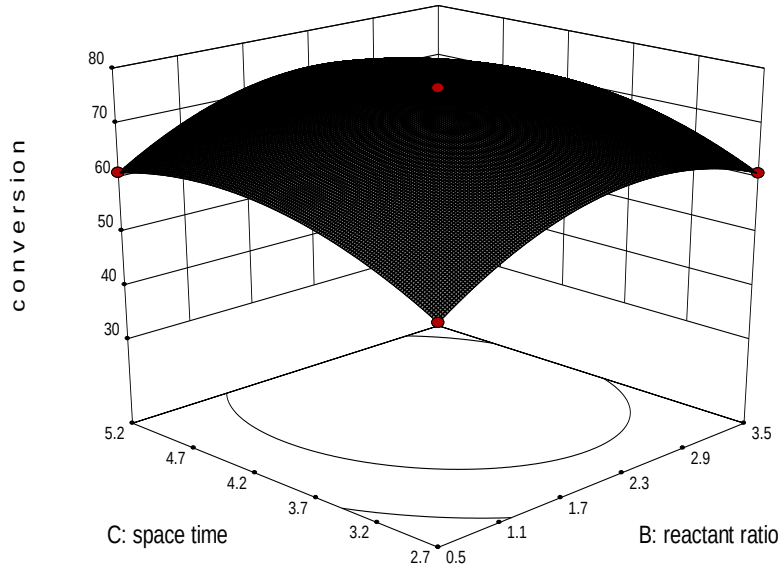

(c)

Figure 5.27: a. Effect of reactant ratio and temperature on toluene conversion. b. Effect of temperature and space time on toluene conversion. c. Effect of space time and reactant ratio on toluene conversion

The effect of temperature on xylene selectivity is shown in Figure 5.28 (a, b). It is clear from the Figures that xylene selectivity is not much influenced by recation temperature, as the secondary reactions' rates are also increasing with temperature. The Figures 5.28 (b, c) show a sharp decline in the selectivity with increase in the reactant ratio. This may be attributed to the fact that with more amount of TMB in the feed the yields of byproducts increases as TMB undergoes both disproportionation and isomerisation reactions. The effect of space time on xylene selectivity is depicted in Figures 5.28 (c, a). At very high values of space time, the secondary reactions occurring in the system causes the xylene selectivity to decrease.

Figure 5.28 (a) shows that a maximum xylene selectivity of 77.46% can be achieved at 400 ºC and reactant ratio of 1.32. As depicted in Figure 5.28 (b), a maximum selectivity of 80.59% can be obtained at 396 ºC and at a space time of 4.81 kg h/kmol. Maximum xylene selectivity of 83.07% can be obtained at a reactant ratio of 1.27 and a space time of 4.83 kg h/kmol [Figure 5.28 (c)].

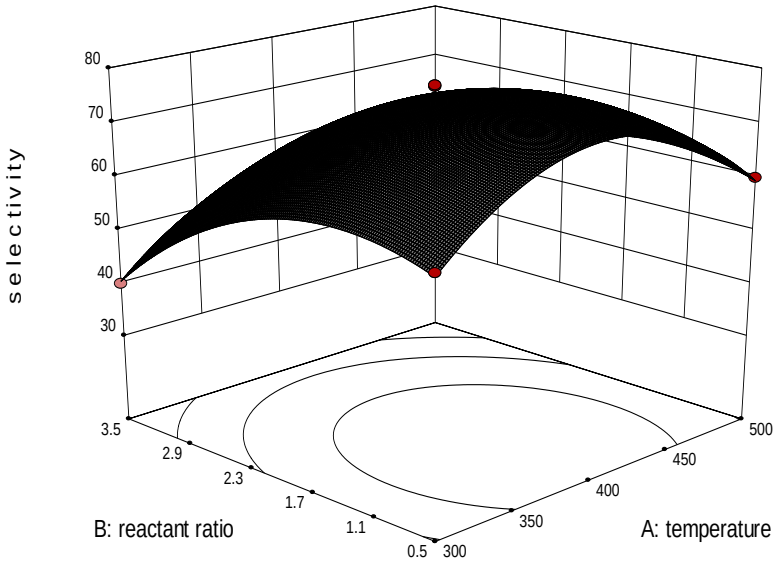
selectivity
80
70
60
50
40
30
3.5
2.9
2.3
1.7
1.1
0.5
B: reactant ratio
300
350
400
450
500
A: temperature

(a)

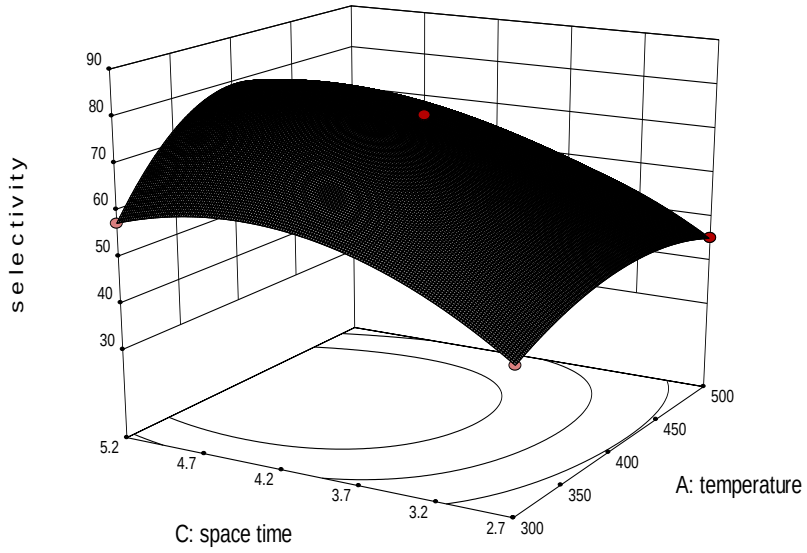
selectivity
90
80
70
60
50
40
30
5.2
4.7
4.2
3.7
3.2
2.7
C: space time
300
350
400
450
500
A: temperature

(b)

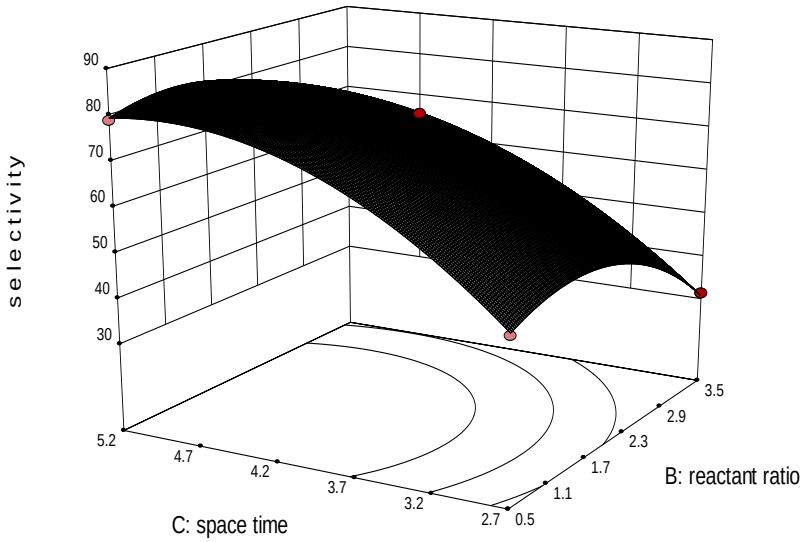

(c)

Figure 5.28: a. Effect of reactant ratio and temperature on xylene selectivity. b. Effect of space time and temperature on xylene selectivity. c. Effect of reactant ratio and space time on xylene selectivity.

Numerical optimization module of the RSM predicted the optimum conditions for the responses (toluene conversion and xylene selectivity). The predicted maximum toluene conversion was 76.51% and xylene selectivity was 79.27% at a temperature of 409.7 °C (~410 °C), reactant ratio of 2.024 (~2.0) and space time of 4.451 kg h/kmol(4.45). From the experimental run at optimized conditions predicted by the model, the toluene conversion of 75.83% and xylene selectivity of 78.62% were obtained which match closely with the results predicted by the model.

5.3.4 CONCLUSION

Box-Behnken method was used to investigate and optimize the effect of various process parameters (temperature, reactant ratio and space time) on toluene conversion and xylene selectivity. All the process variables selected for the study (temperature, reactant ratio and space time) have a significant effect on toluene conversion. The xylene selectivity was found not to vary appreciably with the reaction temperature. The optimum values of the reaction parameters, predicted by the model to maximize toluene conversion and xylene selectivity

are: temperature 409.7 °C (~410 °C), reactant ratio of 2.024 (~2.0) and space time of 4.451 kg h/kmol (4.45). At these conditions, the model predicted toluene conversion is 76.51% and xylene selectivity is 79.27%. There is a very close agreement between the responses predicted by RSM at optimized conditions and results of experiment run at these optimized conditions.

CHAPTER- 6

Transalkylation of Toluene with Cumene

This chapter deals with transalkylation of toluene with cumene over modified Hbeta and NaX zeolite. A comparative study was done to evaluate the catalytic performance of various beta and NaX zeolites modified with different rare earth metals lanthanum (La), cerium (Ce) and praseodymium (Pr) for gas-phase transalkylation reaction of toluene with cumene in a continuous plug flow reactor.

6.1 INTRODUCTION

Aromatics have numerous applications in the chemical and petrochemical industries [Odedairo and Khattaf, 2011]. The products of transalkylation reactions have commercial importance as they are derived from low valued by-products like toluene and benzene. Cymene is one such product which is derived by cumene-toluene transalkylation. Cymenes are important products because it leads to the production of number of end products like cresols, pharmaceuticals, pesticides, herbicides, fragrances, polymers and solvents [Welstead, 1978; Fraenkel and Levy., 1989; Reddy *et al*., 1995]. Cymene is also used as heat transfer media and a starting material in much organic synthesis [Derfer and Derfer, 1978]. Alkylation of toluene with propylene or isopropyl alcohol is a well known industrial route for cymene production. This method yields a mixture of cymene isomers (i.e. o-, m- and p-). The main disadvantage of this method of cymene production is that this method uses hazardous liquid catalysts such as H_2SO_4, $AlCl_3$, $TiCl_4$, supported alumina, supported H_3PO_4, supported titania [Meyer and Bernhauer, 1929; Cullinane and Leyshan, 1954; UOP, 1978; Sabu *et al*., 1973] etc. Various zeolites like ZSM-5, ZSM-12, ZSM-48,Y [Ismailov *et al*., 1973; Burres *et al*., 1980; Young, 1983; Flockhart *et al*., 1989] have also been reported for this reaction. The liquid catalysts are replaced by these solid acid catalysts as the solid catalysts are easy to regenerate, easy to separate from product and also have higher activity, selectivity and noncorrosiveness. Among benzene, toluene, and xylenes (BTX), the price of toluene is always the lowest. Therefore, an attempt to transalkylate low valued toluene to cymene is of great commercial value. The present study will focus on the catalytic performance of beta zeolite modified with rare earth metal ions. A simplified kinetic model was developed which will account for all the primary and secondary reactions.

Various products like aliphatics, benzene, toluene, xylene, cumene and cymene were identified for the said reaction. The proposed mechanism of toluene-cumene transalkylation is as follows (Figure 6.1):

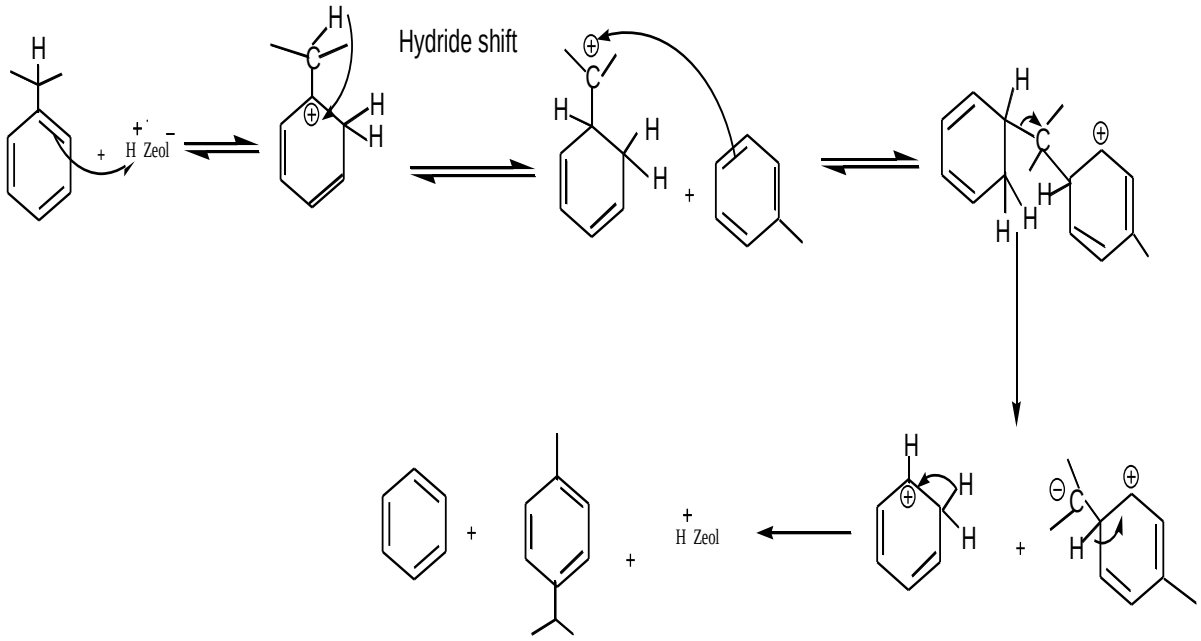

Figure 6.1: Proposed Mechanism of transalkylation of toluene with cumene

According to the product distribution, the transalkylation of toluene with cumene was accompanied with dispropotionation and isomerisation. These reactions are as follows:

(i) Transalkylation reaction

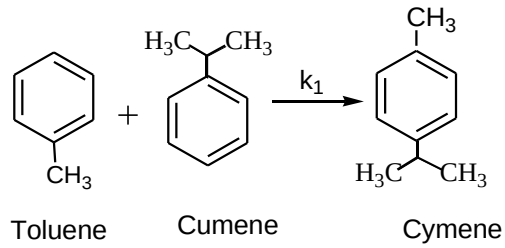

Toluene Cumene Cymene

(ii) Dealkylation

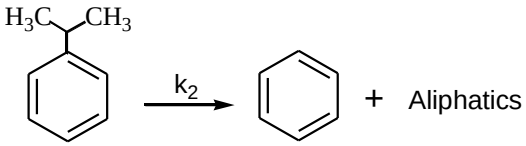

Cumene Benzene

(iii) Disproportionation

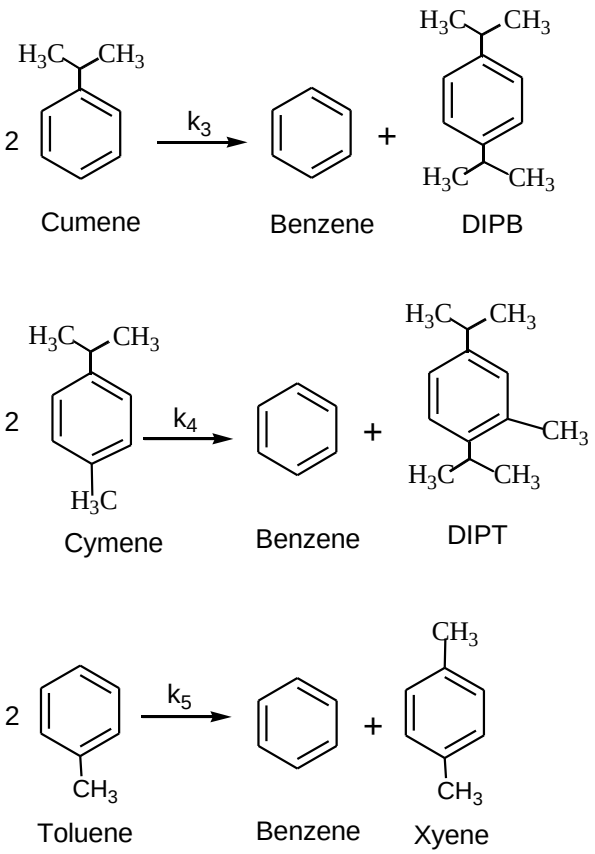

In this chemical reaction, **"cymene yield"** is the fraction of reactant converted to the cymene. The conversion of toluene and selectivity of xylene was calculated according to following formula:

$$\text{Cumene conversion} = \frac{\text{Cumene in feed} - \text{Cumene in exit}}{\text{Cumene in feed}} \times 100 \quad (59)$$

$$\text{Cymene selectivity} = \frac{\text{Cymene in product mixture}}{\text{Aromatics in products excluding toluene and cumene}} \times 100 \quad (60)$$

6.2 EXPERIMENTAL

Rare earth metals modified Hbeta and NaX zeolite were used as acid catalyst in the present study. The effect of various process parameters like metal loading (2-14 wt%), catalyst loading (1.44-8.63 w/w%), temperature (448-573 K), reactant ratio (1-15) and space time (3.2-9.29 kg h/kmol) on the conversion of reactant and selectivity of product were studied over modified large pore zeolites. To investigate external diffusional effects, experiments were carried out over different weight of catalyst (2 g and 4 g) at constant space-time. To find the intraparticle diffusional effects, experiments were carried out at constant space-time with different particle size ranging from 0.5-1.5 mm.

6.3 RESULTS AND DISCUSSION

From the catalyst characterization it was found that lanthanum, cerium and praseodymium ions have been incorporated into the Hbeta and NaX zeolite framework. All metal modified Hbeta and NaX zeolite were found to possess the same topology as of the parent zeolite which showed that the zeolite structure was preserved even after ion exchange. From SEM studies it was found that average particle size and paticle morphology was similar in all modified and unmodified zeolite catalysts. TPD results showed that praseodymium modification of Hbeta and NaX zeolite enhanced its acidity. PrB and PrX were found to have 1.91 mmol/gm and 1.33 mmol/gm acidity respectively. Among all modified and unmodified zeolites PrB possessed maximum acidity which resulted into better activity reflected in terms of better reactant conversion, product yield and selectivity.

6.3.1 Effect of zeolite activity on product distribution

Effect of nature of metal ion loading on beta and NaX zeolite catalyst on product distribution is shown in Figure 6.2. For 3 h time-on-stream it was observed that all the metal exchanged zeolites were active in catalyzing the transalkylation of cumene to cymene. Specifically, the catalytic activity decreases in the order: PrB> CeB> LaB> Hbeta> PrX> CeX> LaX>NaX. Difference in the activity of these zeolites may be attributed to the zeolite structure, acidity and nature of metal ions. From the graph, it is clear that beta zeolites show better results in transalkylation than NaX zeolites. As it was seen that the most active catalyst exhibits the highest acidity therefore, the activity of catalyst was directly related to the acidity of the catalyst. The best activity of PrB may be due to highest charge to size ratio of praseodymium ions which causes formation of high acidic sites which is also supported by TPD results. As praseodymium modified beta zeolite was found to be most active catalyst therefore, all the further runs were done using this catalyst.

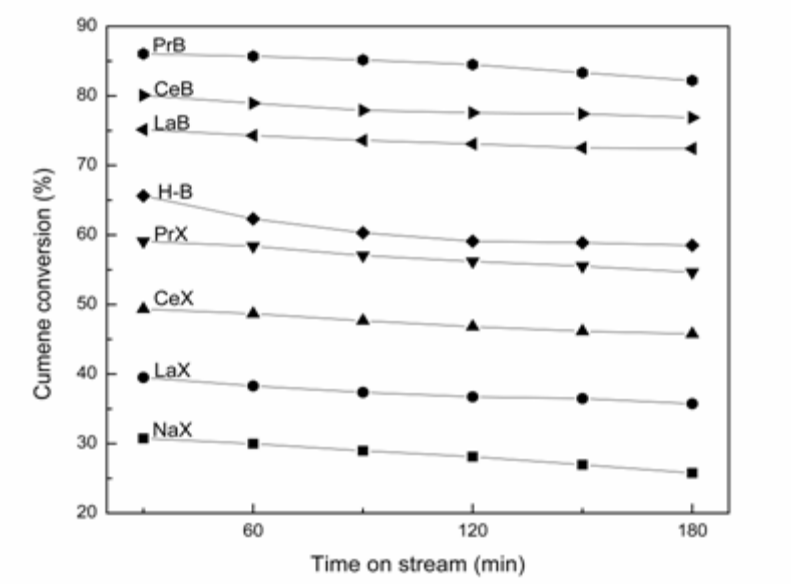

Figure 6.2: **Effect of rare earth metal ion modification on cumene conversion.** Reaction conditions: Pressure- 1 atm, Temperature – 523 K, Toluene/Cumene mole ratio– 9:1, space time –9.29 kg h/kmol, 2 g catalyst, N_2: feed flow rate - 0.20.

6.3.2 Effect of praseodymium loading in the zeolite

As it was observed from time-on-stream study that catalytic performance of PrB is superior than other catalyst. Therefore, to study the effect of praseodymium loading in beta zeolite, the zeolite catalyst was loaded with different concentration of praseodymium (2 wt%, 6 wt%, 10 wt% and 14 wt%) Effect of loading (2-14 wt%) in Hbeta zeolite catalyst on product distribution is shown in Figure 6.3. The Figure shows that cumene conversion increases with increase in praseodymium loading on the catalyst. However, the catalyst with praseodymium loading of 14 wt% showed considerable declination in cumene conversion with time-on-stream. This may be due to the fact that generated acid sites are very strong to initiate side reactions thereby increasing side products and coke which leads to deactivation of catalyst fastly. Therefore, further study was done using PrB_{10} catalyst.

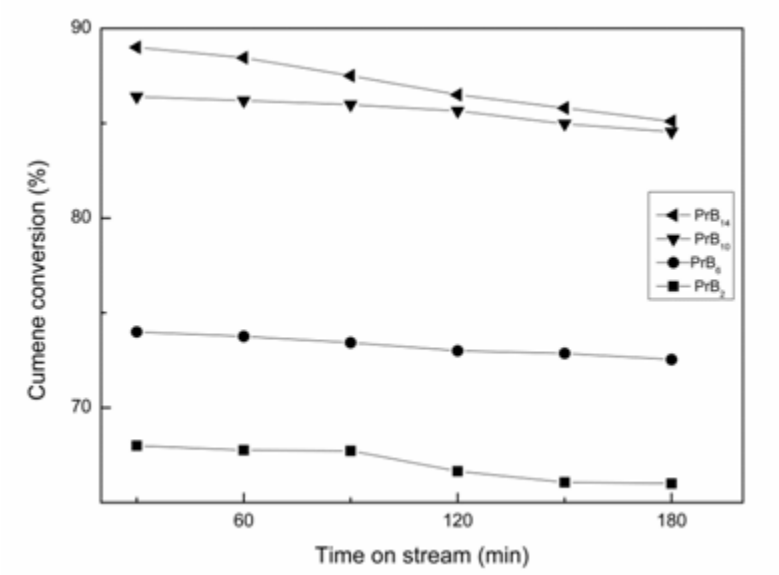

Figure 6.3: **Effect of praseodymium loading on cumene conversion.** Reaction conditions: Pressure- 1 atm, Temperature– 523 K, Toluene/Cumene mole ratio– 9:1, space time –9.29 kg h/kmol, 2 g catalyst, N_2: feed flow rate - 0.20.

6.3.3 Effect of catalyst loading in the reactor

Catalyst loading was varied from 1.44-8.63% (w/w) of the reactants as shown in the Figure 6.4. The conversion of reactant showed sharp increase with increase in catalyst loading from 1.44% (w/w) to 5.76% (w/w) very sharply due to the presence of large number of active sites available for the reactants. However, above catalyst loading of 5.76% (w/w) increase in cumene conversion was not significant (86.4-87.3 wt%) showing a increase of only 0.9 wt%. The 5.76% (w/w) loading of catalyst in the reactor is found to be optimum.

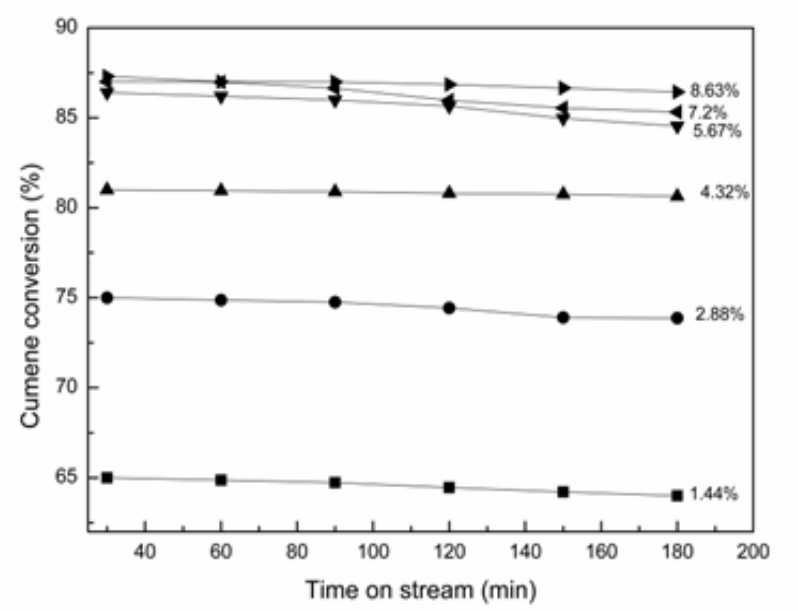

Figure 6.4: **Effect of catalyst loading (PrB_{10}) on cumene conversion in 3 h time-on-stream**. Reaction conditions: Pressure- 1 atm, Temperature- 523 K, Toluene/Cumene mole ratio- 9:1, space time - 9.29 kg h/kmol, N_2: feed flow rate - 0.20.

6.3.4 Effect of reaction temperature

To study the effect of reaction temperature on reactant conversion and product selectivity reactions were carried out in the temperature range of 448-573 K. The product distribution at different temperatures is summarized in Table 6.1 which shows that the reaction temperature has significant effects on product distribution. The cumene conversion increases with rise in temperature. However, the increase is not appreciable after 523 K showing a increase of only 2.2% (86.40-88.59%) up to 573 K. Also, cymene yield (16.21 wt%) and cymene selectivity (65.73 wt %)was found to be maximum at 523K. At higher temperature (723 K), side products like benzene, xylene and DIPT yield increases due to favored dealkylation and disproportionation reaction. Disproportionation of cumene and cymene was negligible as DIPB and DIPT was not formed in negligible amount. Among the side products, yield of benzene was maximum.

Table 6.1- Product distribution of toluene-cumene transalkylation over different temperatures over PrB_{10} zeolite catalyst

Product distribution (wt %)	Temperature(K)					
	448	**473**	**500**	**523**	**548**	**573**
Aliphatics	0.10	0.12	0.12	0.13	0.11	0.10
Benzene	2.98	4.93	5.84	7.12	7.89	8.03
Toluene	82.7	79.18	76.93	73.60	73.39	73.81
Xylene	0.09	0.10	0.17	0.21	0.32	0.54
Cumene	7.22	4.54	3.12	1.74	1.61	1.46
Cymene	6.21	10.32	12.92	16.21	15.43	14.83
DIPT	0.70	0.81	0.90	0.99	1.25	1.23
Cumene conv. (wt %)	43.60	64.52	75.62	86.40	87.42	88.59
Cymene selectivity(wt%)	61.60	63.40	64.76	65.73	61.72	60.00

Reaction conditions: Pressure, 1 atm; Toluene/Cumene mole ratio of – 9:1, space time – 9.29kg h/kmol, 2g catalyst, N_2: feed flow rate - 0.20.

6.3.5 Effect of reactant ratio

The transalkylation reactions were carried out by varying toluene to cumene mole ratio from 1 to 15 at a reaction temperature of 523 K and space time of 9.29 kg h/kmol. As shown in Figure 6.5, the cumene conversion was maximum (86.4 wt%) at a toluene to cumene mole ratio of 9:1. Above this mole ratio, the active sites are crowded by the excess reactant (toluene) which decrease the availability of active sites to limiting reactant (cumene) and hence lead to decrease in cumene conversion. Cymene selectivity was found to increase with increase in toluene to cumene mole ratio. Benzene yield decreases with increasing toluene to cumene mole ratio which shows that benzene is formed by dissosciation of cumene rather than toluene disproportionation.

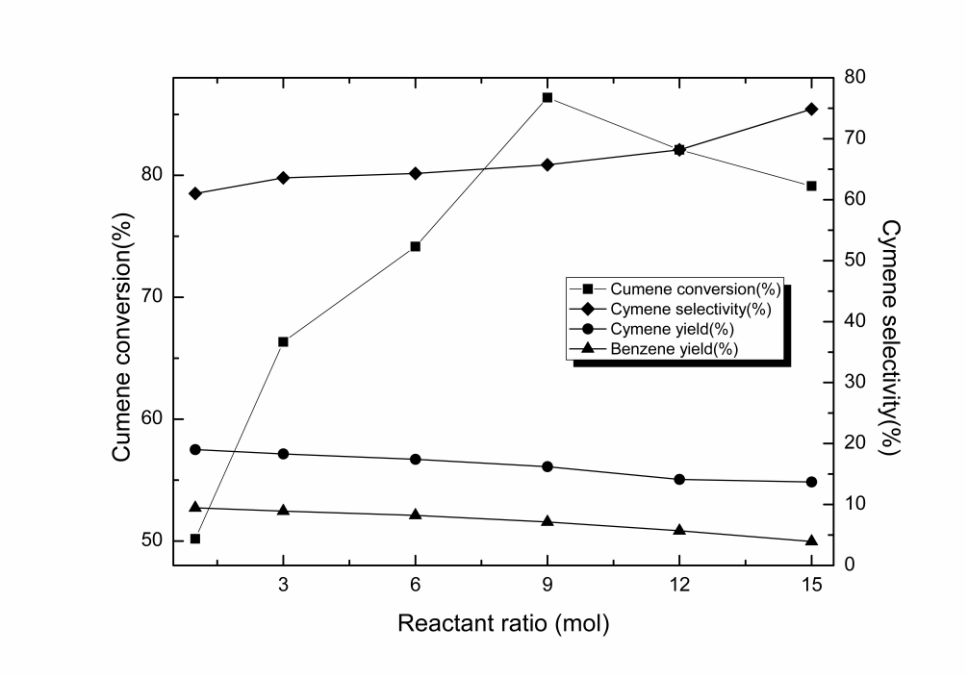

Figure 6.5: Effect of reactant ratio on product distribution over PrB_{10} zeolite catalyst. Reaction conditions: Pressure- 1 atm, Temperature– 523 K, 2 g catalyst, space time –9.29 kg h/kmol, N_2: feed flow rate - 0.20.

6.3.6 Effect of space time

The effect of space time was studied by keeping the weight of catalyst constant and varying the flow rate of the feed. The space time range chosen for study was 3.20 – 9.29 kg h/kmol at a temperature of 523 K and reactant ratio of 9:1. Cumene conversion was found to increase with increase in space time. The higher space time allows the reactant molecules to stay over the catalyst for enough time to react resulting in higher yield of the product. The product distribution is given in Table 6.2. With increase in space time, cymene yield and selectivity were also found to increase. Disproportionation of toluene and cymene both increased with increase in space time which is evident from high yield of side products.

Table 6.2- Product distribution of toluene-cumene transalkylation at different space time at 523K over PrB_{10} zeolite catalyst

Product distribution (wt%)	Space time (kg h/kmol)					
	3.2	**3.57**	**4.04**	**5.16**	**6.507**	**9.29**
Aliphatics	0.3	0.08	0.09	0.13	0.11	0.13
Benzene	4.29	5.08	5.30	6.63	6.82	7.12
Toluene	84.10	82.94	81.30	78.23	77.10	73.60
Xylene	0.0	0.11	0.14	0.17	0.19	0.21
Cumene	5.91	4.74	3.59	2.31	1.94	1.74
Cymene	5.19	7.03	9.14	11.9	13.03	16.21
DIPT	0.12	0.29	0.44	0.63	0.81	0.99
Cumene conv. (wt%)	53.82	62.96	71.95	81.95	84.84	86.40
Cymene selectivity (wt%)	51.95	52.84	60.50	61.15	62.17	65.73

Reaction conditions: Pressure, 1 atm; Temperature – 523 K, 2 g catalyst, N_2: feed flow rate - 0.20.

6.4. KINETICS OF TRANSALKYLATION

6.4.1 Mass transfer considerations

In any kinetic regime, the effect of external and internal mass transfer resistance should be negligible. Experiments were carried out using different amount of catalyst (2 g and 4 g) at constant space-time to investigate external diffusional effects. Feed rates were varied during the runs so as to keep the space time constant. The results are presented in Table 6.3. The results show that cumene conversion remains almost same in both the cases which confirms complete absence of external diffusional resistance.

To find the intraparticle diffusional effects, experiments were carried out at constant space-time with different particle size (0.5-1.5 mm). Cumene conversion remained same over different size of catalyst particles (Table 6.4). This showed that the catalyst used in the kinetic study was free from the intraparticle diffusion resistance.

Table 6.3- Effect of External diffusion for toluene-cumene transalkylation over PrB_{10} zeolite catalyst

Space-time (kg h/kmol)	Conversion of Cumene (%)	
	Catalyst weight = 0.002 kg	**Catalyst weight =0.004 kg**
4.04	62.78	63.49
5.16	66.58	67.18
6.20	70.40	71.23

Reaction conditions: Pressure- 1 atm, Reaction temperature – 498 K, Toluene/Cumene mole ratio of – 9:1, space time –9.29 kg h/kmol, PrB_{10} (1.5 mm) catalyst, N_2: feed flow rate - 0.20.

Table 6.4- Effect of Internal diffusion for toluene-cumene transalkylation over PrB_{10} zeolite catalyst

Particle size dp (mm)	Conversion of Cumene (%)		
	space-time(kg h/kmol) =4.04	**space-time(kg h/kmol) =5.16**	**space-time(kg h/kmol) =6.20**
0.50	63.56	62.73	71.43
1.00	63.18	66.98	70.91
1.50	62.78	66.98	70.40

Reaction conditions: Pressure- 1 atm, Reaction temperature – 498 K, Toluene/Cumene mole ratio of – 9:1, space time –9.29 kg h/kmol, PrB_{10} (1.5 mm) catalyst, N_2: feed flow rate - 0.20.

6.4.2 Kinetic modeling

Langmuir-Hinshelwood-Hougen-Watson model

The experimental data was fitted in LHHW model to evaluate various rate constants of hypothetical reaction scheme. It is seen from the product distribution, cymene and benzene are formed in fair amount. As DIPB was produced in negligible amount, cumene dispropotionation was neglected in the prepared model equations.

The dual site, single site and stoichiometric models rate equations were derived as following

Dual-site mechanism:

In dual site mechanism, both the reactants are assumed to be adsorbed on catalytic sites.

Cumene-toluene transalkylation: Cumene . C_v +Toluene . C_v ⟶ Cymene . C_v + Benzene . C_v

Dispropotionation: Cumene . C_v ⟶ Benzene . C_v + Aliphatics . C_v

Dissosciation: 2 Cumene . $2C_v$ ⟶ DIPPB . C_v + Toluene . C_v

A rate equation can be represented as,

$$Rate = k\, k_{ads} p_{reactant} C_v$$

Where, k is rate constant, k_{ads} is adsorption coefficient of any reactant, $p_{reactant}$ is partial pressure of any reactant, and C_v is concentration of vacant active sites available in the surface.

Total rate of disappearance of Cumene = Rate of Ist reaction + Rate of IInd reaction + Rate of IIIrd reaction (61)

$$\text{Rate of Ist reaction} = k_1 k_T p_T k_{Cum} p_{Cum} C_v^2 \quad (62)$$

$$\text{Rate of IInd reaction} = k_2 k_{Cum} p_{Cum} C_v \quad (63)$$

$$\text{Rate of IIIrd reaction} = k_3 k_{Cum}^2 p_{Cum}^2 C_v^2 \quad (64)$$

$$\text{Net rate} = k_1 k_T p_T k_{Cum} p_{Cum} C_v^2 + k_2 k_{Cum} p_{Cum} C_v + k_3 k_{Cum}^2 p_{Cum}^2 C_v^2 \quad (65)$$

$$= (C_v^2)\left[k_1\, K_t K_{cum} p_t p_{cum} + \left(\frac{k_2}{C_v}\right) K_{cum} p_{cum} + k_3\, (K_{cum}^2)(p_{cum}^2)\right] \quad (66)$$

$$= \left(\frac{1}{Z}\right)^2 \left[k_1\, K_t K_{cum} p_t p_{cum} + \left(\frac{k_2}{C_v}\right) K_{cum} p_{cum} + k_3\, (K_{cum}^2)(p_{cum}^2)\right] \quad (67)$$

Where, $C_v = \frac{1}{1 + K_{Cum} p_{Cum} + K_T p_T}$ (68)

Where p_{Cum} and p_T were calculated from the values of concentration of the reactants and C_v was calculated as follows,

$$C_t = C_v + C_{T.S} + C_{Cum.S} \quad (69)$$

$$C_t = C_v + k_{T.} C_T C_v + k_{Cum} C_{Cum} C_v \quad (70)$$

$$= C_v[\,1 + k_{T.} C_T + k_{Cum} C_{Cum}] \quad (71)$$

$$C_v = \frac{C_t}{1 + k_{T.} C_T + k_{Cum} C_{Cum}} \quad (72)$$

As total number of sites are equal to 1,

$$C_v = \frac{1}{1+k_{T.}C_T+k_{Cum}C_{Cum}} \quad (73)$$

$$C_v = \frac{1}{Z}$$

$$Z = 1 + k_{T.}C_T + k_{Cum}C_{Cum} \quad (74)$$

Single-site mechanism:

In single site mechanism, only the limiting reactant is assumed to be adsorbed on catalytic sites.

Cumene-toluene transalkylation: Cumene . C_v + Toluene ⟶ Cymene . C_v+ Benzene . C_v

Dispropotionation: Cumene . C_v ⟶ Benzene . C_v + Aliphatics . C_v

Dissosciation: 2 Cumene . $2C_v$ ⟶ DIPPB . C_v + Toluene . C_v

Total rate of disappearance of Cumene = Rate of Ist reaction + Rate of IInd reaction + Rate of IIIrd reaction

Rate of Ist reaction = $k_1 p_T k_{Cum} p_{Cum} C_v$ (75)

Rate of IInd reaction = $k_2 k_{Cum} p_{Cum} C_v$ (76)

Rate of IIIrd reaction = $k_3 k_{Cum}^2 p_{Cum}^2 C_v^2$ (77)

Net rate = $k_1 p_T k_{Cum} p_{Cum} C_v + k_2 k_{Cum} p_{Cum} C_v + k_3 k_{Cum}^2 p_{Cum}^2 C_v^2$ (78)

$$= (C_v^2)\left[\left(\frac{k_1}{C_v}\right) K_t K_{cum} p_t p_{cum} + \left(\frac{k_2}{C_v}\right) K_{cum} p_{cum} + k_3 (K_{cum}^2)(p_{cum}^2)\right] \quad (79)$$

$$= \left(\frac{1}{Z}\right)^2 \left[k_1 K_t K_{cum} p_t p_{cum} + \left(\frac{k_2}{C_v}\right) K_{cum} p_{cum} + k_3 (K_{cum}^2)(p_{cum}^2)\right] \quad (80)$$

Where, $C_v = \frac{1}{1+ K_{Cum} p_{Cum}}$ (81)

And was calculated as follows,

$$C_t = C_v + C_{Cum.S} \quad (82)$$

$$C_t = C_v + k_{Cum} C_{Cum} C_v \quad (83)$$

$$= C_v[\,1 + k_{Cum} C_{Cum}] \quad (84)$$

$$C_v = \frac{C_t}{1+k_{Cum}C_{Cum}} \quad (85)$$

As total number of sites are equal to 1,

$$C_v = \frac{1}{1+k_{Cum}C_{Cum}} \quad (86)$$

$$C_v = \frac{1}{Z}$$

$$Z = 1 + k_{Cum}C_{Cum} \quad (87)$$

Stoichiometricmodel:

In this model, rate of disappearance of cumene was considered to be independent of adsorption of any species.

$$\text{Net rate} = k_1\, p_T\, p_{Cum} + k_2\, p_{Cum} + k_3\, p_{cum}^2 \quad (88)$$

The following rate expression using LHHW model with surface reaction as a rate controlling step and dual site (both reactant adsorbed on catalyst) mechanism was found to fit the kinetic data significantly better than the other models.

$$-r_{cum} = \left(k_1\, K_t K_{cum} p_t p_{cum} + \left(\frac{k_2}{C_v}\right) K_{cum} p_{cum} + k_3\, (K_{cum}^2)(p_{cum}^2) \right) (C_v^2)$$

Where, $C_v = 1/[1 + K_{Cum}p_{Cum} + K_T p_T]$

The partial pressures in the above equations were calculated using the fractional conversions and total pressure P as given by following expressions. For the reaction system, the total number of moles of different components was found to be 12. The values of p_T and p_{cum} were calculated at various space time and is reported in Table 6.5.

$$p_T = (9 - X_T)P/\ 12 \quad (89)$$

$$p_{cum} = (1 - X_{cum})P/\ 12 \quad (90)$$

$$p_{cymene} = (X_{cymene})P/\ 12 \quad (91)$$

$$p_{ben} = (X_{ben})P/\ 12 \quad (92)$$

$$p_{xyl} = (X_{xyl})P/\ 12 \quad (93)$$

$$p_{DIPT} = (X_{DIPT})P/\ 12 \quad (94)$$

$$p_A = (X_A)P/\ 12 \quad (95)$$

Table 6.5- Calculated p_{cum} and p_t at various temperatures and space time

Space time (kg h/kmol)	**P_c=(1-X_c)P/12 (atm)**				**p_t =(9- X_t)P/12 (atm)**			
	523K	**498K**	**473K**	**448K**	**523K**	**498K**	**473K**	**448K**
4.04	0.0233	0.0372	0.0417	0.0598	0.7443	0.7464	0.7473	0.7486
5.16	0.0150	0.0278	0.0381	0.0543	0.7413	0.7433	0.7446	0.7474
6.20	0.0126	0.0246	0.0345	0.0506	0.7403	0.7417	0.7438	0.7464
9.29	0.0113	0.0203	0.0295	0.0469	0.7370	0.7401	0.7423	0.7457

A non-linear regression was used for model parameter estimation. The optimum value of the parameters was estimated by minimizing the objective function given by equation (43). The experimental rates at various temperature and space time were calculated by using formula and the values are reported in Table 6.6.

$$-r_{cum} = dX_{cum}/d\tau \quad (96)$$

Table 6.6- Experimental rate of cumene conversion at various temperatures and space time

Space time (kg h/kmol)	**Experimental Rate (kmol/kg h)**			
	523K	**498K**	**473K**	**448K**
4.04	0.1780	0.1554	0.1235	0.0656
5.16	0.1588	0.1290	0.1050	0.0627
6.20	0.1366	0.1134	0.0941	0.0631
9.29	0.0930	0.0813	0.0694	0.0470

For model equation, the standard error of estimate for the rate of disappearance of cumene was 6.90×10^{-4} which was calculated using the values of constants from Table 6.7. Figure 6.6 shows experimental and predicted rate are quite comparable having an R^2 value of 0.97.

Table 6.7- Kinetic and adsorption parameters for dual site for toluene-cumene transalkylation over PrB_{10} zeolite catalyst

Kinetic and adsorption parameters	Temperature			
	448K	**473K**	**498K**	**523K**
K_1 (kmol/kg h)	3.99	12.39	21.54	38.98
K_2 (kmol/kg h)	2.55	7.54	12.60	29.99
K_3 (kmol/kg h)	2.30	3.79	7.09	11.76
Kc (atm^{-1})	0.940	0.75	0.65	0.564
Kt (atm^{-1})	1.805	1.604	1.40	1.205

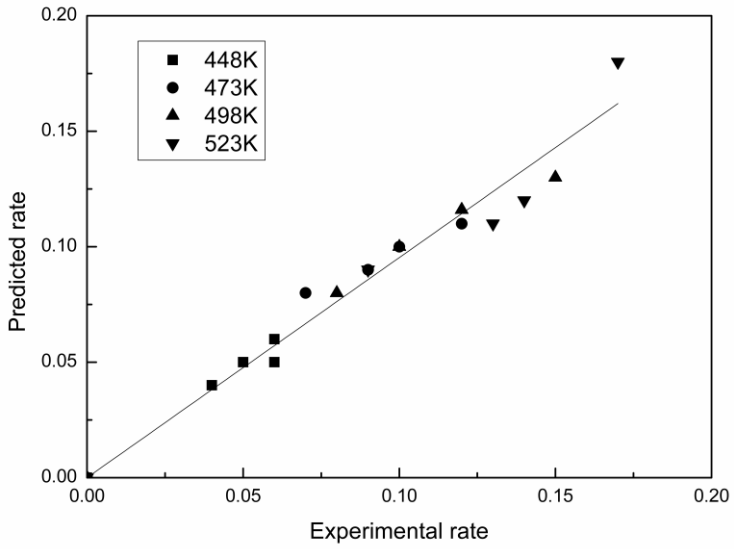

Figure 6.6: Experimental vs predicted values of reaction rate of cumene conversion over PrB_{10} zeolite catalyst

Activation energy and pre exponential factor for transalkylation reaction was found to be 61.44 kJ/mol and 5.37×10^9 respectively which was calculated form Arrhenius equation (44). Similar observation was reported in the temperature range 483–543 K for the transalkylation of *m*-diethylbenzene over beta zeolite [Forni *et al*., 1995].

6.4.3 Deactivation kinetics

To study the deactivation kinetics similar method was followed as described in section 5.1.3.3. The deactivation constant was determined using equation (46). A plot of $\ln[\ln(C_{A0}/C_A)]$ vs t using CeX_{10} catalyst at four temperatures is shown in Figure 6.7; the slopes of the lines at different temperatures represent the deactivation constant k_d. The values of ln k_d were plotted against 1/Temperature (Figure 6.8) to find the apparent activation energy for deactivation of catalyst which was found to be 14.8 kJ/kmol.

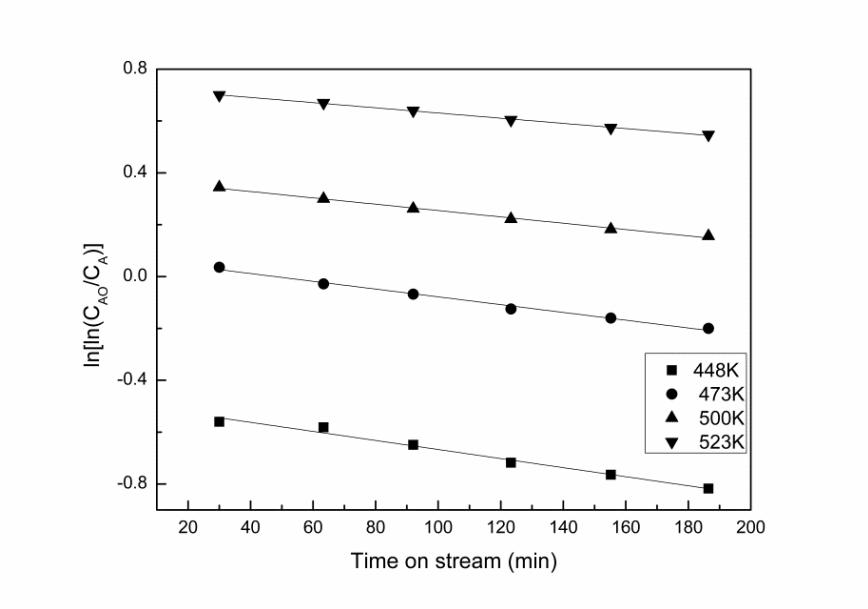

Figure 6.7: Plots of $\ln[\ln(C_{AO}/C_A)]$ *vs* time at different temperatures for toluene-cumene transalkylation over PrB_{10} zeolite catalyst

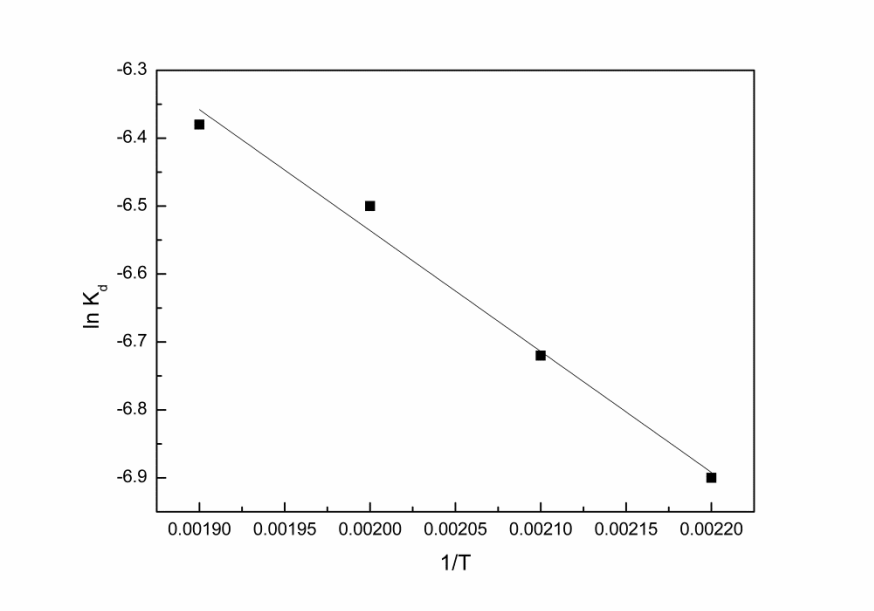

Figure 6.8: Arrhenius plot for deactivation energy for toluene-cumene over PrB_{10} zeolite catalyst

6.5 CONCLUSION

In transalkylation of toluene with cumene, metal exchanged zeolites were highly active. Modification of zeolite with rare earth metals bring out a significant change in acidity of zeolites and thus activity of catalyst. Modified zeolites shows higher reactant conversion and higher yield and selectivity of desired product compared to unmodified zeolite. Catalytic performance of praseodymium modified beta zeolite was found to be the best among various catalysts studied for this system. Praseodymium modified large pore beta zeolite shows highest activity at 523 K among all the metal modified zeolites. Maximum cumene conversion of 89% was achieved at 573K over PrB comparative to CeB (71.5%), LaB (60.9%), Hbeta (55.7%), PrX (51.5%), CeX (43.2%) and LaX (35.8%). It was seen that catalytic performance of beta zeolite is better than X zeolites. Maximum cymene yield (16.21%) and cymene selectivity (65.73%) were achieved at 523 K, toluene/cumene mole ratio of 9:1, 9.29 kg h/kmol space time, over PrB which were higher than cymene yield (10.7%) and cymene selectivity (48.7%) over PrX zeolite. At high reaction temperature of 573K dealkylation and disproportionation is favored which leads to decrease in yield and selectivity of cymene at higher temperature. High toluene to cumene ratio was required for maximum cumene conversion and cymene yield. Cumene conversion was found to increase with increase in space time.

Based on the product distribution, a reaction mechanism was proposed together with a rate expression for the disappearance of toluene using LHHW approach. The kinetic and the adsorption constants of the rate equation during their various transformation reactions were estimated by the best fit. The activation energy for the cymene synthesis reaction over PrB zeolite was estimated to be around 61.44 kJ/mol.

CHAPTER- 7

Transalkylation of 1,4 DIPB with Benzene

In this chapter, transalkylation of 1,4 diispropylbenzene (DIPB) with benzene over cerium modified Hbeta and NaX zeolite are reported. This chapter is further divided into two sections 7.1 and 7.2. These sections present a detailed study of transalkylation of DIPB with benzene over CeB and CeX zeolite respectively.

INTRODUCTION

Cumene is a colourless liquid having boiling-range motor fuel of high antiknock value. It is of industrial demand for the production of high molecular weight hydrocarbons such as cymene and polyalkylated benzene. The main end uses of cumene are for the production of phenolic resins, bisphenol A and caprolactam. However, 5-10 wt% diisopropylbenzene (DIPB) isomers are produced as low value byproduct during the isopropylation of benzene to cumene [Reddy *et al*., 1993; Sridevi *et al*., 2001]. The by-product can be recycled for cumene production making this process more economical. Another problem assosciated with this process is the use of hazardous liquid catalysts which are difficult to separate from the product mixture and hence reuse [Ercan *et al*., 1998; Barman *et al*., 2005; Maity *et al*., 2006]. In that respect, ecofriendly zeolites can exhibit acidities close to those of traditional mineral acid solutions [Best and Wojciechowski, 1978; Slaugh, 1983]. Moreover, the number and strength of acid sites in zeolite can be changed to a great extent by exchanging its H^+/Na^+ ions with rare earth cations into the zeolite framework. The catalysts such as zeolite X, MCM-22, MCM-49, PSH-3, SSZ-25, zeolite Y, zeolite beta [Huang *et al*., 1997(a); Yeh *et al*., 2008] were used in transalkylation reaction. These studies show that choice of catalyst, its Si/Al ratio and acidity of catalyst highly affects the process. Replacement of sodium ions in zeolites with polyvalent cations like rare earth metals (La, Ce, etc.) has been reported to produce materials of superior catalytic activity [Venuto *et al*., 1966; Rabo *et al*., 1968; Hunter and Scherzer, 1971]. However, very scarce literature is available on the use of rare earth metal modified zeolite Hbeta and NaX zeolite for cumene synthesis. In this work, the kinetics of this commercially important reaction over zeolite Hbeta modified by exchanging H^+ ions with cerium ions.

The transalkylation of 1,4 DIPB with benzene is a complex reaction. The mechanism of transalkylation of 1,4 DIPB with benzene is shown in Figure 7.1.

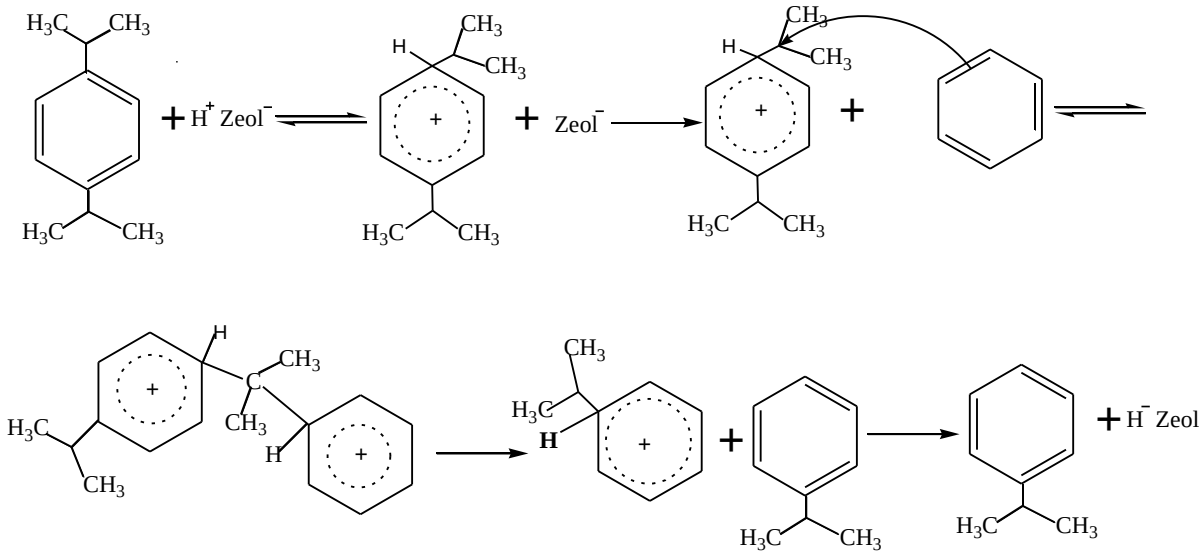

Figure 7.1: Proposed mechanism of transalkylation of 1,4 DIPB with benzene

Transalkylation of 1,4 DIPB with benzene is a complex reaction which is followed by isomerization and disproportionation reaction.

i) 1,4 DIPB transalkylation:

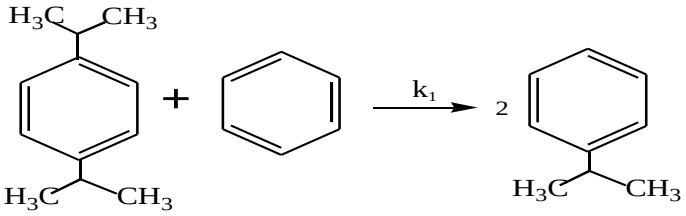

1,4 DIPB Benzene Cumene

ii) Isomerisation:

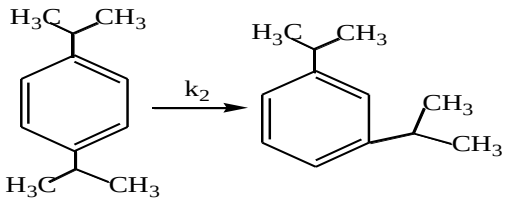

1,4 DIPB 1,3 DIPB

iii) Dealkylation:

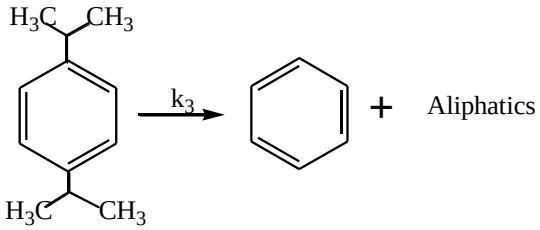

iv) Alkylation

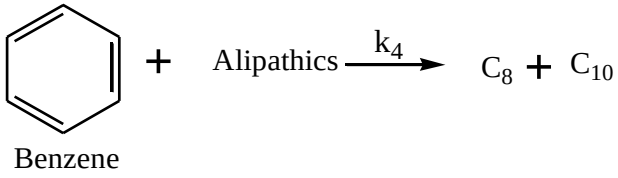

In this chemical reaction scheme, **"cumene yield"** is the fraction of reactant converted to the cumene. The selectivity of cumene, 1,3 DIPB and conversion of 1,4 DIPB were calculated as:

$$\text{1,4 DIPB conversion} = \frac{(\text{1,4 DIPB in feed} - \text{1,4 DIPB in exit})}{(\text{1,4 DIPB in feed})} \times 100 \tag{97}$$

$$\text{Cumene Selectivity} = \frac{(\text{Cumene in the product mixtrure})}{(\text{aromatics in product excluding 1,4 DIPB and Benzene})} \times 100 \tag{98}$$

$$\text{1,3 DIPB Selectivity} = \frac{(\text{1,3 DIPB in the product mixtrure})}{(\text{aromatics in product excluding 1,4 DIPB and Benzene})} \times 100 \tag{99}$$

7.1 Benzene and 1,4 DIPB Transalkylation over Cerium modified Hbeta zeolite

7.1.1 EXPERIMENTAL

The effect of various process parameters like metal loading (6-10 wt%), time on stream (0-3.5 h) catalyst loading (3.06-10.72 w/w%), temperature (493-593 K), reactant ratio (1-15) and space time (4.2-9.03 kg h/kmol) on the conversion of reactant and selectivity of product were studied over cerium modified Hbeta zeolite. To investigate external and internal diffusional effects, experiments were carried out over different weight (2 g and 4 g) and particle size (0.5-1.5 mm) of catalyst at constant space-time.

7.1.2 RESULTS AND DISCUSSION

7.1.2.1 Effect of cerium loading and time on stream

The activity of CeB zeolites and unmodified Hbeta zeolite were tested in 3.5 h time-on-stream at 573 K and atmospheric pressure. The Figure 7.2 shows that 83.82% selectivity of cumene was obtained over CeB_{10} which decreased to a value of 81.09 % after 3.5 h time-on-stream. This may be due to the deactivation of zeolite by formation of coke particles which block the catalyst surface. Selectivity of cumene decreases with cerium content and was found to be 81.33%, 77.87% and 73.23% over CeB_8, CeB_6, and Hbeta zeolite respectively.

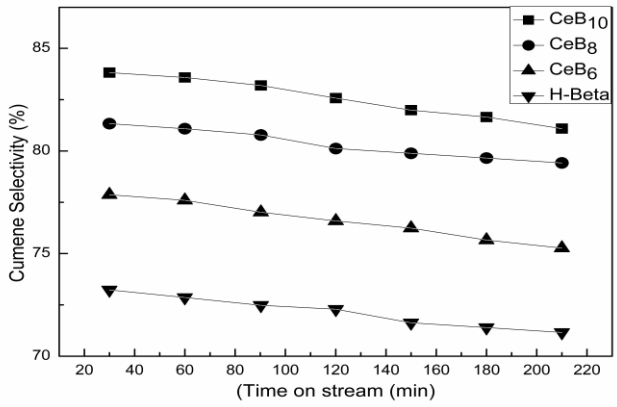

Figure 7.2: Cumene selectivity as a function of time-on-stream over Hbeta and cerium modified beta zeolites. Reaction conditions: Pressure- 1 atm, temperature- 573K, benzene/1,4DIPB– 5:1, space time- 9.03 kg h/ kmol, N_2 to feed ratio- 0.2.

7.1.2.2 Effect of catalyst loading in the reactor

Catalyst loading was varied from 1.93-11.6% (w/w) of the reactants as shown in the Figure 7.3. The conversion of reactant was found to increase with increase in catalyst loading from 1.93% to 11.6% (w/w). It was observed that with increase in catalyst loading conversion of 1,4DIPB increased sharply due to the presence of large number of active sites available for the reactants. The conversion increased from 58.91% in case of 1.93% (w/w) catalyst loading to 97.99% in case of 11.6% (w/w) catalyst loading.

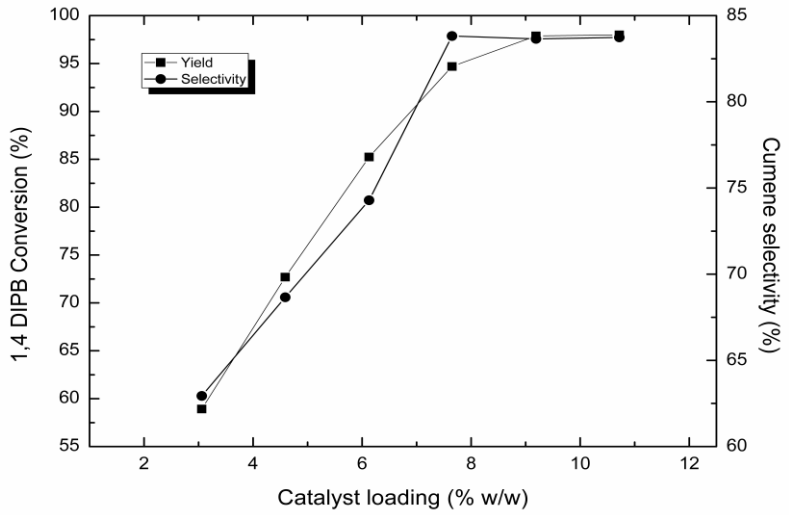

Figure 7.3: 1,4 DIPB conversion and cumene selectivity as a function of catalyst loading (CeB_{10}). Reaction conditions: Pressure- 1atm, temperature- 573 K, benzene/1,4DIPB– 5:1, space time- 9.03 kg h/ kmol, N_2 to feed ratio- 0.2.

7.1.2.3 Effect of reaction temperature

The effect of temperature on product selectivity is shown in Figure 7.4. The experiments were conducted in the temperature range of 493-593K over CeB_{10} catalyst. With the increase in temperature, the cumene selectivity increases gradually and reaches maximum (83.82 %) at 573 K but above this temperatures the cumene selectivity is decreased due to the formation of side product xylene. The product distribution at different reaction temperatures is shown in Table 7.1. The conversion of DIPB was maximum (94.69%) at a temperature of 573 K and then decreased to 85.12 % at 613 K. At higher temperature the decrease in conversion is due to deactivation of catalyst by deposition of coke at catalyst surface.

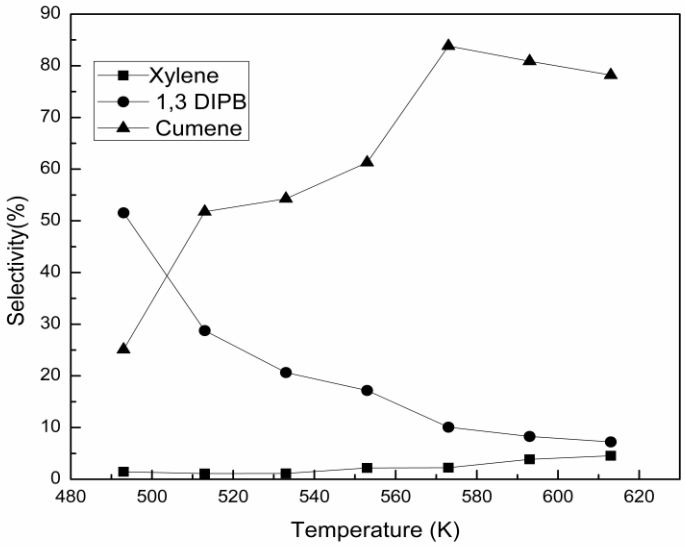

Figure 7.4: Effect of temperature on product selectivity for 1,4 DIPB-benzene transalkylation over CeB_{10} zeolite catalyst. Reaction conditions: Pressure-1 atm, benzene/1,4DIPB ratio– 5:1, space time- 9.03 kg h/ kmol, N_2 to feed ratio-0.2, catalyst (CeB_{10}) amount- 2 g.

Table 7.1- Product distribution of 1,4DIPB-benzene transalkylation at different temperatures over CeB_{10} zeolite catalyst

Product distribution (wt%)	**Temperature (K)**					
	493	**513**	**533**	**553**	**573**	**593**
Alipathics	0.76	0.79	0.72	0.40	0.07	0.03
Benzene	67.15	67.07	66.91	63.27	47.21	56.40
Toluene	0.12	0.20	0.22	0.30	0.35	0.69
Xylene	0.17	0.23	0.31	0.74	1.14	1.55
Cumene	2.96	10.60	15.03	20.18	42.94	32.54
n-PB	0.29	0.35	0.41	0.50	0.58	1.56
C10	1.39	2.41	5.31	5.16	0.97	0.53
1,3DIPB	6.10	5.89	5.72	5.66	5.17	3.33
1,4DIPB	21.06	12.46	5.40	3.79	1.57	3.37
Cumene yield (%)	2.96	10.60	15.03	20.18	42.94	32.54
1,4DIPB conv(wt%)	29.01	51.69	81.78	87.20	94.69	88.63

Reaction conditions: Pressure-1 atm, benzene/1,4DIPB ratio – 5:1, space time- 9.03 kg h/ kmol, N_2 to feed ratio-0.2, catalyst (CeB_{10}) amount-2 g.

7.1.2.4 Effect of benzene to 1,4DIPB mole ratio

In the transalkylation reaction, the benzene to 1,4 DIPB ratio was varied from 1 to 15 at a reaction temperature of 573 K and space time of 9.03 kg h/kmol. Figure 7.5 shows that the maximum selectivity (83.82%) of cumene was obtained at a benzene to 1,4 DIPB ratio 5:1, beyond this ratio, the isomerisation of para 1,4 DIPB seems to increase and hence a decrease in cumene selectivity was observed. Also, it is evident that 1,4 DIPB conversion increases and is maximum at benzene to 1,4 DIPB ratio 5:1 while further increase in reactant ratio leads to a decrease in 1,4 DIPB conversion. This may be due to crowding of active sites by the excess reactant molecules.

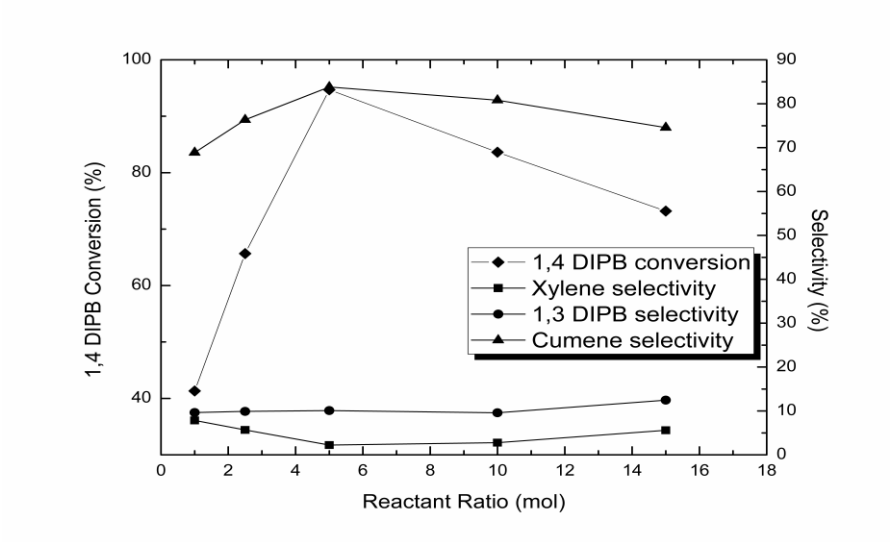

Figure 7.5: Effect of reactant mole ratio on product selectivity for 1,4 DIPB-benzene transalkylation over CeB_{10} zeolite catalyst. Reaction conditions: Pressure-1 atm, temperature- 573 K, space time- 9.03 kg h/ kmol, N_2 to feed ratio- 0.2, catalyst (CeB_{10}) amount- 2 g.

7.1.2.5 Effect of space time

The effect of space-time was studied in the range of 4.21–9.03 kg h/kmol (Table 7.2). The cumene selectivity increased with increase in space time and reached at a maximum of 83.82% at a space time of 9.03 kg h/kmol. Higher contact time allows the reactants to remain in the vicinity of each other and the catalyst surface for longer time therefore favoring transalkylation reaction. Selectivity of products as a function of space time is shown in the Figure 7.6. As can be seen from Figure 7.7, the conversion of 1,4 DIPB increased with increase in space time;

which may be due to the higher contact time between reactants and catalyst. Conversion of 1,4 DIPB was 94.69% at a space time of 9.03 kg h/kmol.

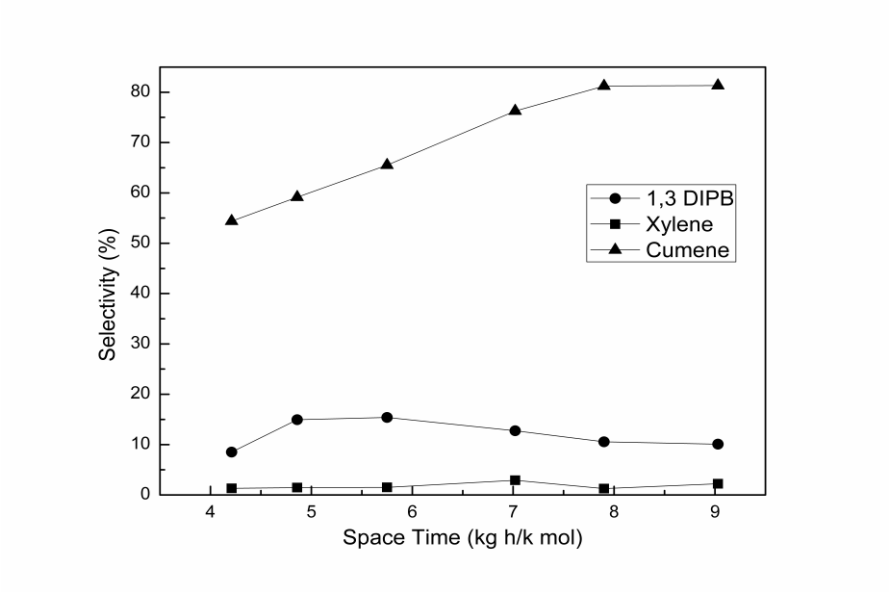

Figure 7.6: Effect of space time on product selectivity for 1,4 DIPB-benzene transalkylation over CeB_{10} zeolite catalyst. Reaction conditions: Pressure- 1 atm, temperature- 573 K, benzene/1,4DIPB ratio– 5:1, N_2 to feed ratio- 0.2, catalyst (CeB_{10}) amount- 2 g.

Table 7.2- Product distribution of 1,4DIPB-benzene transalkylation at different space time over CeB_{10} zeolite catalyst

Product distribution (wt%)	**Space Time (kg h/ k mol)**					
	4.2	**4.8**	**5.75**	**7.02**	**7.9**	**9.03**
Alipathics	0.71	0.49	0.48	0.04	0.10	0.06
Benzene	68.82	68.25	67.91	62.42	53.97	47.26
Toluene	0.94	0.58	0.29	0.48	0.22	0.35
Xylene	0.32	0.39	0.42	1.03	0.56	1.14
Cumene	16.96	18.78	21.02	28.65	37.39	42.93
n-PB	0.11	0.16	0.23	0.36	0.52	0.57
C10	3.34	2.42	1.14	0.14	0.70	0.96
1,3DIPB	2.08	4.01	4.29	4.49	4.66	5.16
1,4DIPB	6.72	4.92	4.22	2.39	1.88	1.57
Cumene yield (wt%)	16.96	18.78	21.02	28.65	37.39	42.93
1,4DIPB conv.(wt%)	77.34	83.41	85.77	92.39	93.69	94.69

Reaction conditions: Pressure-1 atm, temperature- 573 K, benzene/1,4DIPB ratio – 5:1, N_2 to feed ratio-0.2, catalyst (CeB_{10}) amount-2 g.

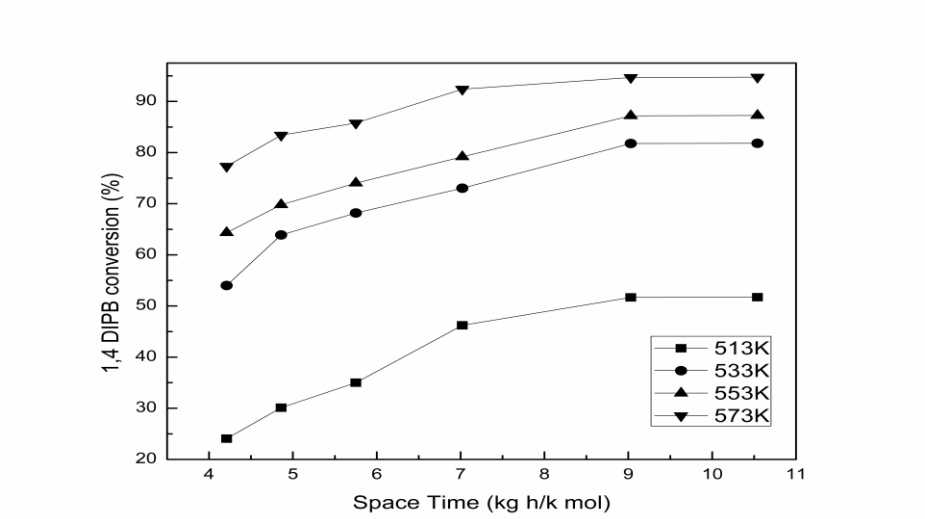

Figure 7.7: Effect of space time on 1,4 DIPB conversion at different temperature over CeB_{10} zeolite catalyst. Reaction conditions: Pressure-1 atm, benzene/1,4DIPB ratio – 5:1, N_2 to feed ratio- 0.2, time-on-stream- 30 min, catalyst (CeB_{10}) amount-2 g.

7.1.3 KINETIC STUDY

7.1.3.1 Mass transfer considerations

Experiments were carried out to find the effect of external diffusional resistance by varying feed rates and catalyst weight at constant space-time. Table 7.3 shows that external mass transfer resistance is negligible as the conversions of 1,4 DIPB at constant space time are independent of feed rate. To investigate the effect of intraparticle diffusion the experiments were carried out keeping space-time constant but varying the catalyst particle size. The conversion of 1,4 DIPB is found to be same over different catalyst size (Table 7.4) which indicates negligible intraparticle mass transfer resistance in the particle size range studied.

Table 7.3- External diffusion results for 1,4 DIPB-benzene transalkylation over CeB_{10} zeolite catalyst

Space-time (kg h/kmol)	**Conversion of DIPB (%)**	
	Catalyst weight = 0.002 kg	**Catalyst weight =0.004 kg**
4.2	64.34	65.11
4.8	69.80	70.87
5.75	74.03	75.12

Reaction conditions: Pressure-1 atm, temperature- 573 K, benzene/1,4DIPB ratio – 5:1, N_2 to feed ratio-0.2.

Table 7.4- Internal diffusion results for 1,4 DIPB-benzene transalkylation over CeB_{10} zeolite catalyst `

Particle size dp (mm)	Conversion of DIPB (%)		
	space-time(kg h/kmol) =4.2	space-time(kg h/kmol) = 4.8	space-time(kg h/kmol)= 5.75
0.50	65.87	70.23	75.34
1.00	65.35	69.98	74.76
1.50	64.34	69.80	74.03

Reaction conditions: Pressure-1 atm, temperature- 573 K, benzene/1,4DIPB ratio – 5:1, N_2 to feed ratio-0.2.

7.1.3.2 Kinetic modeling

The kinetic runs were carried out at four different temperatures. The experiments were conducted in the zone in which the mass transfer effects were negligible. Based on the product distribution various kinetic models were formulated following LHHW approach. These models were tested with the help of the experimental data. A non-linear regression algorithm was used for the kinetic parameter estimation. For the above reactions, the possible rate equations based on different mechanism are presented below. To avoid complexity only those reactions are taken into considerations which has significant yield of product therefore, isomerisation of DIPB and benzene reaction with aliphatics were not considered [Barman *et al*., 2005; Maity *et al*., 2006; Kondamudi and Upadhyayula, 2008]. Also, cumene adsorption on active site is very weak therefore cumene adsorption step is also neglected [Kondamudi and Upadhyayula, 2008].

Dual-site mechanism:

In dual site mechanism, both the reactants are assumed to be adsorbed on catalytic sites.

1,4 DIPB transalkylation: 1,4DIPB . C_v + Benzene . C_v ⟶ 2 Cumene . $2C_v$

Isomerisation: 1,4DIPB . C_v ⟶ 1,3DIPB . C_v

As only cumene and 1,3 DIPB is formed in fair amount and all other products are formed in negligible amount therefore, all other reactions were neglected while preparing the models.

A rate equation can be represented as,

$Rate = k\ k_{ads} p_{reactant} C_v$

Where, k is rate constant, k_{ads} is adsorption coefficient of any reactant, $p_{reactant}$ is partial pressure of any reactant, and C_v is concentration of vacant active sites available in the surface.

Rate of disappearnace of 1,4 DIPB = Rate of Ist reaction + Rate of IInd reaction (100)

Rate of Ist reaction = $k_1 k_B p_B k_{DIPB} p_{DIPB} C_v^2$ (101)

Rate of IInd reaction = $k_2 k_{DIPB} p_{DIPB} C_v$ (102)

Net rate = $k_1\, k_B\, p_B\ \ k_{DIPB}\, p_{DIPB}\, C_v^2 + \ k_2\, k_{DIPB}\, p_{DIPB}\, C_v$ (103)

$= C_v^2\ [k_1\, k_B\, p_B\ \ k_{DIPB}\, p_{DIPB} + \ (\frac{k_2}{C_v})\, k_{DIPB}\, p_{DIPB}\ ]$ (104)

$= \frac{1}{Z}^2\ [k_1\, k_B\, p_B\ \ k_{DIPB}\, p_{DIPB} + \ (\frac{k_2}{C_v})\, k_{DIPB}\, p_{DIPB}\ ]$ (105)

Where, $C_v = \frac{1}{(1 + k_B\, p_B + k_{DIPB}\, p_{DIPB})}$ (106)

And was calculated as follows,

$C_t = C_v + C_{B.S} + C_{DIPB.S}$ (107)

$C_t = C_v + k_{B.} C_B C_v + k_{DIPB.} C_{DIPB} C_v$ (108)

$C_t = C_v[\ 1 + k_{B.} C_B + k_{DIPB.} C_{DIPB}]$ (109)

$C_v = \frac{C_t}{1 + k_{B.} C_B + k_{DIPB.} C_{DIPB}}$ (110)

As total number of sites are equal to 1,

$C_v = \frac{1}{1 + k_{B.} C_B + k_{DIPB.} C_{DIPB}}$ (111)

$C_v = \frac{1}{Z}$

Z= $1 + k_{B.} C_B + k_{DIPB.} C_{DIPB}$ (112)

Single-site mechanism:

In single site mechanism, only the limiting reactant is assumed to be adsorbed on catalytic sites.

1,4 DIPB transalkylation: 1,4DIPB . C_v+ Benzene $\longrightarrow$ 2 Cumene . $2C_v$

Isomerisation: 1,4DIPB . C_v ⟶ 1,3DIPB . C_v

Total rate of disappearance of 1,4 DIPB = Rate of Ist reaction + Rate of IInd reaction

Rate of Ist reaction = $k_1 p_B k_{DIPB} p_{DIPB} C_v$ (113)

Rate of IInd reaction = $k_2 k_{DIPB} p_{DIPB} C_v$ (114)

Net rate = $k_1\, p_B\ k_{DIPB}\, p_{DIPB}\, C_v + k_2\, k_{DIPB}\, p_{DIPB}\, C_v$ (115)

$= C_v\, [k_1\, p_B\, k_{DIPB}\, p_{DIPB} + k_2\, k_{DIPB}\, p_{DIPB}\,]$ (116)

$= \frac{1}{Z}\ [k_1\ p_B\ k_{DIPB}\, p_{DIPB} + k_2\, k_{DIPB}\, p_{DIPB}\,]$ (117)

Where, $C_v = \frac{1}{(1 + k_{DIPB}\, p_{DIPB})}$ (118)

And was calculated as follows,

$C_t = C_v + C_{DIPB.S}$ (119)

$C_t = C_v + k_{DIPB.} C_{DIPB} C_v$ (120)

$C_t = C_v[\, 1 + k_{DIPB.} C_{DIPB}]$ (121)

$C_v = \frac{C_t}{1+k_{DIPB.} C_{DIPB}}$ (122)

As total number of sites are equal to 1,

$C_v = \frac{1}{1+k_{DIPB.} C_{DIPB}}$ (123)

$C_v = \frac{1}{Z}$

Z= $1 + k_{DIPB.} C_{DIPB}$ (124)

Stoichiometric model:

In this model, rate of disappearance of DIPB was considered to be independent of adsorption of any species.

Net rate = $k_1\, p_B\ p_{DIPB} + k_2\ p_{DIPB}$ (125)

The following rate equation based on surface reaction as controlling step was found to fit the experimental data satisfactorily.

Dual-sitemechanism:

$$-r_{DIPB} = \left[\, k_1 k_B k_{DIPB} p_B p_{DIPB} + \left(\frac{k_2}{C_v}\right) k_{DIPB} p_{DIPB} \right] C_v^2$$

where,

$$C_v = \frac{1}{(1+k_B p_B + k_{DIPB} p_{DIPB})}$$

The partial pressure of 1,4 DIPB and benzene are related to the fractional conversions and the total pressure (P) by these following equations :

$$p_{DIPB} = (1 - X_{DIPB})P/\ 7.2 \quad (126)$$

$$p_B = (5 - X_B)P/\ 7.2 \quad (127)$$

$$p_c = (X_c)/7.2 \quad (128)$$

The optimum values of the parameters were obtained by minimizing the objective function given by equation (43).

Model selection

By using the values of the constants for dual site mechanism, as shown in Table 7.5, the standard error of estimate for the rate of disappearance of 1, 4 DIPB was ±2.53 x 10^{-4}. The experimental and the predicted 1,4 DIPB conversions at four different temperatures are plotted in Figure 7.8. The Figure shows that the proposed reaction rate expression predicts the 1,4 DIPB conversion values which are comparable to the experimental values with R^2 value of 0.99. The kinetic constants evaluated at various temperatures were used to determine the activation energy for cumene synthesis (transalkylation) which was estimated to be 116.53 kJ/mol and for isomerisation reaction activation energy was found to be 176.01 kJ/mol by the Arrhenius equation (44). The plot of ln K vs 1/T is presented in Fig 7.9. The activation energy values for various reactions compare well with the values of similar reactions over zeolites obtained by other investigators [Kondamudi and Upadhyayula, 2008].

Table 7.5- Kinetic and adsorption constants at different temperature for 1,4 DIPB-benzene transalkylation over CeB_{10} zeolite catalyst

Kinetic and adsorption parameters	Temperature (K)			
	493	**513**	**533**	**553**
K_1 (kmol/kg h)	1.11	2.34	10.49	20.53
K_2 (kmol/kg h)	0.097	0.534	4.54	10.54
K_{Dipb} (atm^{-1})	1.223	0.839	0.689	0.459
K_B (atm^{-1})	2.345	2.00	1.80	1.50

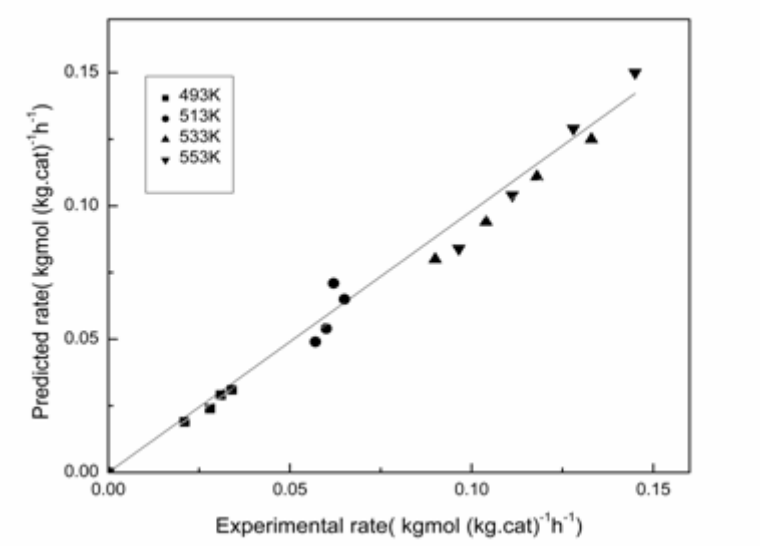

Figure 7.8: Experimental vs predicted rate of reaction of 1,4 DIPB conversion over CeB_{10} zeolite catalyst

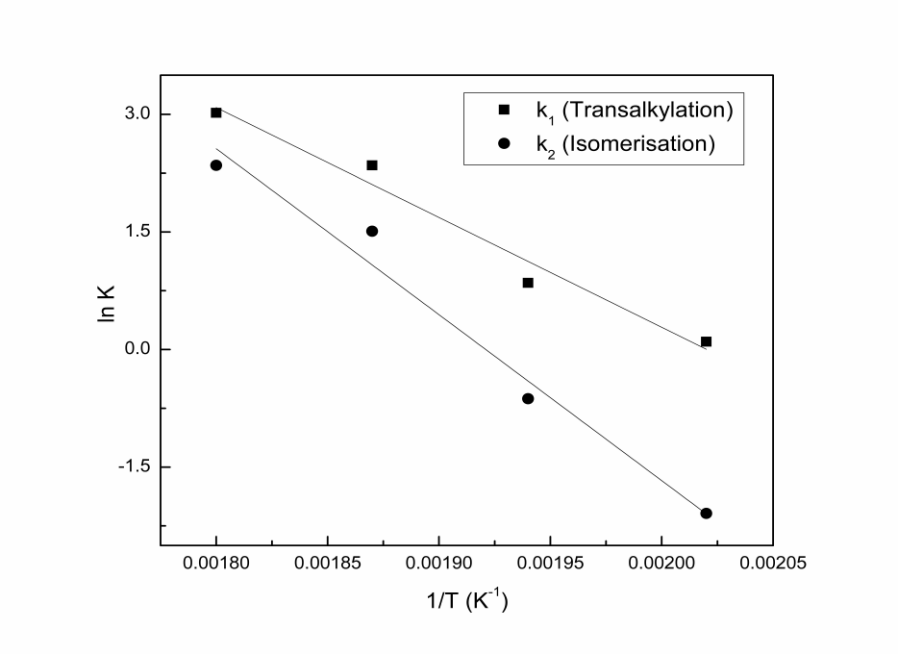

Figure 7.9: A plot of ln K vs 1/T for activation energy of 1,4 DIPB-benzene transalkylation over CeB_{10} zeolite catalyst

Thermodynamic adsorption parameters like enthalpy and entropy of adsorption were calculated using the equation (45). The values of enthalpy and entropy change are reported in Table 7.6. The adsorption equilibrium constants are plotted in Figure 7.10 which shows a satisfactory trend.

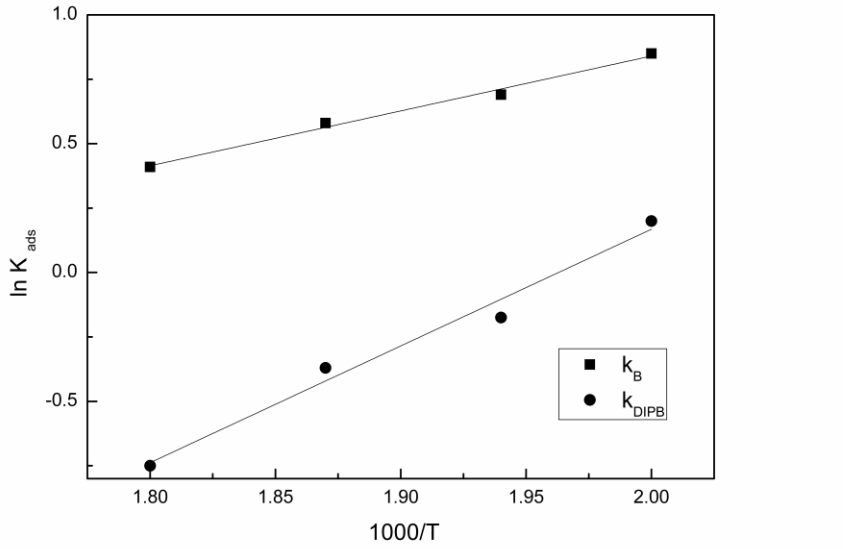

Figure 7.10: Arrhenius plot for adsorption equilibrium constants for 1,4 DIPB-benzene transalkylation over CeB_{10} zeolite catalyst

Table 7.6- Thermodynamic adsorption parameters for 1,4 DIPB-benzene transalkylation over CeB_{10} zeolite catalyst

Reactants	ΔHads (kJ/mol)	ΔSads (J/mol K)
Benzene	-17.32	-28.43
1,4 DIPB	-37.413	-73.91

7.1.3.3 Deactivation kinetics

The deactivation constant was determined using equation (46). A plot of $\ln[\ln(C_{A0}/C_A)]$ vs t using CeB_{10} catalyst at four temperatures is shown in Figure 7.11; the slopes of the lines at different temperatures were used to find the deactivation constant k_d. The values of $\ln k_d$ were plotted against 1/Temperature (Figure 7.12) to find the apparent activation energy for deactivation of catalyst which was found to be 25.44 kJ/kmol.

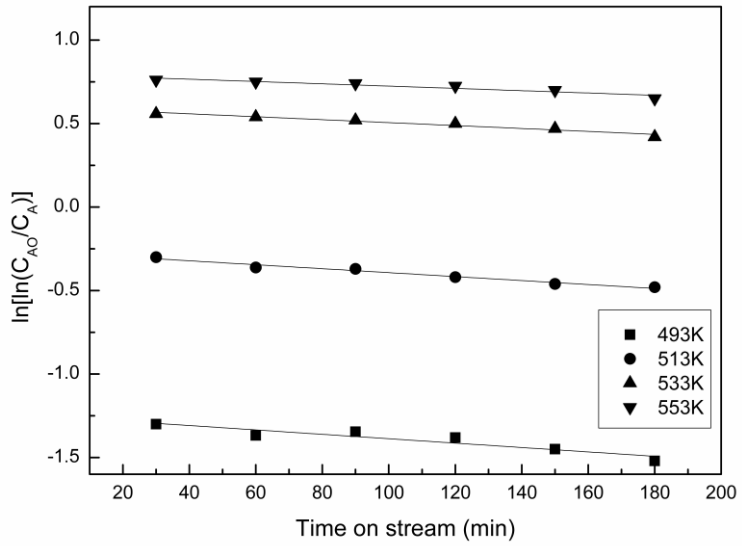

Figure 7.11: Plots of $\ln[\ln(C_{AO}/C_A)]$ *vs* time at different temperatures for 1,4 DIPB-benzene transalkylation over CeB_{10} zeolite catalyst

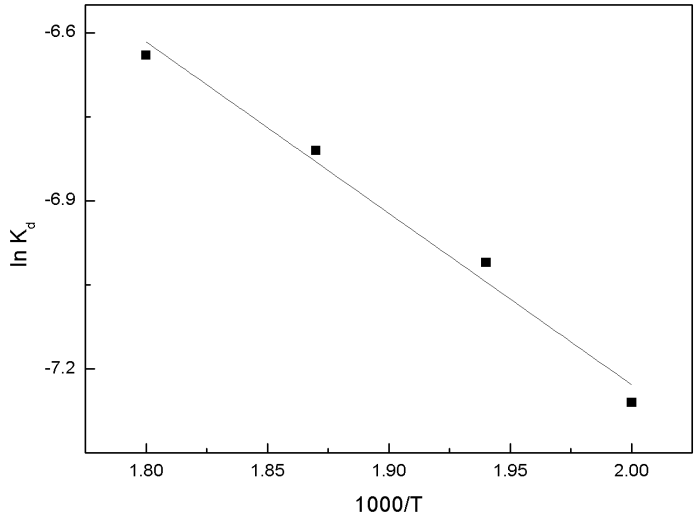

Figure 7.12: Arrhenius plot for deactivation energy for 1,4 DIPB-benzene transalkylation over CeB_{10} zeolite catalyst

7.1.4 CONCLUSION

The catalytic performance of cerium exchanged beta zeolite was evaluated for commercially important cumene synthesis. The Hbeta zeolite was successfully modified with cerium and it was found that activity and selectivity of the cerium modified zeolite was higher than parent zeolite due to the presence of strong acid sites in the exchanged zeolite. 94.69% conversion of 1,4 DIPB was obtained over CeB_{10} zeolite at 573 K and benzene to 1,4 DIPB reactant ratio of 5:1. The cumene selectivity at these conditions was 83.82%. Based on the product distribution pattern, a kinetic model was proposed and the parameters of the model were estimated. The activation energies for transalkylation and isomerisation reactions were found to be 116.53 kJ/mol and 176.01 kJ/mol respectively.

7.2. Benzene and 1,4 DIPB Transalkylation over Cerium modified NaX zeolite

7.2.1 EXPERIMENTAL

The effect of various process parameters like metal loading (2-12 wt%), catalyst loading (1.91-9.55 w/w%), temperature (533-593 K), reactant ratio (1-12.5) and space time (5.271-10.54 kg h/kmol) on the product distribution were studied over CeX zeolite. To investigate external and internal diffusional effects, experiments were carried out over different weight (2 g and 4 g) and particle size (0.5-1.5mm) of catalyst at constant space-time.

7.2.2 RESULTS AND DISCUSSION

7.2.2.1 Effect of cerium loading on product distribution

Commercially available NaX zeolite was treated with 2% (CeX_2), 5% (CeX_5), 7% (CeX_7) 10% (CeX_{10}) and 12% (CeX_{12}) cerium nitrate solutions. In Figure 7.13, it is seen that the DIPB conversion and cumene selectivity both increases with an increase in cerium content in the NaX zeolite. This is due to the strong acid sites generated by high cerium content. CeX_{12} zeolite shows comparable conversion of 84% while selectivity of cumene was less in case of CeX_{12} than CeX_{10}. Therefore, all the reactions were carried out over CeX_{10} zeolite catalyst.

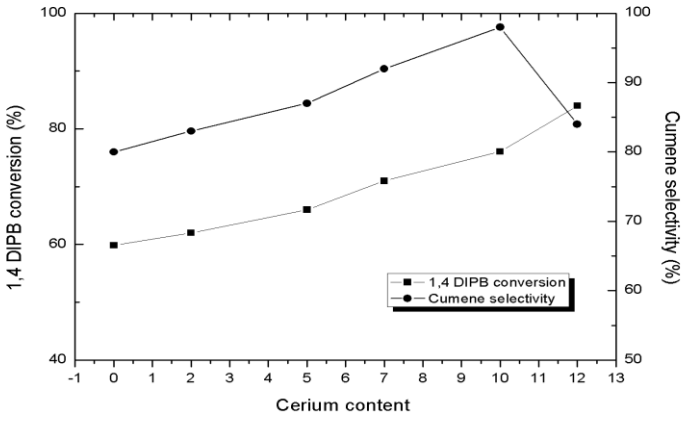

Figure 7.13: Effect of cerium loading on DIPB conversion and Cumene selectivity over CeX zeolite. Reaction conditions: pressure-1 atm, temperature- 573 K, space-time- 10.54 kg h/kmol, benzene to 1,4DIPB mole ratio- 7.5:1, N_2 to feed ratio- 0.2.

7.2.2.2 Effect of catalyst loading in the reactor

Catalyst loading was varied from 1.91-9.55% (w/w) of the reactants as shown in the Figure 7.14. The reactant conversion and cumene selectivity was found to increase with increase in catalyst loading from 1.91% to 9.55% (w/w). It was observed that with the catalyst loading conversion of 1,4DIPB increases sharply due to the presence of large number of active sites available for the reactants. The conversion was found to show a sharp increase from 42.43% in case of 1.91% (w/w) catalyst loading to 76.06% in case of 7.64% (w/w) catalyst loading. However, above catalyst loading of 7.64% although the surface area is provided for reaction, the increase in reactant conversion and cumene selectivity was negligible.

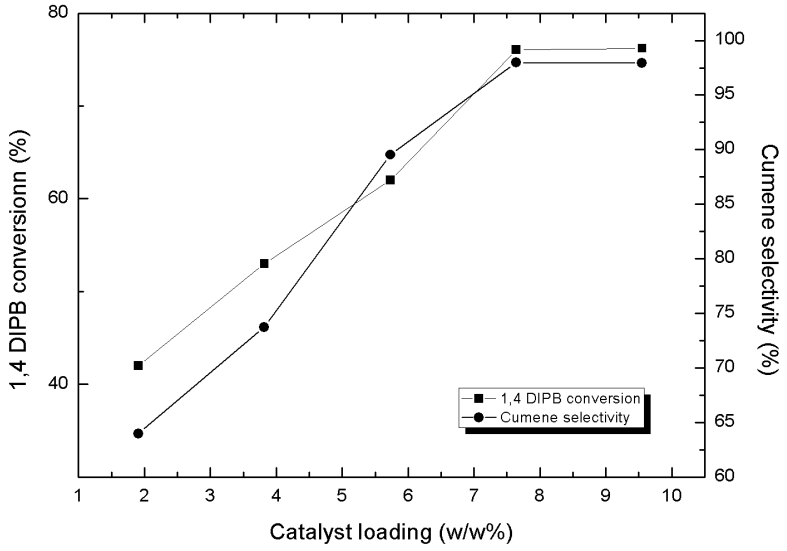

Figure 7.14: 1,4 DIPB conversion and Cumene selectivity as a function of catalyst loading (CeX_{10}). Reaction conditions: Pressure- 1 atm, temperature- 573 K, benzene/1,4DIPB– 7.5:1, space time- 10.54 kg h/ kmol, N_2 to feed ratio-0.2.

7.2.2.3 Effect of reaction temperature

The effect of temperature on product selectivity was studied in the temperature range of 533-593 K over CeX_{10} catalyst. With the increase in temperature, the cumene selectivity increased gradually and reached maximum (98.19%) at 593 K. This shows that high temperature favours transalkylation reaction. The product distribution at different reaction temperatures is shown in Table 7.7. The conversion of DIPB was maximum (76.06%) at a temperature of 573

K and then decreased to 71.40 % at 593 K. At higher temperatures, the decrease in conversion is due to deactivation of catalyst by deposition of coke at catalyst surface.

Table 7.7- Product distribution of 1,4DIPB-benzene transalkylation at different temperatures over CeX_{10} zeolite catalyst

Product distribution (wt%)	**Temperature (K)**			
	533	**553**	**573**	**593**
Alipathics	0.00	0.01	0.00	0.02
Benzene	73.53	71.32	68.38	75.23
Toluene	0.03	0.16	0.07	0.06
Xylene	0.10	0.09	0.07	0.03
Cumene	18.75	21.67	25.60	17.86
n-PB	0.03	0.04	0.04	0.05
C10	0.13	0.02	0.16	0.00
1,3DIPB	0.29	0.22	0.18	0.17
1,4DIPB	7.14	6.47	5.50	6.58
Cumene yield (%)	18.75	21.67	25.60	17.86
Cumene selectivity(%)	96.95	97.54	97.98	98.19
1,4DIPB conv.(wt%)	68.94	71.87	76.06	71.40

Reaction conditions: Pressure-1 atm, benzene/1,4DIPB ratio– 7.5:1, space time- 10.54 kg h/ kmol, N_2 to feed ratio-0.2, catalyst (CeX_{10}) amount- 2 g.

7.2.2.4 Effect of reactant mole ratio on product distribution

To investigate the effect of reactant ratio on 1,4 DIPB conversion and cumene selectivity, the benzene to 1,4DIPB ratio was varied from 1 to 12.5. At 553 K and at a reactant ratio of 7.5, 71.87% conversion of 1,4 DIPB was achieved over CeX_{10}. It can be seen from the Figure 7. 15 with the increase in reactant ratio, 1,4 DIPB conversion increases and reaches maximum at the ratio of 7.5 above which conversion of 1,4 DIPB decreases due to the less availability of the limiting reactant. Benzene molecules being smaller in size can easily enter deep into the pores of zeolites and is not sufficiently present at external surface for the reaction to occur. Therefore, high benzene to 1,4 DIPB ratio is required for high 1,4 DIPB conversion, as at higher benzene to 1,4 DIPB ratio, benzene is present in such a large amount that besides being present inside the pores it is available at the surface also and 1,4 DIPB can react with it. But, on further increase in benzene/DIPB ratio benzene molecules will compete with 1,4

DIPB molecules for adsorption sites therefore less availability of 1,4 DIPB at active sites which leads to decreased 1,4 DIPB conversion. However, on the other hand a maximum cumene selectivity of 98.18% was obtained at molar ratio of 10 and decreased to 91.92% at mole ratio of 12.5 over CeX_{10}. Decrease of cumene selectivity at higher ratio is due to the increase in formation of side products like xylene, n-propylbenzene and C_{10}.

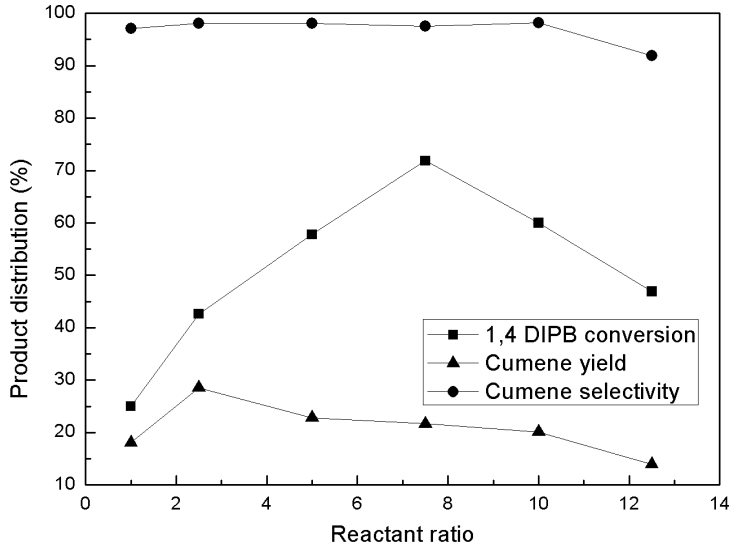

Figure 7.15: Effect of reactant mole ratio on product selectivity for 1,4 DIPB-benzene transalkylation over CeX_{10} zeolite catalyst. Reaction conditions: Pressure- 1 atm, temperature- 553 K, space time- 10.54 kg h/ kmol, N_2 to feed ratio-0.2, catalyst (CeX_{10}) amount- 2 g.

7.2.2.5 Effect of space time on products distribution

The effect of space time on conversion of 1,4 DIPB and selectivity of cumene was investigated in the range of 5.27-10.54 kg h/kmol and the results are Table 7.8. 1,4 DIPB conversion increases with increase in space time over the catalyst CeX_{10} as evident from the Figure 7.16. This is due to the fact that more is the contact time more interaction of reactant molecules with the surface of the catalyst. At higher contact time, the feed molecules remained in contact with the catalyst particle for longer time thus more reactants get converted into products. In case of CeX_{10} zeolite, selectivity of cumene remains almost constant from 98% to 97.54%. However, the yield of cumene was found to increase from a value of 8.64% to 21.62% with increase in space time up to a value of 10.54 kg h/kmol.

Table 7.8- Product distribution of 1,4DIPB-benzene transalkylation at different space time over CeX_{10} zeolite catalyst

Product distribution (wt%)	Space Time (kg h/ kmol)			
	5.2	**6.32**	**7.91**	**10.54**
Alipathics	0.01	0.01	0.00	0.02
Benzene	75.25	73.14	72.36	71.32
Toluene	0.01	0.02	0.04	0.16
Xylene	0.03	0.04	0.07	0.10
Cumene	8.64	16.34	18.56	21.63
n-PB	0.01	0.02	0.03	0.04
C10	0.01	0.01	0.02	0.04
1,3DIPB	0.10	0.12	0.13	0.22
1,4DIPB	15.94	10.21	8.8	6.47
Cumene yield (%)	8.654	16.34	18.56	21.63
Cumene selectivity (%)	98.09	98.73	98.35	97.54
1,4DIPB conv.(wt%)	30.67	55.6	61.7	71.87

Reaction conditions: Pressure-1 atm, temperature- 573 K, benzene/1,4DIPB ratio– 7.5:1, N_2 to feed ratio-0.2, catalyst (CeX_{10}) amount- 2 g.

7.2.3 KINETIC STUDY

7.2.3.1 Mass transfer considerations

For gas-solid heterogeneous reactions, the resistance may be external or internal, within the catalyst particles. Experiments were carried out to estimate the external diffusional effects by varying feed rates and catalyst size but at constant space-time. The results shown in Table 7.9 indicate that the conversions of 1,4 DIPB at constant space velocity are independent of feed rate. Therefore, the external mass transfer resistance is negligible. Experiments were carried out to investigate the effect of intraparticle diffusion by varying the catalyst particle size at constant space-time. The experimental data are presented in the Table 7.10. It is seen that there was no change in conversion of 1,4 DIPB with catalyst size which indicates negligible intraparticle mass transfer resistance in the particle size range studied. The kinetic study were done within the intraparticle diffusion free range.

Table 7.9- External diffusion results for 1,4DIPB-benzene transalkylation over CeX_{10} zeolite catalyst

Space-time (kg h/kmol)	Conversion of DIPB (%)	
	Catalyst weight = 0.002 kg	**Catalyst weight =0.004 kg**
5.75	46.01	46.79
6.3	49.32	49.92
7.9	60.18	60.87

Reaction conditions: pressure-1 atm; temperature 553 K; benzene to 1,4DIPB mole ratio, 7.5:1; N_2 to feed ratio-0.2

Table 7.10- Internal diffusion results for 1,4DIPB-benzene transalkylation over CeX_{10} zeolite catalyst

Particle size dp (mm)	Conversion of DIPB (%)		
	space-time(kg h/kmol) =5.75	**space-time(kg h/kmol) = 6.3**	**space-time(kg h/kmol)= 7.9**
0.50	47.98	51.01	61.78
1.00	47.12	51.86	60.97
1.50	46.01	49.32	60.18

Reaction conditions: pressure- 1 atm, temperature- 553 K, benzene to 1,4DIPB mole ratio- 7.5:1, N_2 to feed ratio- 0.2.

7.2.3.2 Kinetic modeling

The kinetic runs were carried out at four different temperatures and the results are shown in the Figure 7.16. The experiments were carried in the zone in which the mass transfer effects were negligible. In accordance with the product distribution, the system can be described by the following reaction scheme. Transalkylation of 1,4 DIPB with benzene is a complex reaction which is accompanied by the reactions shown in section 7.1.

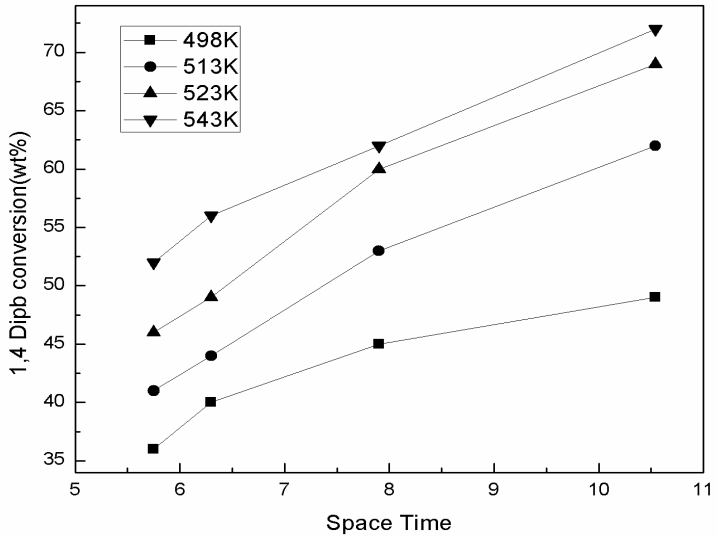

Figure 7.16: Effect of space time on 1,4 DIPB conversion over CeX_{10} at different temperature. Reaction conditions: pressure-1 atm, benzene to 1,4DIPB mole ratio- 7.5:1, N_2 to feed ratio- 0.2.

With the help of the reaction scheme, various reaction rate models were formulated following Langmuir-Hinshelwood approach. The models were tested with the help of the experimental data. All models, except the surface reaction controlling one, gave negative constants. Hence they were not considered. For the rate of disappearance of 1,4 DIPB, Langmuir-Hinshelwood-Hougen-Watson model was attempted to fit the kinetic data. The derivation of rate equations for dual site, single site and stoichiometric models is shown in section 7.1.3.2. The partial pressure of 1,4 DIPB and benzene are related to the fractional conversions and the total pressure (P) by these following equations :

$$p_{DIPB} = (1 - X_{DIPB})P/\ 10.2 \quad (129)$$

$$p_B = (7.5 - X_B)P/\ 10.2 \quad (130)$$

$$p_c = (X_c)/10.2 \quad (131)$$

Where, the value 10.2 corresponds to total number of moles (benzene, 1,4 DIPB, nitrogen) in the reaction. A non-linear regression algorithm was used for parameter estimation. The kinetic parameters in the three models were estimated by nonlinear regression analysis using least square method. The optimum values of the kinetic parameters were estimated by minimizing the objective function given by the equation (43).

By using the values of the constants for dual site mechanism as shown in Table 7.11, the standard error of estimate for the rate of disappearance of 1,4 DIPB was 4.53×10^{-4}. The experimental and the predicted 1,4 DIPB conversions at four different temperatures were plotted in Figure 7.17. The Figure shows that the proposed reaction rate expression predicts the 1,4 DIPB conversion values comparable with the experimental ones. The kinetic constants evaluated and tabulated at various temperatures (Table 7.11) were used to determine the activation energy and frequency factor using Arrhenius relationships as shown in the Figure 7.18. Activation energy for both reactions were calculated using equation (44). The activation energy values for transalkylation reactions were found to be 78.54 kJ/mol which was similar with the same type of reactions over zeolites obtained by other investigators [Forni *et al*., 1995; Kondamudi and Upadhyayula, 2008]. Activation energy for isomerization reaction was found to be 84.56 kJ/mol.

Table 7.11- Kinetic and adsorption constants at different temperature for 1,4 DIPB-benzene transalkylation over CeX_{10} zeolite catalyst

Kinetic and adsorption parameters	**Temperature**			
	498K	**513K**	**533K**	**553K**
K_1 (kmol/kg h)	2.58	4.83	8.04	17.64
K_2 (kmol/kg h)	1.04	2.03	4.59	8.14
K_{Dipb} (atm^{-1})	1.49	0.83	0.53	0.26
K_B (atm^{-1})	2.50	2.20	1.80	0.31

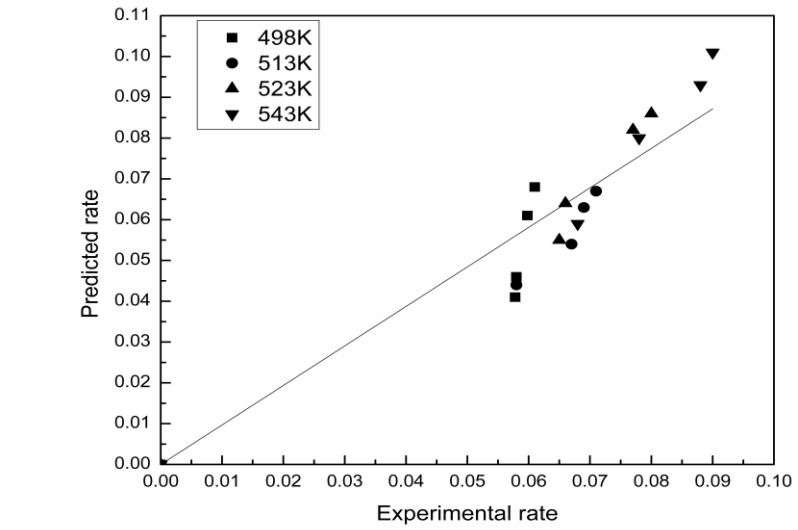

Figure 7.17: Experimental vs predicted rate of reaction 1,4 DIPB conversion over CeX_{10} zeolite catalyst

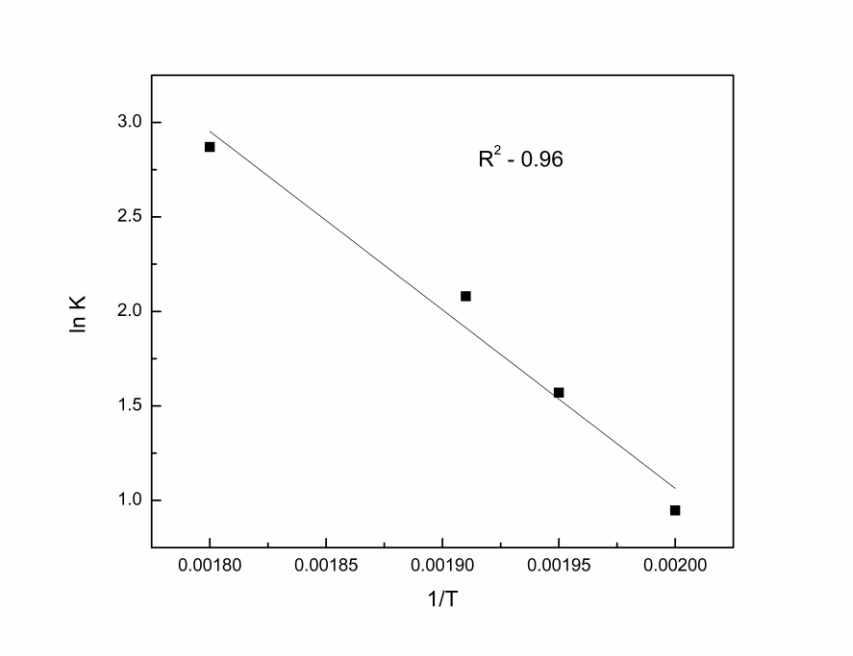

Figure 7.18: A plot of ln K vs 1/T for activation energy of 1,4 DIPB-benzene transalkylation over CeX_{10} zeolite catalyst

Thermodynamic adsorption parameters like enthalpy and entropy of adsorption were calculated using the equation 45. The values of enthalpy and entropy change are reported in Table 7.12.

Table 7.12- Thermodynamic adsorption parameters for 1,4 DIPB-benzene transalkylation over CeX_{10} zeolite catalyst

Reactants	ΔHads (kJ/mol)	ΔSads (J/mol K)
Benzene	-21.11	-34.75
1,4 DIPB	-65.43	-124.71

7.2.3.3 Deactivation kinetics

The deactivation constant was determined using equation (46). A plot of $\ln[\ln(C_{A0}/C_A)]$ vs t using CeX_{10} catalyst at four temperatures is shown in Figure 7.19; the slopes of the lines at different temperatures represent the deactivation constant k_d. The values of ln k_d were plotted against 1/Temperature (Figure 7.20) to find the apparent activation energy for deactivation of catalyst which was found to be 29.93 kJ/kmol.

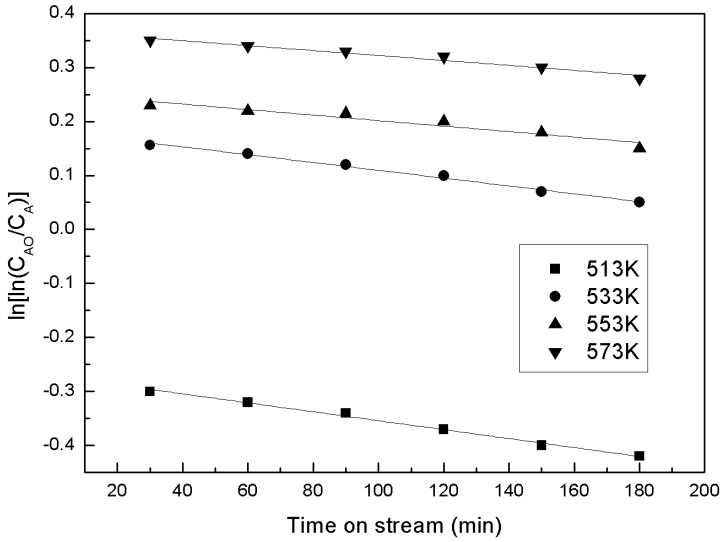

”

Figure 7.19: A plot of ln[ln(C_{AO}/C_A) *vs* time at different temperatures for 1,4 DIPB-benzene transalkylation over CeX_{10} zeolite catalyst

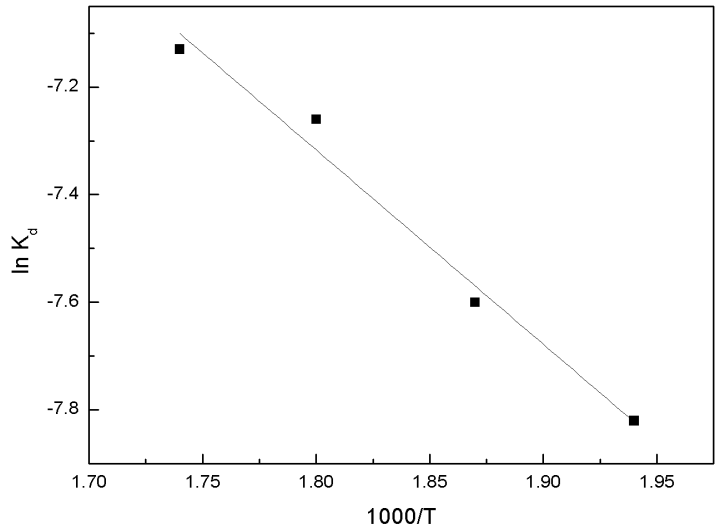

Figure 7.20: Arrhenius plot for deactivation energy for 1,4 DIPB-benzene transalkylation over CeX_{10} zeolite catalyst

7.2.4 CONCLUSION

NaX zeolite was modified with cerium ions to check the effect of ion exchange on acidity and hence activity of the catalyst. Time-on-stream study shows that CeX_{10} zeolite exhibits much higher conversion and stability than NaX. 1,4 DIPB conversion of 76.06% and cumene selectivity of 98% were achieved over CeX. From the experimental results it can be concluded that acidity affects the activity and selectivity to a great extent. A kinetic model was proposed for the reactions and the parameters of the model equation were estimated. A good correlation was obtained between experimental and predicted rate. From the estimated kinetic constant, the apparent activation energy for 1,4 DIPB transalkylation reaction was estimated to be 78.54 kJ/mol and apparent activation energy for isomerisation reaction was found to be 84.56kJ/mol.

In transalkylation of benzene with DIPB, metal exchanged Hbeta and NaX zeolites were showed high activity than the parent zeolites. Catalytic performance of cerium modified beta zeolite was found to be the better than cerium modified NaX zeolite. Cerium modified large pore beta zeolite shows highest activity at 573 K giving a maximum DIPB conversion of 94..69% compare to CeX (76.06%) at 573 K. Maximum cumene yield (42.94%) and cumene selectivity (98.9%)were achieved at 573 K, benzene/DIPB mole ratio of 5:1, 9.03 kg h/kmol space time, over CeB which were higher than cumene yield (25.26%) and cumene selectivity (97.98%) over CeX zeolite at 573 K, benzene/DIPB mole ratio of 7.5:1, 10.54 kg h/kmol space time. The activation energy for the xylene synthesis reaction over CeB and CeX zeolite was estimated to be 116.5 kJ/mol and 78.5 kJ/mol respectively, whereas the value of deactivation energy was 25.4 kJ/mol and 29.9 kJ/mol respectively.

CHAPTER-8

Conclusions and Futuristic aspects

8.1 INTRODUCTION

In the present investigation, research was carried out for the preparation and characterization of zeolites modified withrare earth metal ions and their application as solid catalysts for the commercially important transalkylation systems.

8.2 CONCLUSIONS FROM PRESENT THESIS

In ***Chapter 4,*** large pore zeolites modified with different rare earth metal ions (lanthanum, cerium and praseodymium) were characterized using various characterization techniques. From the results it was found that ion exchange of both large pore zeolites Hbeta and NaX were successfully carried out. The structure of modified zeolite was found to be well preserved and intact after the ion exchange. However, at high loading of metal ions on the zeolite some metal ions were found to appear on the zeolite surface in the form of metal oxide. SEM images showed that both parent and modified Hbeta zeolite crystals were round in shape, but both parent and modified NaX zeolite showed octahedral crystals. Modified zeolite was found to have less surface area compared to parent zeolite due to decrease in pore volume by metal exchange. The rare earth metal ions exchange leads to increase in both quantity and strength of the acid sites in zeolite. TPD results showed that acidity of the modified zeolites increase with increase in metal loading in the zeolite.

In ***Chapter 5,*** transalkylation of toluene with TMB was carried out over cerium modified Hbeta and NaX zeolite catalysts. Cerium modification enhanced the activity and stability of Hbeta and NaX for toluene-trimethylbenzene transalkylation reaction. Toluene conversion obtained over CeB (58.77%) and CeX (45%) zeolites were higher in comparison to unmodified Hbeta (41.42%) and NaX (21.28%) zeolites. Modified zeolites also possess higher xylene yield and selectivity than parent zeolites. Transalkylation reaction of toluene-trimethylbenzene was accompanied by disproportionation and isomerisation reactions. Box-Benkehn design of RSM was used for fitting the response surface and was found to accurately predict the optimum conditions giving maximum conversion and selectivity. A good correlation between experimental results and RSM predicted response values indicated the importance of DOE tools to understand the importance of interactions among the process parameters using less number of experiments.

In ***Chapter 6,*** toluene with cumene transalkylation was studied over lanthanum, cerium and praseodymium modified Hbeta and NaX zeolites. Dealkylation of cumene and disproportionation of cumene, cymene and toluene were the side reactions observed during toluene-cumene transalkylation reaction. Modification of Hbeta and NaX zeolites with different rare earth metal ions bring out a significant change in the activity of catalyst. Higher conversion, yield and selectivity were obtained over modified zeolites. Praseodymium modified beta zeolite gave maximum cumene conversion (89%) and cymene selectivity (66%) among all the rare earth metal ion modified zeolite catalyst. Moreover, beta zeolites were found to be more active than X zeolites. The trend of activity followed the order: PrB> CeB> LaB> HB> PrX> CeX> LaX> NaX. Acidity of these catalysts was found to have direct influence on their catalytic activity. The activation energy for the cymene synthesis reaction over PrB zeolite was estimated to be 61.44 kJ/mol.

In ***Chapter 7,*** catalytic performance of cerium exchanged beta and NaX zeolite was evaluated for commercially important cumene synthesis. DIPB-benzene transalkylation is accompanied by various side reactions like isomerisation, dealkylation and alkylation reaction however, dispropotionation reaction involving two bulky molecules of DIPB did not occurred at all. Modified zeolites were found to be more active, stable and selective for DIPB-benzene transalkylation. 94.69% conversion of 1,4 DIPB was obtained over CeB zeolite while maximum conversion obtained over CeX was 76.06%. CeB gave maximum cumene selectivity (83.82%) whereas, 98% selectivity was obtained over CeX.

For transalkylation reactions, high acidity of the catalyst resulting from high metal loading leads to high reactant conversion but decreases the selectivity of the catalyst to some extent as side reactions are favored due to presence of high acidic sites. In the fixed bed reactor, the conversion of the reactant depends on the amount of the catalyst loading. Reaction temperatures higher than 523 K favor transalkylation reaction whereas very high temperatures (> 725 K) will lead to dispropotionation and dealkylation. Among the various isomers formed in the reaction the yield of sterically stable isomer is more whereas high temperature can favor steric hindered product. Reactant ratio plays a crucial role in product distribution of transalkylation reactions. Transalkylation reaction between highly substituted molecule and mono substituted molecule favors high conversion if the highly substituted molecule is taken in excess which leads to increase in the number of alkyl groups in the system. However, if transalkylation reaction occurs between two mono substituted molecules

then the molecule having smaller alkyl group must be taken in excess in order to achieve high conversion. Higher space time allows the molecular moieties to remain in the vicinity of the catalyst surface for more time therefore favoring high conversion and selectivity. LHHW model with surface reaction as a rate controlling step and dual site (both reactant adsorbed on catalyst) mechanism fits the kinetic data significantly better than the other models. Activation energy for transalkylation reactions studied in the present thesis was in the range of 60-125 kJ/mol. Dispropotionation and isomerisation reactions were found to have more activation energy than transalkylation reaction. Deactivation energy for the three transalkylation reaction systems was in the range of 14-30 kJ/mol which shows that very low temperatures will lead to rapid deactivation by molecular retention and might not favour formation of products.

Thus, all modified catalysts have shown excellent activity and have the potential to convert low value polyalkylated aromatics to commercially important monoalkyllated or dialkylated products. The catalyst used in the present study showed better results for reactant conversion, product yield and selectivity in comparison to others reported in the literature. Maximum toluene conversion obtained in case of toluene-1,2,4TMB transalkylation reaction using CeB zeolite was 59% which was higher in comparison to values reported by other workers [Haag and Olson, 1979 (conv-23%); Nacamuli *et al.*, 1999 (conv- 37%); Khattaf *et al*., 2007(conv-40%,); Krejci *et al*., 2010 (conv- 52%)]. PrB zeolite used as a catalyst for toluene-cumene transalkylation gave cumene conversion (89%), cymene yield (16.2%) higher than other catalysts like dual catalyst of ZSM-5 and mordenite [Odedario and Khattaf, 2011 (conv-54.15, yield-3%)], Hbeta [Reddy *et al*., 1995 (conv- 71.4%, yield-9.45%)], NH_4Y [Mavrodinova *et al*., 2003 (conv- 84.5%, yield-3.78%)] reported in the literature. CeB and CeX zeolites also showed better results for 1,4DIPB-benzene transalkylation reaction. The maximum DIPB conversion and cumene yield obtained over CeB was 94.6% and 43% respectively whereas CeX zeolite gave 76% DIPB conversion and 26% cumene yield. These catalysts showed superior results when compared to work of Kondamudi and Upadhyayula (2008) (conv- 93%, yield-22%), Maity *et al*. (2006) (conv- 43%), Bozga *et al*. (2001) (conv-61.5%, yield-24%), Pradhan and Rao (1993) (conv- 90%, yield-12.54%).

In the industry, using this catalyst, rate of reaction can be increased which can save the fixed cost as well as the operating cost by minimizing energy consumption, reactor volume, reaction time and make the process more economic. The derived kinetic model for the said

reactions can provide necessary information to scale up the reactor for large scale production in the industry.

8.3 FUTURE ASPECTS

Few futuristic suggestions related with the present work are listed below:

1. Using the rate equation obtained from the study, a suitable reactor can be designed to meet the desired selectivity and yield of products which can be useful for large scale production.
2. Large pore nanozeolites can be synthesised and used for transalkylation reactions as nonozeolites have high surface area which can reduce the diffusional resistance and enhance the rate of reaction.
3. Alkylation and transalkylation reaction can be studied in a single reactor to maximize the yield of specific product and minimize the fixed cost.
4. Varying the synthesis conditions, suitable catalysts can be synthesized with different Si/Al ratio for other important transalkylation reactions.

REFERENCES

References

Aitani, A. M.; Ali, A.; Waziri, S. M.; Khattaf, A. S.,*Chemical Engineering & Technology,* **2010,** *33* (7), 1193–1202.

Ali, A. S.; Aitani, A. M.; Ercan, C.; Wang, Y.; Khattaf. S., *Chemical Engineering Research & Design,* **2011**, *89* (10), 2125-2135.

Al-Zahrani, S. M.; Al-Kinany, M. C.; Al-Humaizi, K. I.; Al-Khowaiter, S. H., *International Journal of Chemical Kinetics,* **2003***, 35* (11), *555-563.*

Amin, N. A. S.; Anggoro, D. D., *Journal of Natural Gas Chemistry,* **2003**, *12* (2), 123-134.

Anastas, P. T.; Warner, J. C., *Green Chemistry*: *Theory and Practice*, Oxford University Press: New York, **2000**.

Anderson, J. R.; Mole, T.; Christov. V., *Journal of Catalysis,* **1980**, *61*, 477-484.

Angulakshmi, V. S.; Sivakumar, N.; Karthikeyan, S., *Journal of Environmental Nanotechnology*, **2012**, *1* (1), 40-45.

Anupama, M. P.; Mahesh D. G.; Ayyanna. C., *International Journal of Applied Biology and PharmaceuticalTechnology*, **2010**, *1* (1), 34-45.

Arshadi, M.; Ghiaci, M., *Iranian Journal of Organic Chemistry*, **2010**, *2* (4) 491-500.

Arvela, M. P.; Kumar, N.; Diaz, S. F.; Aho, A.; Tenho, M.; Salonen, J., *Journal of Molecular Catalysis A Chemical*, **2013**, *366* , 228–237.

Bagnasco, G., *Journal of Catalysis*, **1996**, *159* (1), 249-252.

Balogh, M.; Laszlo, P., *Organic Chemistry Using Clays*, Springer-Verlag: Berlin, **1993**.

Bandyopadhyay, R.; Singh. S. P.; Shaikh. R. A., *Applied Catalysis A: General*, **1996**, *135* (1), 249-259.

Bandyopadhyay, R.; Sugi. Y.; Kubota. Y.; Rao, S. B., *Catalysis Today*, **1998**, *44* (1-4), 245-252.

Barman, S.; Pradhan, N. C.; Maity, S. K., *Journal of Chemical Engineering*, **2005**, *114* (1), 39-45.

Barrer, R. M., *Hydrothermal Chemistry of Zeolite,* Academic Press, London, **1982**, 251-305.

Barthomeuf, D.; ACS Symposium Series, Mol. Sieves-2, Int. Conf., 4th, **1977**, *40*, 453-472.

Bennet, J.M.; Chang, C.D.; Cheng, J.C.; Lawton, S.L.; Leonowicz, E.M.; Lissy, D.N.; Rubin, M.K.; Smith, C.M.; Walsh, D.E., *US Patent No. 5371310,* **1994.**

Best, D. A.; Wojciechowski, B. W., .*Journal of Catalysis*, **1978**, *53* (2), 243-250.

Bogdan, P.L.; James. R.B.; Maher, G.F., *US Patent No. 20050215839,* **2005.**

Borgna, A.; Sepulveda, J.; Magni S. I.; Apesteguia, C. R., **2004**, *Applied Catalysis A: General, 276* (1-2), 207—215.

Bozga, G.; Lupascu, M.; Zaharia, E.; Malacea. R., *Romanian International Conference on Chemistry and Chemical Engineering,* **2001**, 344-349.

Breck, D. W., Zeolite Molecular Sieves, Structure, Chemistry and Use. *Wiley*, New York, **1974,** 752.

Brown, H.C; Nelson, K.L., *Journal of American Chemical Society,* **1953,** *75,* 6292–6299.

Burres, G.T.; Kaeding, W.W.; Wu, M.M.; Young, L.B., *US Patent No. 4197413,* **1980**.

Camiloti, A.M.; Jahn, S.L.; Velasco, N.D.; Moura, L. F.; Cardoso, D., *Applied Catalysis A: General,* **1999,** *182* (1), 107-113.

Canattieri, E. V.; Rocha, G. J. M.; Carvalho, J. A.; Silva, J.B.A., *Bioresource Technology*, **2007**, *98* (2), 422-428.

Canizares, P.; Carrero, A.; Sanchez, P., *Applied Catalysis A: General*, **2000**, *190* (1-2), 93–105.

Cavani, F.; Corazzari, M.; Bencini, E.; Goffredi, G., *Applied Catalysis A: General,* **2002**, *226* (1-2), 31–40.

Cejka, J.; Wicheterlova, B., *Catalysis Review,* **2002**, *44* (3), 375–421.

Chao, K.; Leu, L., *Zeolites*, **1989**, *9* (3), 193-196.

Chen, N. Y., *Studies in Surface Science and Catalysis*, **1988**, *38*, 153-163.

Chen, N. Y.; Degnan, T. F., *Chemical Engineering Progress*, **1988**, *84* (2), 32-41.

Cheng, J. Y.; Brown, S. H.; Better, M. A., Dandekar, A. B.; Smith, C. M.; Steckel, M. A.; Weber, W. A., *US Patent No. 6936744,* **2005.**

Cheng K.; Zhenhuan, Z.; Xiao-Bing, F., *Petroleum Processing and Petrochemicals*, **2013**, *44*(12), 35-40.

Cheun, Y. Y.; Jinsou. X.; Phillip. J. A., *US Patent No. 7371910,* **2008.**

Clark, M. C.; Cheng, J. C.; Dandekar, A. B., *US Patent No.7951986,* **2011**.

Clark, J. H., *Account of Chemical Research*, **2002**, *35*,791-797.

Collins, N. A.; Mazzone, D. N.; Venkat, C. R., *US Patent No. 5902917*, **1999.**

Crejka, J.; Krejci, A.; Hanika, J., *Studies in Surface Science and Catalysis*, **2001***, 135,* 281.

Crejka, J.; Krejci, A., *Studies in Surface Science and Catalysis*, **2000**, *130*, 2627-2632.

Csicsery, S.M., *Journal of Catalysis*, **1971**, *23*, 124-130.

Csicsery, S.M.; Kiricsi,I., *Encyclopedia of Catalysis*, Horvath, I.T., Ed.; Wiley: New York, **2003,** *6*, 307-338.

Cullinane, N. M.; Leyshan, D. M., *Journal of Chemical Society*, **1954**, *4*, 2942-2947.

Das, J.; Bhat, S. Y.; Bhardwaj, A. I.; Halgeri**,** A. B., *Applied Catalysis A: General*, **1994**, *116*, 71-79.

Dasgupta, S.; Torok, B., *Organic Preparations and Procedures International*, **2008**, *40* (3), 215-291.

Derfer, J.M.; Defter, M.M., *Kirk-Othmer Encyclopedia of Chemical Technology*, **1978**, *22*, 709-715.

Dumitriu, E.; Guimon, C.; Hulea, V.; Lutic, D.; Fechete, I., *Applied Catalysis A: General*, **2002**, *237* (1), 211-221.

Dumitriu, E.; Hulea,V.; Kaliaguine, S.; Huang,M.M., *Applied Catalysis A: General*, **1996**, *135* (1), 57-81.

Elavarasan, P.; Kondamudi, K.; Upadhyayula, S., *Chemical Engineering Journal*, **2009**, *155* (1-2), 355-360.

Elliot, A.D.; Zhang, D., World of Coal Ash (WOCA), Lexington, Kentucky, USA, **2005**.

Emana, A.N.; Chand, S., *Applied Petrochemical Resource*, **2015**, *5*, 121–134.

Ercan, C.; Dautzenberg, F. M.; Yeh, C. Y.; Barner, H. E., *Industrial Engineering Chemistry Research*, **1998**, *37* (5), 1724-1728.

Ernest, L., *US Patent No. 3527825*, **1970.**

Ernest, L., *US Patent No. 3780122*, **1973.**

Fang, H.; Zhao, C.; Song, X., *Bioresource Technology*, **2010**. *101*, 4111-4119.

Faramawy, S., *Petroleum Science and Technology*, **1999**, *17* (3-4), 249-271.

Feinstein, A.I.; Bertolacini, R.J., *US Patent No. 4172813*,**1979.**

Ferreira, S.L.C.; Bruns, R.E.; Silva, E.G.P.; Santos, W.N.L.; Quintella, C.M.; David, J. M.; Andrade, J.B.; Breitkreitz, M. C.; Jardim I.C.F.S.; Neto. B. B., *Journal of Chromatography A*, **2007**, *1158* (1-2), 2-14.

Flockhart, B. D.; Liew, K. Y.; Pink, R. C., *Journal of Catalysis*, **1989**, *118*, 10-21.

Forni, L.; Cremona, G.; Missineo, F.; Bellussi, G.; Perego, C.; Pazzuconi, G., *Applied Catalysis A: General*, **1995,** *121* (2), 261-272.

Frankel, D.; Levy, M., *Journal of Catalysis*, **1989**, *118* (2), 487-493.

Friedel, C.; Crafts, J.M., *Comptes Rendus Chimie*, **1877**, *84*, 1450-1454.

Garcia, F. A. C.; Araujo, D. R.; Silva, J. C. M.; Macedo, J. L.; Ghesti, G. F.; Dias, S. C. L.; Diasa, J. A.; Geraldo, N. R., *Journal of Brazilian Chemical Society*, **2011**, *22* (10), 1894-1902.

Gates, B.C.; Catalysis by Solid Acids, in *Encyclopedia of Catalysis*, Horvath, I.T., Ed.; Wiley: New York, **2003,** *2*, 104-142.

Ghosh, A. S.; Elbaccouch, M.; Shafiei, M.; Gopalakrishnan, M., *US Patent No.* 2015036284A1, **2015.**

Gottipati, R.; Susmita, M., *Research Journal of Chemical Sciences*, **2012**, *2* (2), 40-48.

Haag, W. O.; Lago, R. M.; Weisz, P.B., *Nature*, **1984**, *309*, 589-591.

Haag, W. O.; Olson, D. H., *US Patent No.4136128*, **1979.**

Hafizi, A.; Ahmadpour, A.; Heravi, M. M.; Bamoharram F. F.; Khosroshahi. M., *Chinese Journal of Catalysis*, **2012**, *33* (2), 494-501.

Hanika, J.; Smejkal, Q.; Krejci, A.; Kolena, J., *Petroleum and Coal*, **2003,** *45* (1-2), **78-82.**

Hedge, S.G.; Kumar, R.; Bhat, R.N.; Ratnasamy, P., *Zeolites*, **1989,** *9*, 231-237.

Higgins, J. B.; La-Pierre, R. B.; Schlenker, J. L.; Rohrman, A. C.; Wood, J. D.; Kerr, G. T.; Rohrbaugh, W. J., *Zeolites*, **1998**, *8*, 446-452.

Hino, M.; Arata, K., *Chemistry Letter*, **1977**, *6* (3), 273-277.

Huang, X.; Suna, X.; Zhua, S.; Liua, Z., *Reaction Kinetics and Catalysis Letter*, **2007**, *91*, 385-390.

Huang, Z.; Tian, S.; Xu, Y.; Zhu, B.; Wang, W.; Zhang, F.; Wang, X., *US Patent No. 5600050*, **1997 (a).**

Huang, Z.; Tian, S.; Xu, Y.; Zhu, B.; Wang, W., *US Patent No. 5600050*, **1997 (b).**

Hulea, V.; Bilba, N.; Lupascu, M.; Dumitriu, E.; Nibou, D.; Lebaili, S.; Kessler, H.; *Microporous Materials*, **1997**, *8* (5-6), 201-206.

Hutchings, G. J.; Bartley, J. K.; Rhodes, C.; Taylor, S. H.; Wells, R. P. K.; Willock, D. J.; *Encyclopedia of Catalysis*, Horvath, I.T., Ed.; Wiley: New York, **2003,** *4*, 602-694.

Hwang, S. Y. H.; Johnson, D.E., *US Patent No. 20150183695*, **2015**.

Ichioka, R.; Yamakawa, S.; Okino, H.; Kato, H.; Iwayama,K.; Konta , H.; Kitamura, A., *US Patent No.6040490*, **2000.**

Innes, R. A.; Zones, S. I.; Nacamuli, G. J., *US Patent No. 4891458*, **1990.**

Innes, R. A.; Zones, S. I.; Nacamuli, G. J., *US Patent No. 5081323*, **1992**.

Ismailov, R. G.; Aliev, S. M.; Guseinov, N. I.; Ahmed, Z. A.; Guseinov, R. I., *Khim Technol Topl Masel*, **1973**, *18* (1), 6.

Jan, D. Y.; Schmidt, R. J.; Woodle, G. B.; Koljack, M. P.; Maurukas, E. Z.; Reynolds, T. M.; Garrett, C. J., *US Patent No. 20080171901*, **2008 (a).**

Jan, D. Y.; Schmidt, R. J.; Woodle, G. B.; Koljack, M. P.; Maurukas, E. Z.; Reynolds, T. M.; Garrett, C. J., *US Patent No. 20080171902*, **2008 (b).**

Jansen, J. C.; Creighton, E. J.; Njo, S. L.; Koningsveid, H.; Bekkum, H. V., *Catalysis Today*, **1997**, *38*, 205-212.

Janssens, B.; Catry, P.; Claessens, R.; Baron, G.; Jacobs, P. A., *Studies of Surface Science and Catalysis*, **1997**, *105*, 1211-1218.

Kaeding, W. W.; Holland, E. R., *Journal of Catalysis*, **1988**, *109* (1), 212-216.

Kato, H.; Tanaka, H.; Iwayama, K., *US Patent No. 6060417*, **2000.**

Kauffman, S., *US Patent No.3385906*, **1968**.

Khattaf, A. S.; Tukur, N. M.; Amer, A. A., *Industrial & Engineering Chemistry Research*, **2007**, *46* (13) , 4459–4467.

Khattaf, A. S.; Syed, A. A.; Osman, M. S.; Aitani, A. M., *Journal of Industrial & Engineering Chemistry Research*, **2015**, *21*, 1077-1088.

Kondamudi, K.; Upadhyayula, S., *Journal of Chemical Technolgy & Biotechnol*ogy, **2008**, *83*, 699-706.

Kozhevnikov, I.V., *Applied Catalysis A: General*, **2003**, *256* (1-2), 3-18.

Krejci, A.; Khattaf, A.S.; Ali, M.A.; Bejblova, M.; Cejka,J., *Applied Catalysis A: General*, **2010**, *377* (1-2), 99-106.

Kubicka, D.; Kumar, N.; Maki-Arvela, P.; Tiitta, M.; Niemi, V.; Karhu, H.; Sami, T.; Murzin, D.Y., *Journal of Catalysis*, **2004**, *227* (2), 313-327.

Kucherov, A. V.; Slinkin, A. A., *Zeolites*, **1986**, 6, 175-187.

Kucherov, A.V.; Slinkin, A.A.; Beyer, G.K.; Bordley, G., *Journal of Chemical Society*, **1989**, *85*, 3087-3094.

Lee, J.; Hong, U. G.; Hwang, S.; Youn, M. H.; Song, I. K. J., *Journal of Nanoscience and Nanotechnology*, **2014**, *14* (11), 8817-8822.

Lee, Y. K.; Park, S. H.; Rhee, H. Q., *Catalysis Today*, **1998**, *44* (1-4), 223-233.

Li,Y.; Wang,H.; Dong, M.; Li.J.; Qin, Z.;Wang, J.; Fan, WW., *RSC Advances*, **2015**, *5*, 66301-66310.

Lishchiner, I.I.; Plakhotnik, V.A.; Levin, D.Z.; Mortikov, E.S.; Ilyin, V. F., *Reaction kinetics and Catalysis lett*ers, **1983** , *23* (3), 261-265.

Lobo, R. F., Handbook of Zeolite Science and Technology, Marcel Dekker Inc. **2003**.

Mahajan, S.S.; Ghatpande, S.S., *Research Journal of Chemical and Environment*, **2005**, *9*, 100-103.

Maity, S. K.; Seetaram, C. H.; Pradan, N. C., *CHEMCON*, Ankleswar, Gujrat, India, **2006**.

Mavrodinova, V.; Popova, M.; Mihályi, R.M.; Borbely, G.P.; Minchev, C., *Applied Catalysis A: General*, **2003**, *248*, 197-209.

Meier, W.M.; Olson, D.H.; Boerlocher, C., *Atlas of Zeolite Structure types*, 4th edition Amsterdam: International Zeolite Association, **1996**.

Meshram, N. R.; kulkarni, S. B.; Ratnasamy, P., *Journal of Chemical Technology and Biotechnology*, **1984,** *34*, 119-126.

Meyer, H; Bernhauer, K., *Monatsh Chem*, **1929**, *53-54*, 721-743.

Mirzabekova, R.S.; Dorogochinskii, Z.A.; Mortikov, S.E., *Chemistry and Technology of fuels and oil*, **1977**,*13*, 840-842.

Misono, M., *Encyclopedia of Catalysis*, Horvath, I.T. ed.; Wiley: New York, **2003,** *3*, 433-447.

Mitche , R.T., *US Patent No. 3677973*, **1972.**

Molnar, A., *Current Organic Chemistry*, **2008**, *12*, 159.

Nacamuli, G. J.; Vogel, R. F.; Zones, S. I., *US Patent No. 5952536*, **1999.**

Nikaljeet, M. D.; Phukan, P.; Sudalai, A., *Organic Preparations and Procedures International*, **2000**, *32*, 1.

Nowinska, K.; Cław, A.; WIzbinska, A., *Applied Catalysis A: General*, **2003**, 243, 225–236.

Odedairo, T.; Al-Khattaf, S., *Chemical Engineering Journal*, **2011**, *167*, 240-254.

Olah, G. A., *Friedel-Crafts and Related Reactions*, Ed., Wiley:New York, **1964,** Chapter 14, 1

Olah, G. A.; Molnar, A., *Hydrocarbon Chemistry*, 2nd ed.; Wiley: New York, **2003**, 229-248.

Park, J.; Ali, S. A.; Alhooshani, K.; Azizi, N.; Miyawaki, J.; Kim, T.; Lee, Y.; Kim, H.; Yoon, S.; Mochida, I., *Journal of Industrial and Engineering Chemistry*, **2013**, 19 (2), 627–632.

Pathak, A. S.; Agarwal, S.; Gera, V.; Kaistha, N., *Industrial Engineering Chemical Research*, **2011**, *50* (6), 3312–3326.

Patkin, S. H.; Friedmann, B. S., Friedel Crafts and Related Reactions, **1964**, *2*, 1.

Patrick, B. J.; Lankton, S. P.; Schmidt, R. J., *US Patent No. 20100292519*, **2010.**

Plank, C. J.; Rosinski, E. J.; Hawthorne, W. P., *Industrial & Engineering Chemistry Product Research and Development*, **1964**, *3*, 165-169.

Pless, J. D.; Maxwell, R. S.; Philips, M. L. F.; Helean, K. B.; Axness, M. Y.; Nenoff, T. A., *Chemistry of Materials*, **2005**, *17*, 5101-5124.

Pradhan, A. R.; Rao, B. S., *Applied Catalysis A: General*, **1993**, *106*, 143-153.

Rahimi, N.; Karimzadeh, Ramin., *Applied Catalysis A: General*, **2011**, *398*, 1-17.

Ramesh, P.; Panwar, N. R.; Singh, A. B.; Ramana, S., *Indian Journal of Agricultural Science* **2010**, *78*, 351-354.

Qinhua, Xn.; Aizhen, Yan., *Crystal Growth and Characterization*, **1990,** *21*, 29–70.

Rao, B. S., *European Patent No. 0538518*, **1993.**

Reddy, S. N.; Rao, B. S.; Shiralkar, V. P., *Applied Catalysis A: General*, **1995**, *121*, 191-201.

Sabu, K. R.; Rao, K. V. C.; Nair, C. G. R., *Indian Jounal of Chemistry*, **1973**, *35*, 151-157.

Schultz. M.; Lankton. P.S.; Tagamolila. P.C., *US Patent No. 20080293986,* **2008.**

Schulz, R. C.; Gajda, G. J.; Woodle, G. B.; Zarchy, A. S., *US Patent No. 6339179,* **2002.**

Serra, M. J.; Guillon, E.; Corma, A., *Journal of Catalysis*, **2005**, *232*, 342-354.

Simon, L.; Guillon, E., *US Patent No. 20110108459 A1*, **2011**.

Siregar, T. B.; Amin, N. A. S., *Jurnal Teknologi*, **2006**, *44*, 69-82.

Slaugh, L. H., *US Patent No. 4375574 A*, **1983**.

Sotelo, J. L.; Calvo, L.; Velazquez, P. A.; Capilla, D.; Cavani, F.; Bolognini, M., *Applied Catalysis A: General*, **2006**, *312*, 194-201.

Sridevi , U.; Rao, B.; Pradhan, N. C., *Journal of Chemical Engineering*, **2001**, *83*, 185-189.

Srilatha, K; Prabhavathi Devi, B. L. A.; Lingaiah, N.; Prasad, R. B. N.; Sai Prasad P. S., *Bioresource Technology*, **2012**, *119*, 306–311.

Sulikowski, B.; Rachwalik, R., *Applied Catalysis A: General*, **2003**, *256*, 173–182.

Szostak, R., Molecular Sieves: Principles of synthesis and Identification. Van Nostrand Reinhold, New York, **1989.**

Tang, B.; Dai, W.; Sun, X.; Guan, N.; Li, L.; Hunger. M., *Green Chemistry*, **2014**, *16*, 2281-2291.

Tao, K.; Li, W.; Li, H.; Qi, X., *Applied Catalysis A:General*, **1996**, *139*, 43-49.

Thomas, O. H.; Thomas, A. B.; Wickman, R. F., *US Patent No. 3551509*, **1970.**

Treacy, M. M. J.; Higgins, J. B.; Ballmoos, R. V., Collection of Simulated XRD Powder Patterns for Zeolites. 3rd edition. Amsterdam: Elsevier, **1996**.

Tsai, T. C.; Chenb, W. H.; Liu, S. B.; Tsai, C. H.; Wang. I., *Catalysis Today*, **2002**, *73*, 39–47.

UOP, Inc., *US Patent No. 4128593*, **1978.**

Ushikubo, T. *Catalysis Today*, **2000**, *57*, 331.

Venuto, P. B.; Hamilton, L. A.; Landis, P. S.; Wise, J. J., *Journal of Catalysis*, **1966**, *5*, 81-83

Verma, R. S. *Tetrahedron*, **2002**, *58*, 12-35.

Villegas, J. I.; Kumar, N.; Heikkila, T.; Lehto, V. P.; Salmi, T.; Murzin, D. Y., *Chemical Engineering Journal*, **2006**, 120, 83–89.

Wachs, I. E.; Briand, L. E.; Jehng, J. M., *Catalysis Today*, **2000**, *57*,323.

Wadlinger, R. L.; Kerr, G. T.; Rosinski, E. J., *US Patent No. 3308069*, **1967**.

Wang.Y.; Ali, S. A.; Aitani, A. M.; Ali, M. A.; Ercanb, C.; Khattaf, A. S., *20th Annual Saudi-Japan Symposium, Dhahran, Saudi Arabia - December* **2010**.

Wang, H.; Zou, Y., *Catalysis Letters*, **2003**, *86*, 163-167.

Wang, I.; Tsai, T.C., *Industrial & Engineering Chemistry Research*, **1990,** *29*, 2005-2012.

Ward, J. W.; Hansford, R. C., *Journal of Catalysis*, **1969**, *13*, 364 –372.

Waziri, S. M.; Aitani, A. M.; Khattaf, A. S., *Industrial & Engineering Chemistry Research*, **2010**, *49*, 6376–6387.

Welstead, W. J., *Kirk-Othmer Encyclopedia Chemical Technology*, **1978**, *9*, 544-549.

West, M.; Abdo, S. F., *US Patent No. 5036033,* **1991.**

Yang, H.; Liu, Z.; Gao, H.; Xie, Z., *Applied Catalysis A: General*, **2010**, *379*, 166-171.

Yeh, C.Y.; Xu, J.; Hillsborough, N. J.; Angevine, P.J.; Woodbury, N. J., *US Patent No. 737190B2,* **2008**.

Young, L. B., *US Patent No. 4375573,* **1983**.

Zhang, Q.; Ming, W.; Ma, J.; Zhang, J.; Wang. P.; Li. R., *Journal of Materials Chemistry A*, **2014**, *2*, 8712-8718.

Zhixi, Z.; Zhang, L.; Chen, P.; Kun,Y., *The Open Materials Science Journal*, **2015**, 9, 194-197.

Publications

A comparative study of catalytic performance of rare earth metal modified beta zeolites for synthesis of Cymene, Ruchika Thakur, Raj Kumar Gupta, Sanghamitra Barman, ***Chemical Papers,*** (SCI journal), **Accepted**, July **2016**.

Optimization of Process Parameters for Transalkylation of Toluene to Xylene using Response Surface Methodology, Ruchika Thakur, Raj Kumar Gupta, Sanghamitra Barman, ***Particulate Science and Technology*** (SCI journal), 34(3), 332-340, **2016** .

Synthesis of cumene by transalkylation over modified beta zeolite: A kinetic study, Ruchika Thakur, Sanghamitra Barman, Raj Kumar Gupta, ***Brazilian Journal of Chemical Engineering***, (SCI journal), **Accepted**, Oct **2015**.

Synthesis of Xylene over cerium modified large pore zeolite: A kinetic study., Ruchika Thakur, Sanghamitra Barman, Raj Kumar Gupta, ***Indian journal of Chemical Technology*** (SCI journal), 21(5-6), 379-385, **2014**.

Kinetic investigation in Transalkylation of 1,2,4 Trimethylbenzene with Toluene over Rare Earth Metal modified Large Pore Zeolite, Ruchika Thakur, Sanghamitra Barman, Raj Kumar Gupta (Communicated).

Conferences

Optimization of various process variables in Transalkylation of Toluene with 1, 2, 4 Trimethylbenzene by Response Surface Method, Ruchika Thakur*, Sanghamitra Barman, Raj Kumar Gupta, *National conference on innovative molecules for sustainable future NCIMSF-2013*, Thapar University, 24-26 Oct, **2013**.

Synthesis of Cumene over Large Pore Zeolite, Ruchika Thakur*, Sanghamitra Barman, Raj Kumar Gupta, *CHEMCON*, PU Chandigarh, India, 27-30 Dec, **2014**.

Catalytic performance of rare earth metal modified large pore zeolite in synthesis of xylene, Ruchika Thakur*, Sanghamitra Barman, Raj Kumar Gupta, *CHEMCON*, IIT Guwahati, 27-30 Dec, **2015**.